

*Department of Civil and Environmental Engineering
University College Cork*



**Observations and modelling of
carbon dioxide, nitrous oxide and
methane using PaSim at an Irish
grassland site**

By

Delphine Lawton

*A Thesis submitted to the National University of Ireland, Cork
In part candidature for the Degree of Master of Engineering Science*

October 2005

Acknowledgements

I would like to express my thanks to the following people:

Prof. Gerard Kiely, my supervisor, for his guidance and his encouragement.

Prof. J.P.J. O’Kane, for the use of the facilities of the Department of Civil and Environmental Engineering, UCC.

Dr. Michael Creed for his administrative support.

Dr. Pierluigi Calanca of the Swiss Federal Research Station for Agroecology and Agriculture, Zurich, Switzerland, for his help and comments on the model PaSim.

Dr. Cécile Delolme for her help in my coming in Ireland.

Adrian Birky for his technical support.

Dr. Paul Leahy and **Dr. Ken Byrne**, for their helpful comments and discussion.

The students of the Civil and Environmental Engineering, **Anna Laine**, **Emmanuel Steinmann**, **Matteo Sottocornola**, **Jean-Baptiste Gobert** and **Pierre François** for their help and friendship.

The fellow graduates before me, **Charlotte Le Bris** and **Vesna Jaksic**, for their work on the carbon fluxes.

Eléonore Bagué, for her coming to Ireland with me and her permanent telephonic support.

My family for their permanent support and encouragements.

David Zillhardt, my fiancé, for his support, understanding and love.

Executive summary

Temperate grasslands are one of the most widespread ecosystems in the world and cover approximately 45% of the area of Ireland. The Pasture Simulation (PaSim) model is a process-based biogeochemical model for examining the fluxes of carbon, nitrogen, energy and water for grassland ecosystems. PaSim can incorporate land management practices such as grass cuttings (forage), grazing and the application of fertilizers. It is driven by hourly time series of meteorological data. The model's outputs include greenhouse gases (GHG) such as carbon dioxide (CO₂), nitrous oxide (N₂O) and methane (CH₄) fluxes.

Firstly, the model was calibrated using the observations of CO₂ and N₂O fluxes for the three years of data (2002, 2003 and 2004). The model simulated the observations well, particularly during the growing season. However, the cumulative annual CO₂ and N₂O fluxes were higher in the model than in the observations (with the exception of the year 2003 for N₂O emissions). There are no CH₄ measurements on site, but we estimated them through the IPCC guidelines. The PaSim modelled CH₄ fluxes were comparable to the IPCC estimations. Combining the contribution from each gas to their global warming potential (GWP) over the year, the model confirmed that this humid grassland in southwest Ireland acted as a sink for GHG during this period.

Secondly, the model was run with IS92a climate change (CC) scenario and elevated CO₂ (CO₂*2). The GHG sink was reduced under CC perturbations only. Nonetheless, it became a large sink of GHG as measured by radiative forcing under elevated CO₂ only. When combining CC and CO₂*2, the grassland still had a positive balance (i.e. sink) for GHG but in a smaller extent than under CO₂*2 only. When examining at the components of the GHG balance, the role of the grassland as a greenhouse gas sink is enhanced as a consequence of a higher uptake of CO₂ and reduced emissions of N₂O, under CC + CO₂*2. The grassland uptakes 11.3, 10.3 and 15.0 T of CO₂ equiv. ha⁻¹. yr⁻¹, respectively for the three years of simulation, that is to say, this is almost triple for 2002 and 2003 and double for 2004, in comparison with the simulation under ambient conditions. The model was also run with a reduction of application of fertilisers as recommended in the Irish Rural Environmental Protection Scheme (REPS); the balance was improved as the N₂O fluxes were reduced and the CO₂ fluxes did not change.

List of abbreviations

C: Carbon.
CC: Climate Change.
CH₄: Methane.
CO₂: Carbon Dioxide.
CO₂*2: Elevated CO₂.
CFC: Chlorofluorocarbon.
DM: Dry Matter.
EC: Eddy Covariance.
GCM: General Circulation Model
GHG: Greenhouse Gas.
GPP: Gross Primary Productivity.
GWP: Global Warming Potential.
IC: Initial Condition.
IR: Infrared.
LAI: Leaf Area Index.
N: Nitrogen.
NEE: Net Ecosystem Exchange.
NH₃: Ammonia.
NH₄⁺: Ammonium.
N₂O: Nitrous Oxide.
NO₃⁻: Nitrate.
NPP: Net Primary Production.
PAR: Photosynthetically Active Radiation.
REPS: Rural Environment Protection Scheme.
R_{tot}: Total Respiration or Ecosystem respiration.
SOM: Soil Organic Matter.
TDL: Tunable Diode Laser.
WFPS: Water Filled pore space.

Units and sign conventions

Units and conversions

Molar mass:

$$\begin{aligned} \text{C} &= 12 \text{ g. mol}^{-1} \\ \text{N} &= 14 \text{ g. mol}^{-1} \\ \text{O} &= 16 \text{ g. mol}^{-1} \\ \text{H} &= 1 \text{ g. mol}^{-1} \end{aligned}$$

Global warming potential:

$$\begin{aligned} \text{CO}_2 &= 1 \\ \text{N}_2\text{O} &= 296 \\ \text{CH}_4 &= 23 \end{aligned}$$

For carbon dioxide

$$\begin{aligned} 10 \text{ tC. ha}^{-1} &= 1 \text{ kgC. m}^{-2} = 44/12 \text{ kg CO}_2. \text{ m}^{-2} = 3.667 \text{ kg CO}_2. \text{ m}^{-2} \\ &= 3.667 \text{ kg CO}_2 \text{ equiv. m}^{-2} \end{aligned}$$

For nitrous oxide:

$$\begin{aligned} 1 \text{ kg N}_2\text{O} - \text{N. ha}^{-1} &= 14/(2*14) \text{ kg N}_2\text{O. ha}^{-1} = 1.571 \text{ kg N}_2\text{O. ha}^{-1} \\ &= 1.571*10^{-4} \text{ kg N}_2\text{O. m}^{-2} \\ &= 296*1.571*10^{-4} \text{ CO}_2 \text{ equiv. m}^{-2} = 0.046 \text{ kg CO}_2 \text{ equiv. m}^{-2} \end{aligned}$$

For methane:

$$\begin{aligned} 1 \text{ kgC. ha}^{-1} &= 16/12 \text{ kg CH}_4. \text{ ha}^{-1} = 1.333 \text{ kg CH}_4. \text{ ha}^{-1} = 1.333*10^{-4} \text{ kg CH}_4. \text{ m}^{-2} \\ &= 23*1.333*10^{-4} \text{ kg CO}_2 \text{ equiv. m}^{-2} = 0.003 \text{ kg CO}_2 \text{ equiv. m}^{-2} \end{aligned}$$

Sign convention

In this study we use the standard biological convention in which fluxes from the biosphere to the atmosphere are negative. However for more clarity, nitrous oxide and methane emissions that are negative considering the biological convention, will be shown on the positive axis for more legibility.

Contents

<i>Acknowledgements</i>	<i>i</i>
<i>Executive summary</i>	<i>ii</i>
<i>List of abbreviations</i>	<i>iii</i>
<i>Units and sign conventions</i>	<i>iv</i>
<i>Contents</i>	<i>v</i>
Chapter 1 Introduction	2
1.1 General background	2
1.2 Methods	4
1.3 Objectives	5
1.4 Layout of the thesis	5
Chapter 2 Data collection	7
2.1 Site description	7
2.1.1 Location.....	7
2.1.2 Climate	8
2.2 Field history and grassland management	9
2.3 Description of instruments	11
2.3.1 Weather station.....	11
2.3.2 Pyranometer.....	12
2.3.3 Temperature and relative humidity probe	13
2.3.4 Ultrasonic anemometer.....	15
2.3.5 Rain gauge.....	16
2.3.6 Soil temperature probes.....	16
2.3.7 Soil moisture monitors	16
2.3.8 Datalogger	17
2.3.7 Telephone connection.....	18

2.4 Summary of meteorological data	18
2.4.1 Precipitation.....	18
2.4.2 Soil moisture.....	20
2.4.3 Incoming radiation.....	21
2.4.4 Air and soil temperature	22
Chapter 3 <i>Methods</i>.....	24
3.1 Observations	24
3.1.1 Eddy covariance method and footprint.....	24
3.1.2 Carbon dioxide	26
Instrumentation.....	26
Filtering and gap-filling.....	29
3.1.3 Nitrous Oxide	29
Instrumentation.....	29
Filtering and gap-filling.....	32
3.2 Simulation model.....	33
3.2.1 Model description.....	33
Five submodels.....	33
Meteorological input data.....	34
Outputs	35
3.2.2 Model parameterisation	35
Site specific parameters.....	35
Initial conditions.....	36
Management Data.....	38
3.2.3 Sensitivity to changes.....	42
Chapter 4 <i>Greenhouse Gas Balance</i>.....	45
4.1 What is a greenhouse gas balance?	45
4.2 Carbon dioxide	48
4.2.1 Comparison of modelled and observed NEE	48
4.2.2 Components of NEE.....	50
4.3 Nitrous oxide	52
4.4 Methane.....	56

4.5 Greenhouse gas balance	58
4.5.1 Modelled vs. observed GHG balance	58
4.5.2 GHG balance modelled	61
Chapter 5 <i>Climate Change Scenarios</i>	64
5.1 Definition of the scenarios	64
5.1.1 Climate change scenario and elevated CO ₂	64
5.1.2 REPS 2000	65
5.2 Climate change scenario	66
5.2.1 Definition of the scenario in terms of meteorological data	66
5.2.2 Results and analysis.....	67
5.3 Elevated CO₂ scenario	71
5.4 Climate change and elevated CO₂ scenario	74
5.5 REPS scenario	79
5.5.1 Definition of the scenario in terms of management data	79
5.5.2 Results and analysis.....	80
Chapter 6 <i>Conclusion</i>	85
6.1 Conclusion	85
6.2 Suggestion for further investigation	86
<i>References</i>	89
<i>Appendix 1: Glossary of terms</i>	99
<i>Appendix 2: Paper submitted to Global Change Biology</i>	103

Chapter 1

Introduction

Chapter 1

Introduction

1.1 General background

Grasslands cover between 12% and 27% of the total land area of the world [Brown, 1998] and occupy 37% of Europe's agricultural area. They are the dominant ecosystem in Ireland, representing 90% of agricultural land and 45% of the total land area [Gardiner and Radford, 1980]. They play a key role in the carbon cycle through photosynthetic and respiratory processes. Photosynthesis, using inorganic molecules and the energy of light, is the transformation of carbon dioxide (CO₂) into organic matter, which either remains in the plants or is stored in the soils.

CO₂ is a greenhouse gas (GHG). Greenhouse gases also include methane (CH₄), nitrous oxide (N₂O), chlorofluorocarbons (CFCs), and water vapour (H₂O). CO₂, CH₄ and N₂O have significant natural and human sources while only industry produce CFCs [Kiely, 1997]. Water vapour has the largest greenhouse effect, but it is not considered in the greenhouse gas balance for its concentration in the troposphere is determined within the climate system.

Although greenhouse gases together make up less than 0.1% of our atmosphere [Encyclopedia Britannica, 2002], they act as a kind of thermal blanket around the whole earth, preventing a significant amount of incoming solar energy from being radiated back out into space [Kiely, 1997; Sarmiento and Gruber, 2002]. Unfortunately this blanket is getting thicker as the proportion of greenhouse gases increases because of human influences [UNFCCC, 1992], which may be magnifying to dangerous levels an otherwise beneficial natural phenomenon known as the greenhouse effect [Kyoto Protocol, 1997; Sarmiento and Gruber, 2002] and may be causing a significant increase in the average temperature of our planet's atmosphere.

It is estimated that the global temperature would increase by between 1 and 3.5°C if the CO₂ concentration were to double. It is projected that this will happen before the end of the 21st century [IPCC, 1996]. Such changes could trigger major disruptions around the world: food production patterns could shift as agriculture becomes more difficult in some areas and easier in others, large numbers of plant and animal species could become extinct, forests and water supplies could be threatened etc [Environmental Media Service, 2003; Kyoto Protocol, 1997].

The Kyoto Protocol for Ireland requires that emissions of GHG must be no more than 13% above the 1990 levels. As of 2001, emissions are 31% greater than the 1990 levels [EPA, 2000]. By 2008 – 2012 the “business as usual” scenario forecast (produced in 2000 based on 1998 data) is that emissions may be more than 37% greater than the 1990 levels [EPA, 2003]. Agriculture is estimated to be responsible for about 27% (soils 5.5%) of total GHG emissions in 2001 [EPA, 2003].

The study of carbon fluxes between vegetation and the atmosphere is important as carbon (C) uptake by ecosystems may compensate for some emissions of greenhouse gases [IPCC, 2001]. Indeed, the Kyoto Protocol established the concept of credits for C sinks. It is possible to take carbon sinks into account to a certain extent in calculating national greenhouse gas balances. It is therefore important to have reliable quantitative information on current carbon stocks and potential sinks.

As a consequence, long-term measurements of CO₂ fluxes are necessary to determine the seasonal and inter-annual variability of net ecosystem exchange (NEE). CO₂ fluxes between the atmosphere and grasslands in the Great Plains of the USA have been extensively measured with eddy covariance (EC) [Flanagan et al., 2002; Frank, 2002; Frank and Dugas, 2001; Sims and Bradford, 2001], but few long-term studies have been made of grasslands in more temperate humid climates [Saigusa et al., 1998; Novick et al., 2004]. N₂O has been well studied with closed chamber measurements [Dobbie et al., 1999; Mosier et al., 1996; Williams et al., 1999] and now with the EC technique [Volpe Horii et al., 1999; Scanlon et al., 2004]. Methane from cattle has been well observed as well [Johnson and Johnson, 1995; DeRamus et al., 2003] and methods are now available to estimate CH₄ emissions [IPCC, 1996]. In Europe, projects such as GreenGrass (Sources and sinks of greenhouse gases from managed European grasslands and mitigation strategies), launched in 2001, or CarboEurope-IP, 2004-2009 (Assessment of the European terrestrial carbon balance) started to work on carbon fluxes and greenhouse gases. Another integrated project (Nitri-Europe) will be launched in 2006 for five years.

Eddy covariance studies, while valuable, can only measure the NEE. Ecosystem respiration is usually estimated from a combination of: an extrapolation of night-time fluxes under strong turbulence [Falge et al., 2002] and an empirical regression model of night-time fluxes with soil temperature [Xu and Baldocchi, 2004; Jaksic, 2004]. The exceptions include a few studies, in which direct estimates of the respiration have been obtained by locating the EC instruments below the canopy of a forest [Baldocchi et al., 1997] or using isotopic flux measurements of ¹³CO₂ [Bowling et al., 2001]. The variations in soil and ecosystem respiration are commonly linked with soil temperature and soil water content. Some relationships have also been found with soil organic carbon and plant growth rate [Franzluebbers et al., 2002].

Biogeochemical models used to study the carbon cycle of different ecosystems include: Hurley-Pasture (HP) model [Thornley, 1998]; CENTURY model [Parton et al., 1987]; Simulation of Production and Utilization of Rangelands (SPUR) model [Foy et al., 1999]; DeNitrification-DeComposition (DNDC) model [Li et al., 1994] or Multiple-Element Limitation (MEL) model [Rastetter and Shaver, 1992] and the Pasture Simulation (PaSim) model [Riedo et al., 1998]. Models can provide an improved understanding of the seasonal and interannual trends in the NEE through the simulation of the two components of the NEE: the gross primary production (GPP) and the total respiration of the ecosystem (R_{tot}). They can also be used to examine scenarios such as elevated CO₂ (MEL, Rastetter et al., 1997), elevated CO₂ (CO₂*2) combined with climate change scenarios (GEM2, Chen et al., 1996; CEVSA model, Cao and Woodward, 1998; CENTURY model, Parton et al., 1995). The previous models especially focus either on C sequestration, either on net primary production; PaSim is the only one to model all the GHG.

1.2 Methods

The Dripsey flux site in Cork, southwest Ireland, is a perennial ryegrass pasture, very typical of the vegetation of this part of the country, and is grazed for approximately 8 months of the year. The lands are fertilised with approximately 300 kgN. ha⁻¹. yr⁻¹ of nitrogen. The flux tower monitoring CO₂, water vapour and energy was established in June 2001 and we have continuous data since then. CO₂ fluxes have been analysed for the years 2002, 2003 and 2004 [Le Bris, 2002, Jaksic, 2004]. N₂O have been analysed for the years 2003 and 2004 [Leahy et al., 2004].

We used a biogeochemical model PaSim [Riedo et al., 1998] to model the grassland site and study the emissions of CO₂, N₂O and CH₄. First of all, the model has been parameterised using measurements, literature values and model optimisation. Once the simulations of CO₂ and N₂O were in reasonable agreement with the observations (or measurements), PaSim was run with climate change scenarios (changes in temperature and precipitation as well as elevated CO₂) and the new greenhouse gas balance was established. A last simulation was run under a scenario considering a reduction of nitrogen applications according to the recommendations of the Irish Rural Environment Protection Scheme (REPS).

1.3 Objectives

The first objective of this project was to determine the greenhouse gas balance over a humid grassland using a biogeochemical model. Then the second objective was to apply the model with climate change scenarios and nitrogen fertiliser reductions.

1.4 Layout of the thesis

Chapter 2 describes the studied site, the instruments used in experiment and the meteorological data. Chapter 3 describes how CO₂ and N₂O fluxes were measured and analysed on site, and it contains a description of PaSim model and the parameterisation of the latter. Chapter 4 analyses the CO₂, N₂O, CH₄ fluxes and the GHG balance. Chapter 5 provides estimates of the GHG balance according to climate change scenarios and reductions in the application of fertilisers. Chapter 6 presents the conclusions and recommendations and makes suggestions for continuing research. The Appendices include a glossary of terms and the article “Observations and process-based modelling of the net ecosystem exchange and its components for a humid grassland ecosystem”, submitted to Global Biology Change, in June 2005.

Chapter 2

Data Collection

Chapter 2

Data collection

2.1 Site description

2.1.1 Location

The Dripsey experimental grassland is located near the village of Donoughmore, County Cork in southwest Ireland, 25 km northwest of Cork city (52° North latitude, 8° 30' West longitude), (see Figure 2.1).



Figure 2.1: Location of the site area.

The Dripsey grassland at an elevation of ~ 200 m above sea level has a gentle slope to a stream of 3% grade (see Figure 2.2). The soil is classified as brown podzolics [Gardiner and Radford, 1980]. The topsoil is rich in organic matter to a depth of about 15 cm (about 12% organic matter, [Daly, 1999]), overlying a dark brown B-horizon of sand texture. A yellowish

brown B-horizon of sand texture progressively changes to a brown, gravely sand which constitutes the parent material at a depth of approximately 0.3 m. The underlying bedrock is old red sandstone [Scanlon et al., 2004]. Depth averaged over the top 30 cm the volumetric soil porosity was 0.49, the saturation moisture level was 0.45, the field capacity was 0.32, and the wilting point was $0.12 \text{ m}^3 \cdot \text{m}^{-3}$.



Figure 2.2: Dripsey site.

2.1.2 Climate

The climate is temperate and humid (from the influence of the warm Gulf Stream in the North East Atlantic Ocean) with mean annual precipitation in the Cork region of about $1470 \text{ mm} \cdot \text{yr}^{-1}$. The rainfall regime is characterized by long duration events of low intensity (values up to $40 \text{ mm} \cdot \text{day}^{-1}$). Short duration events of high intensity are more seldom and occur in summer.

Daily air temperatures have a very small range of variation during the year, going from a maximum of 20°C to a minimum of 0°C , with an average of 15°C in summer and 5°C in winter. This part of Ireland is windy with a mean wind velocity (at 3 m) of $4 \text{ m} \cdot \text{s}^{-1}$ at the site with peaks up to $16 \text{ m} \cdot \text{s}^{-1}$. The main wind comes from the southwest.

2.2 Field history and grassland management

The site is agricultural grassland, typical of the land use and vegetation in this part of the country. It has been established about 20 years ago. The vegetation cover at Dripsey is grassland of moderately high quality pasture and meadow, whereas the dominant plant species is perennial ryegrass (*Lolium perenne*) with a significant fraction of clover. Considering environmental conditions, warm but not hot temperatures and high humidity with good airflow and the latitude of Ireland, the metabolic pathway for carbon fixation is assumed to be a Calvin-Benson Cycle (C3 grass, Le Bris, 2002).

Like much of the surrounding rural area, the landscape near the meteorological / EC tower is partitioned into small fields. Management strategies for boosting grassland production varied according to the individual farmers. Management data (application of fertilisers, grazing and silage cuts) is collected through monthly surveys completed by the farmers that own fields within the footprint. The land use is a mixture of paddocks for cattle grazing (approximately 2/3rds of fields) and fields for cutting (silage harvesting) (approximately 1/3rd of fields).

Cattle grazing begins in March and ends in October (approximately 8 months). The rotational paddock grazing periods last approximately one week in four. The grass height in the grazing fields varies from 0.05 m to 0.3 m. With wet fields in the autumn of 2002 and 2004, cattle were not grazing outdoors (as cattle damage the fields in wet times) but were housed indoors from late September leaving the standing biomass to its own devices. By contrast, the autumn of 2003 was dry and cattle were grazing (at least during the day) up to November. Livestock density at the site is 2.2 LU. ha⁻¹ [Lewis, 2003], where Livestock Units (LU) is the basis of comparison for different classes and species of stock. The large animal unit (LU) is a reference animal with an energy requirement of 3000 fodder units (1 FU is equivalent to 6.6 kg of grass). It stands for a dairy cow present on the farm for twelve months and producing 3000 litres of milk with a fat content of 40 g, and one calf [FAO, 1988]. Half of the cattle are dairy cows and half are beef cattle.

In the cut fields the grass is harvested in the summer, typically first in May or June and second time in August or September, and exported as silage from the pastureland for winter feed. The height of grass just before cutting in silage fields reaches about 0.5 m in summer, whereas it is down to 0.15 m in wintertime during the resting period. Due to the mild climatic conditions the field stays green all year. No measurement of the biomass of grass has been made on this site; Leaf Area Index (LAI) measurements started in 2004. The annual

yield of silage in the region has been 8 to 12 tonnes of dry matter per hectare per year depending on the weather.

Grass productivity is enhanced with the application of approximately 300 kg of nitrogen in fertiliser and slurry, spread at intervals of approximately six weeks between February and September [Lewis, 2003]. Commercially prepared mineral fertilizer mixtures were used, consisting of almost equal parts $\text{NH}_4^+\text{-N}$ and $\text{NO}_3^-\text{-N}$. Nitrogen in chemical fertilizer was applied at the rate of 214, 204 and 177 $\text{kgN. ha}^{-1}. \text{yr}^{-1}$, and nitrogen in slurry approximately at 91, 130 and 30 $\text{kgN. ha}^{-1}. \text{yr}^{-1}$ in 2002, 2003 and 2004, respectively. Area-weighted values of chemical fertilizer and slurry for 2002, 2003 and 2004 are given in Figure 2.3, 2.4 and 2.5 respectively.

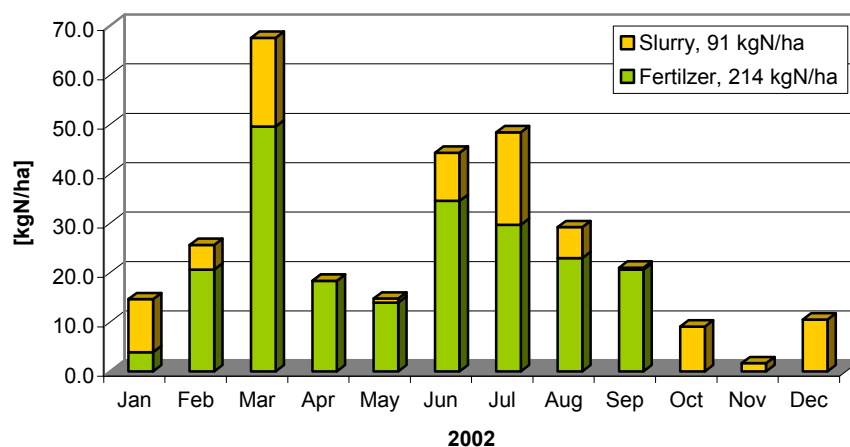


Figure 2.3: Monthly application of nitrogen fertilizer and slurry for 2002 at Dripsey site.

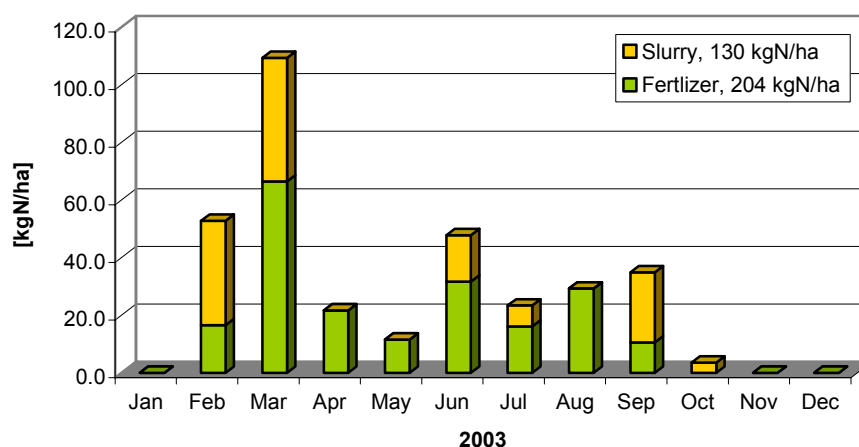


Figure 2.4: Monthly application of nitrogen fertilizer and slurry for 2003 at Dripsey site.

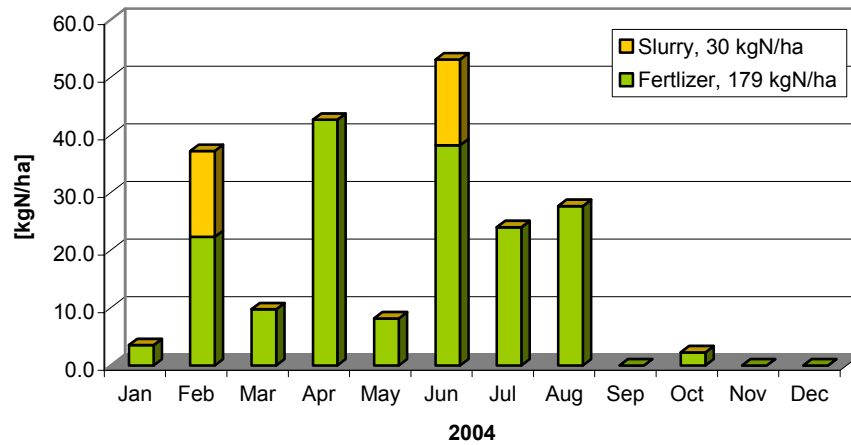


Figure 2.5: Monthly application of nitrogen fertilizer and slurry for 2004 at Dripsey site.

In 2004, it is noted that the amount of chemical fertilizer spread is lower than in 2002 and 2003; and the amount of slurry is much lower than the two previous years. This may come from the fact that the data is given by the farmers, but unfortunately, there are some gaps.

2.3 Description of instruments

The flux tower was established in June 2001 and we have continuous data since then. In this section we present an overview of the sensors and techniques used for data collection.

2.3.1 Weather station

The experimental system used in this study is composed of a 10 m high tower, which supports meteorological, hydrological and eddy covariance sensors connected to a datalogger. The datalogger controls the measurements, data processing and digital storage of the sensor outputs. A secured perimeter has been defined with a wire fence to protect the tower sensors, as well as to define a setting up area for the soil devices (see Figure 2.6).

Figure 2.6 shows the tower in its full height and indicates position of the weather sensors. The tower supports sensors for measuring the relative humidity and air temperature at 3 m and various types of sensors at 10 m of which the net radiometer. The rain gauge is

located on the ground. Meteorological measurements were sampled at one minute and average over 30-minute intervals. The white box near the foot of the tower is called ‘Campbell environmental box’ and houses the datalogger, as well as a modem connection.

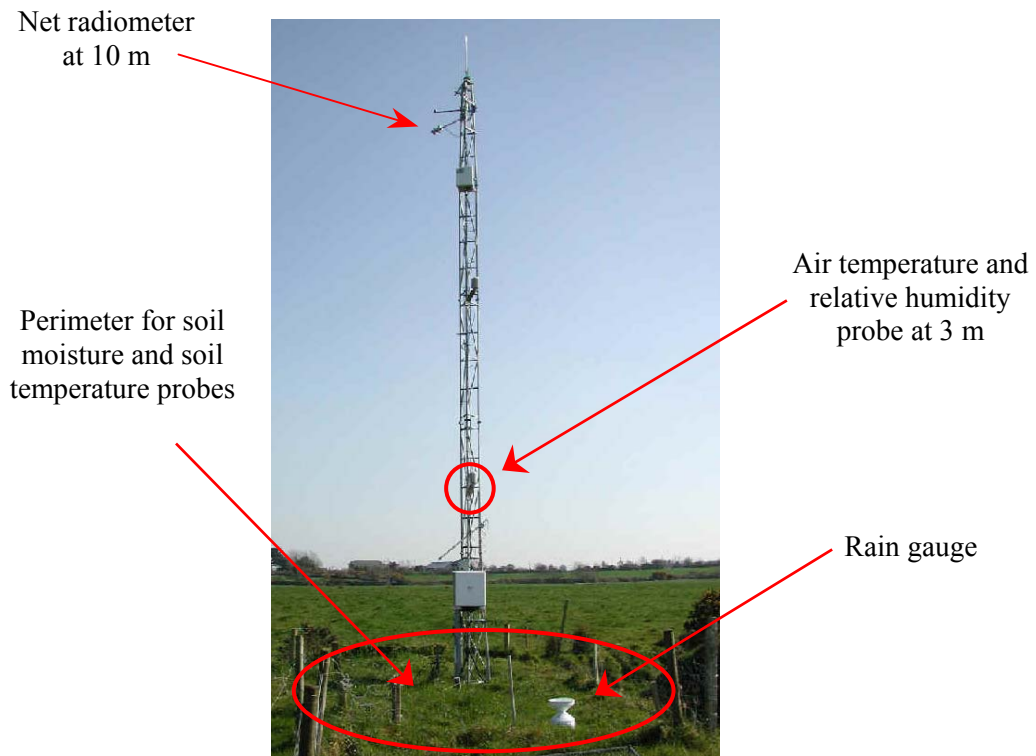


Figure 2.6: Tower at Dripsey site.

2.3.2 Pyranometer

The pyranometer was part of a net radiometer (CNR1 from Kipp & Zonen) positioned horizontally at 10 m above the ground. The net radiometer measures the radiation balance of solar and far infrared radiation. The most common application is the measurement of Net Radiation at the earth's surface. Net radiation is the difference between the incoming and outgoing radiation [Campbell and Norman, 1998]. The instrument consists of a pyranometer and pyrgeometer pair that faces upward and a complementary pair that faces downward (see Figure 2.7). The pyranometers and pyrgeometers measure short-wave and far infrared radiation, respectively. All four sensors are calibrated to an identical sensitivity coefficient [Kipp and Zonen, 2000].

The pyranometer facing upward measures incoming radiation from the sky, and the other, which faces downward, measures the reflected solar radiation (see Figure 2.7). A pyranometer consists of a thermopile sensor, housing, glass dome and a cable. The thermopile

is coated with a black absorbent paint, which absorbs the radiations and converts them into heat. The resulting heat flow causes a temperature difference across the thermopile. The thermopile generates a voltage output. The absorber paint and the dome determine spectral specifications. The thermopile is encapsulated in the housing in such a way that its field of view is 180° degrees, and that its angular characteristics fulfil the so-called cosine response.

The conversion factor between voltage (V) and Watts per square metre of solar irradiance E (incoming or reflected in W/m^2), is the so-called calibration constant C or sensitivity [Kipp and Zonen, 2000].

$$E = \frac{V}{C} \quad \text{Eq. 2.1}$$

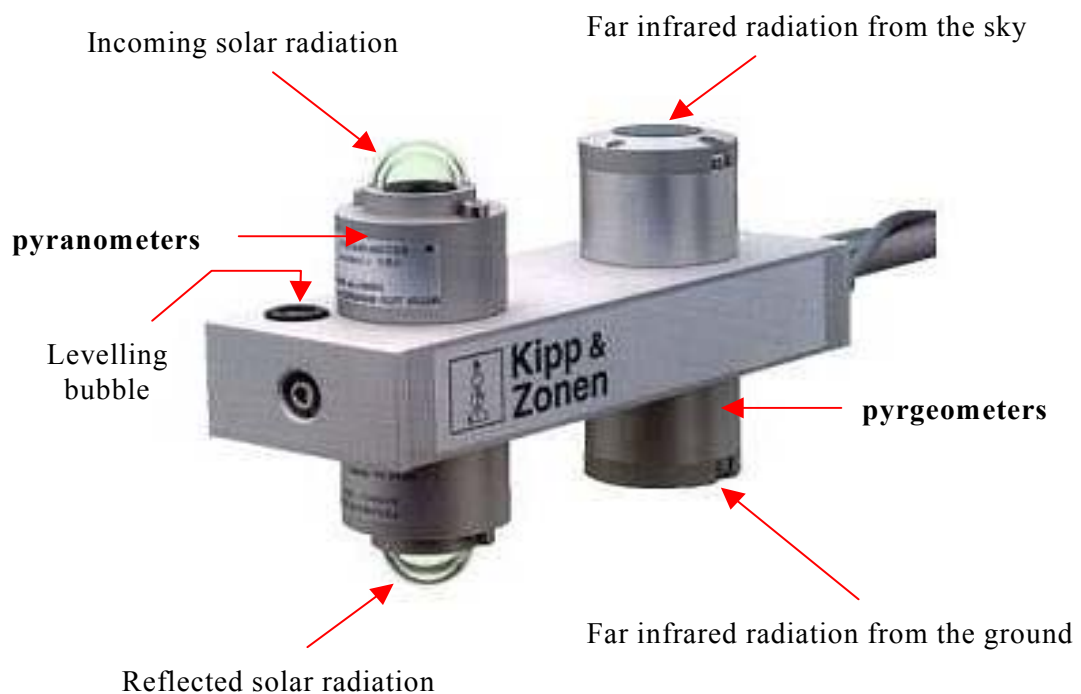
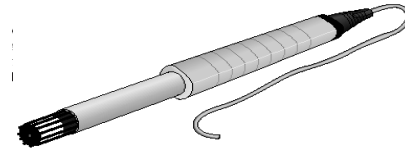


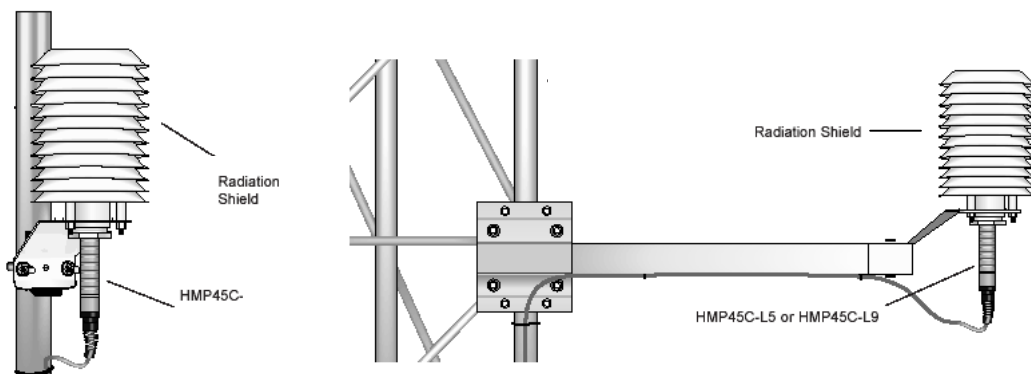
Figure 2.7: Net radiometer and its main components (from Kipp & Zonen manual).

2.3.3 Temperature and relative humidity probe

Air temperature and humidity were monitored at 3 m height and recorded continuously at 30-minute intervals. For that purpose the model HMP45C temperature and relative humidity probe from Campbell Scientific was used. (Figure 2.8). Probe contains a Platinum Resistance Temperature detector (PRT) and a Vaisala HUMICAP® 180 capacitive relative humidity sensor [Campbell, 2003a].



The HMP45C must be housed inside a radiation shield when used in the fields because it should be protected from the sunlight (Figure 2.9).



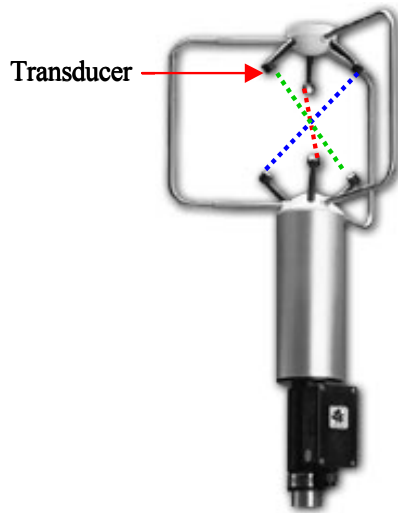
The instrument measures the relative humidity. Relative humidity is defined by the equation below [Campbell, 2003a]:

$$RH = \frac{e}{e_s} \times 100 \quad \text{Eq. 2.2}$$

where RH is the relative humidity, e is the vapour pressure in kPa, and e_s is the saturation vapour pressure in kPa. The vapour pressure, e , is an absolute measure of the amount of water vapour in the air and is related to the dew point temperature [Garatt, 1992; Brutsaert, 1991]. The saturation vapour pressure is the maximum amount of water vapour that air can hold at a given air temperature. When air temperature increases, so does the saturation vapour pressure [Garatt, 1992; Brutsaert, 1991]. Conversely, a decrease in air temperature causes a corresponding decrease in saturation vapour pressure. It follows then from Equation 2.2 that a change in air temperature will change the relative humidity, without causing a change in absolute humidity sensor [Campbell, 2003a].

2.3.4 Ultrasonic anemometer

Wind velocity, wind direction and virtual temperature measurements were performed by the model 81000 ultrasonic anemometer from R. M. Young (Figure 2.10) positioned at the top of the 10 m tower.



It is a 3-dimensional, no-moving-parts wind sensor. Whereas 2-D anemometers ignore the vertical wind component, the 81000 provide a complete picture of the wind. Robust construction, combined with 3 opposing pairs of ultrasonic transducers, provides accurate and reliable wind measurements [Young, 2001].

Figure 2.10: The sonic anemometer with the three paths shown in red (E-W), blue (SW-NE), green (NW-SE), as for a typical orientation of the device (from Young manual).

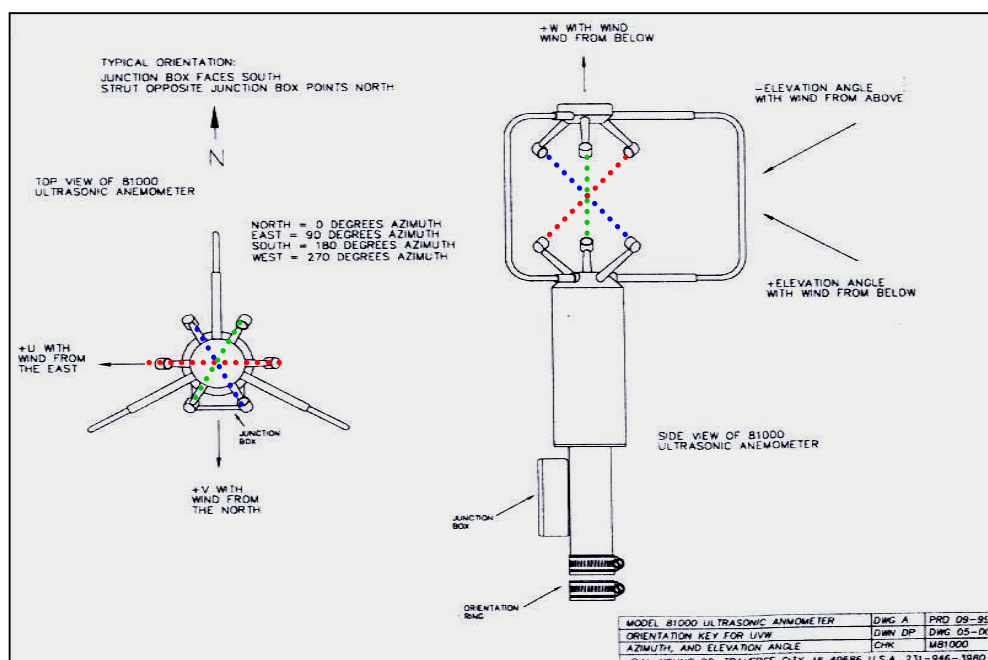


Figure 2.11: Ultrasonic anemometer axis systems (from Young manual).

The instrument makes observations of the wind velocities by measuring the travel time of ultrasonic signals sent between the upper and lower transducers (see Figure 2.11). By measuring the transit time in each direction along all three paths, the three dimensional wind velocity and speed of sound may be calculated. From sonically determined speed of sound,

sonic temperature is derived [Young, 2001]. Sonic temperature is approximately equal to the virtual temperature (it will differ from absolute temperature by an amount proportional to the water vapour of the measured air).

2.3.5 Rain gauge



Figure 2.12: ARG100 rain gauge (from Campbell Scientific manual).

Rain gauge ARG100 Campbell measures total rainfall in mm. Gauges used do not measure snowfall. A conventionally shaped rain gauge interferes with the airflow so that the catch is reduced [Campbell, 2000]. The ARG100 gauge has been designed to minimise this effect by presenting a reduced area to the wind (see Figure 2.12).

The ARG100 is manufactured in UV-resistant plastic. The amount of rain collected is measured by the well-proven tipping bucket method. The contact closure at each tip is recorded by Campbell Scientific datalogger. Standard setting is used of 0.2 mm of rain per tip [Campbell, 2000].

2.3.6 Soil temperature probes

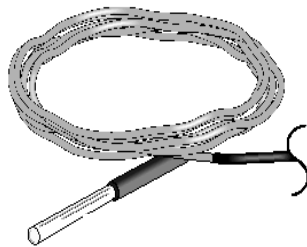


Figure 2.13: Soil temperature probes model 107 (from Campbell Scientific manual).

Soil temperatures were measured in °C with buried temperature probes Model 107 [Campbell, 2003b] (Figure 2.13), two at 2.5 cm deep and one at 7.5 cm deep, and were recorded in 30-minute intervals by Campbell Scientific datalogger.

2.3.7 Soil moisture monitors

Volumetric water content of the soil profile was measured at depths of 5, 10, 25 and 50 cm with CS615 water content reflectometers from Campbell Scientific set horizontally (Figure 2.14). Two CS615 water content reflectometers were installed vertically, one from 0

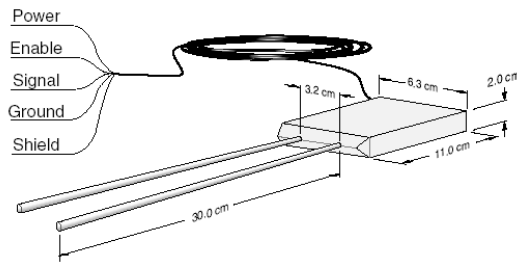


Figure 2.14: CS615 Soil moisture (water content) reflectometer (from Campbell Scientific manual).

to 30 cm, and another from 30 to 60 cm depth. This type of sensor uses time domain reflectometry (TDR) methods that are based on the propagation characteristics of an electromagnetic wave on a transmission line [Campbell, 2002]. The probe consists of two 30 cm long stainless steel rods connected to a printed circuit board. High-speed electronic components on the circuit board are configured as a bistable multivibrator. The output of the multivibrator is connected to the probe rods, which act as a wave travel guide. The travel time of the signal on the probe rods depends on the dielectric permittivity of the material surrounding the rods and the dielectric permittivity depends on the water content. Therefore the oscillation frequency of the multivibrator is dependent on the water content of the media being measured [Campbell, 2002]. The CS615 output is essentially a square wave with amplitude of ± 0.7 Volts with respect to the system ground. The period is then converted into volumetric water content using a calibration equation [Campbell, 2002].

2.3.8 Datalogger

Dataloggers provide sensor measurement, time keeping, data reduction, data or/and program storage and control functions. In this study CR23X datalogger from Campbell Scientific was used (see Figure 2.15).

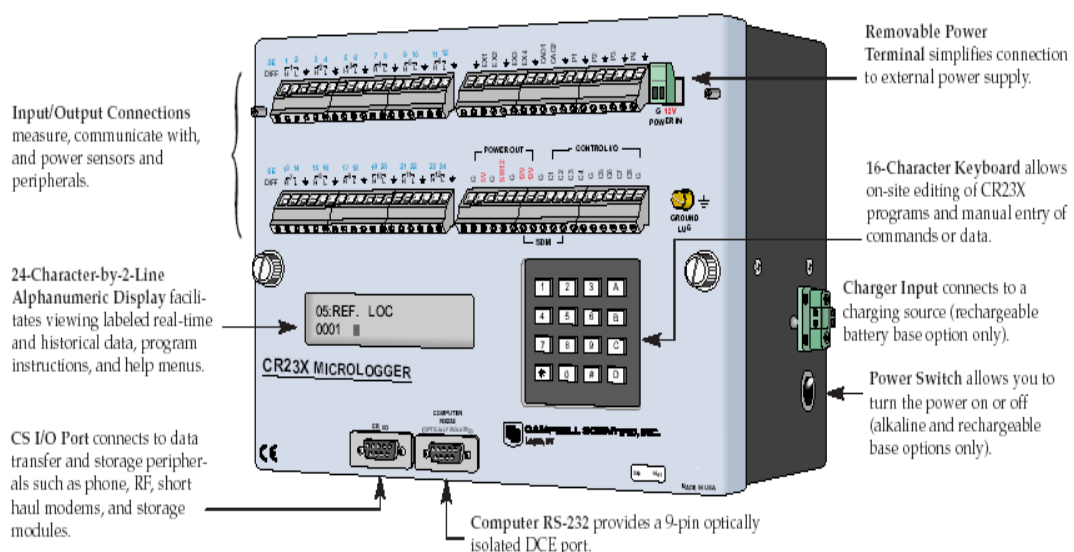


Figure 2.15: CR23X Datalogger (from Campbell Scientific manual).

2.3.7 Telephone connection

The weather station was connected by modem to a network, and was feeding weather data into a retrieval system consisting of a personal computer and telephone communications link.

2.4 Summary of meteorological data

Table 2.1 presents the monthly averages for precipitation, soil moisture at 5 cm depth, incoming radiation, air temperature and soil temperature at 5 cm depth for the three years of measurements.

2.4.1 Precipitation

Figure 2.16 presents the cumulative sum of precipitation. The long-term annual average rainfall for Dripsey is 1470 mm. The year 2002 was wet, with an annual rainfall of 1785 mm (~ 14% above mean annual average). 2003 was dry, with an annual rainfall of 1184 mm (~ 19% less than average). The year 2004 was slightly drier than average, with a cumulative sum of 1341 mm.

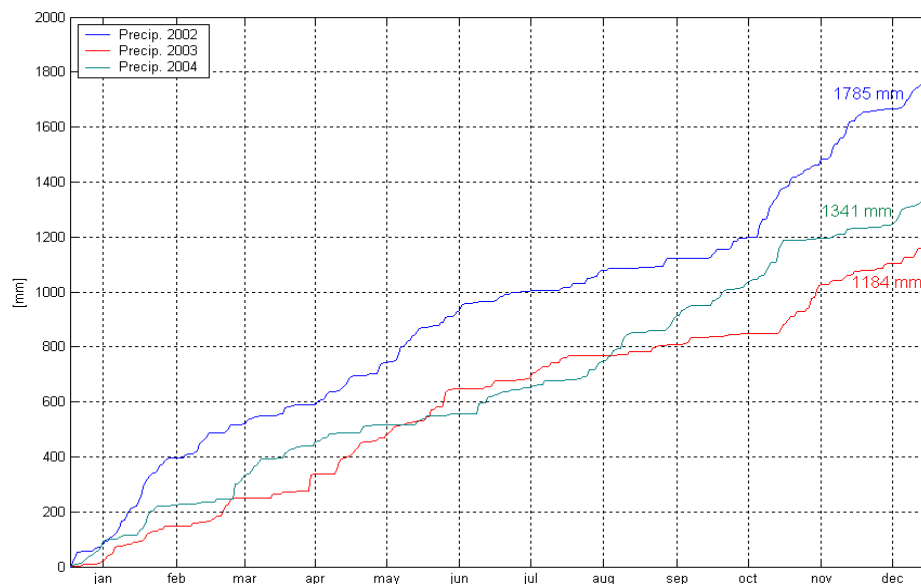


Figure 2.16: Cumulative precipitation in mm for 2002, 2003 and 2004.

Table 2.1: Monthly average for precipitation, soil moisture at 5 cm depth, incoming radiation, air temperature and soil temperature at 5 cm depth for 2002, 2003 and 2004.

	2002											
Month	Jan.	Feb.	Mar.	Apr.	May	Jun.	Jul.	Aug.	Sep.	Oct.	Nov.	Dec.
Precipitation [mm]	254.2	218.2	83.4	136.8	177.8	99.0	47.6	73.4	45.2	244.4	255.2	150.2
Soil moisture at 5 cm	0.59	0.59	0.56	0.53	0.54	0.51	0.39	0.39	0.25	0.45	0.56	0.55
Incoming radiation [$W. m^{-2}$]	27.7	58.5	87.7	154.0	171.1	178.6	171.9	150.3	119.3	69.3	36.8	20.1
Air temperature [°C]	7.5	6.7	7.0	8.0	9.7	11.3	13.4	14.6	13.0	9.7	8.2	6.3
Soil temperature at 5 cm [°C]	6.0	5.7	6.3	8.7	10.7	12.5	14.3	14.8	13.0	10.0	7.8	5.9

	2003											
Month	Jan.	Feb.	Mar.	Apr.	May	Jun.	Jul.	Aug.	Sep.	Oct.	Nov.	Dec.
Precipitation [mm]	94.6	70.0	99.8	143.4	128.2	139.8	91.4	15.4	55.8	46.0	191.6	102.4
Soil moisture at 5 cm	0.54	0.54	0.49	0.44	0.51	0.38	0.27	0.21	0.19	0.19	0.39	0.43
Incoming radiation [$W. m^{-2}$]	36.1	51.5	106.9	149.0	178.9	205.9	155.8	181.1	115.2	71.6	35.5	21.9
Air temperature [°C]	5.4	5.2	7.2	8.7	9.6	12.8	14.3	15.6	13.0	9.3	8.0	6.3
Soil temperature at 5 cm [°C]	4.7	4.5	6.6	8.8	10.1	13.0	14.0	14.6	12.7	9.9	7.7	6.0

	2004											
Month	Jan.	Feb.	Mar.	Apr.	May	Jun.	Jul.	Aug.	Sep.	Oct.	Nov.	Dec.
Precipitation [mm]	137.8	95.8	161.0	92.2	50.6	87.6	55.6	171.6	116.4	218.4	44.0	109.6
Soil moisture at 5 cm	0.50	0.47	0.48	0.46	0.28	0.20	0.22	0.26	0.35	0.45	0.42	0.47
Incoming radiation [$W. m^{-2}$]	29.9	59.8	109.1	143.2	208.2	215.1	196.5	156.9	120.8	73.6	32.9	21.5
Air temperature [°C]	5.8	5.5	6.3	7.7	10.5	13.5	13.2	14.4	13.4	8.6	8.5	7.0
Soil temperature at 5 cm [°C]	4.9	5.5	5.6	7.6	10.1	12.6	12.7	13.6	12.6	9.2	8.3	6.8

The maximum daily rainfall in 2002 was 40 mm. day⁻¹ (20th October), while it was 57 mm. day⁻¹ in 2003 (13th April) and 52 mm. day⁻¹ in 2004 (12th March) (Figure 2.17). We note that summer months of the three years have continuous periods of days with no rain at all. The rainfall regime for the winter is characterized by long duration events of low intensity.

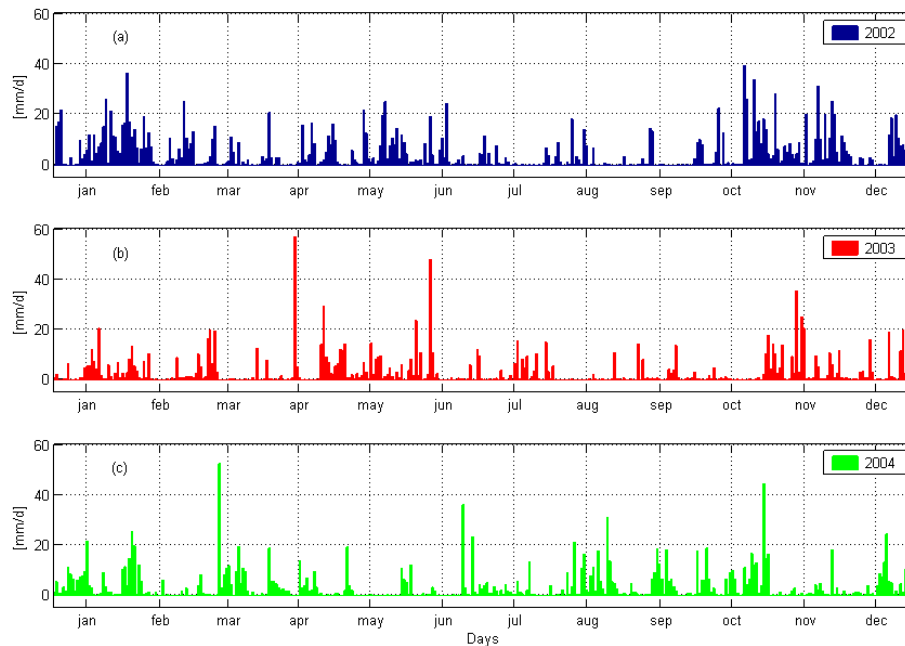


Figure 2.17: Daily precipitation in mm for (a) 2002, (b) 2003 and (c) 2004.

2.4.2 Soil moisture

The volumetric soil moisture in the topsoil at 5 cm (Figure 2.18) shows that during the period from November to May, levels are near saturation at approximately 0.6 m³. m⁻³, and from May to October, the levels fall to 0.2 m³. m⁻³.

Near surface soil moisture shows a strong relationship with precipitation and has a fast response to rain events. Soil moisture in 2003 and 2004 is lower than in 2002 in correspondence with rainfall amounts.

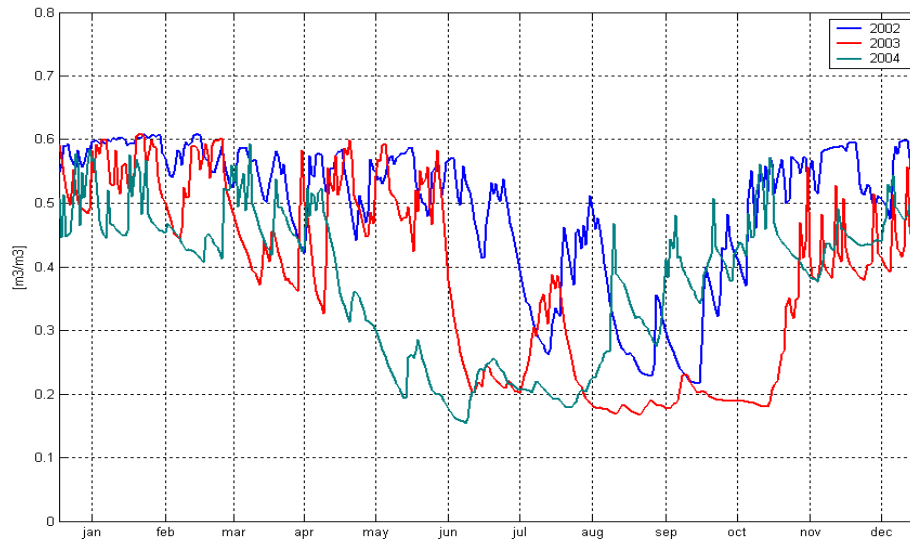


Figure 2.18: Daily soil moisture in $\text{m}^3 \cdot \text{m}^{-3}$ at 5 cm depth, for 2002, 2003 and 2004.

2.4.3 Incoming radiation

The incoming radiation is quite similar for the three years of study (Figure 2.19). The annual averages are respectively 104, 109 and 114 $\text{W} \cdot \text{m}^{-2}$. The incoming radiation is linked the photosynthetic photon flux (Q_{par}). Q_{par} is the fraction of the solar radiation used by the plants for the photosynthesis.

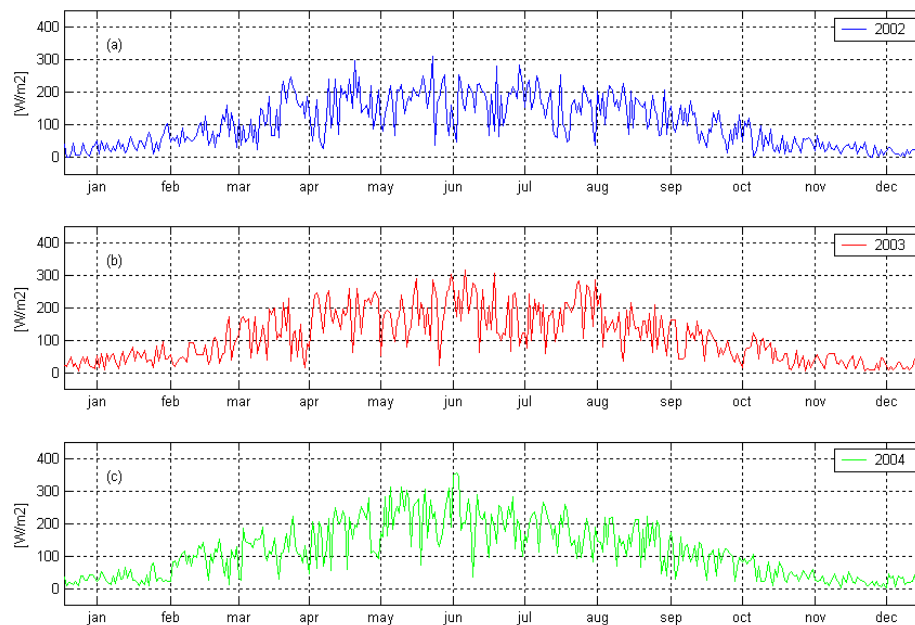


Figure 2.19: Daily incoming radiation, in $\text{W} \cdot \text{m}^{-2}$ for (a) 2002, (b) 2003 and (c) 2004.

2.4.4 Air and soil temperature

The daily air temperatures have a small range of variation (Table 2.2).

Table 2.2: Minimum and maximum daily temperatures in °C.

	2002	2003	2004
Minimum T _{air} (°C)	1.6 (10 th Dec.)	0.4 (4 th Jan.)	0.3 (29 th Jan.)
Maximum T _{air} (°C)	17.4 (5 th Aug.)	19.6 (5 th Aug.)	17.9 (7 th Sept.)

The soil temperature at 5 cm depth follows the same pattern as air temperature (Figure 2.20); however, the amplitude of soil temperature is smaller as soil has a bigger inertia than the air.

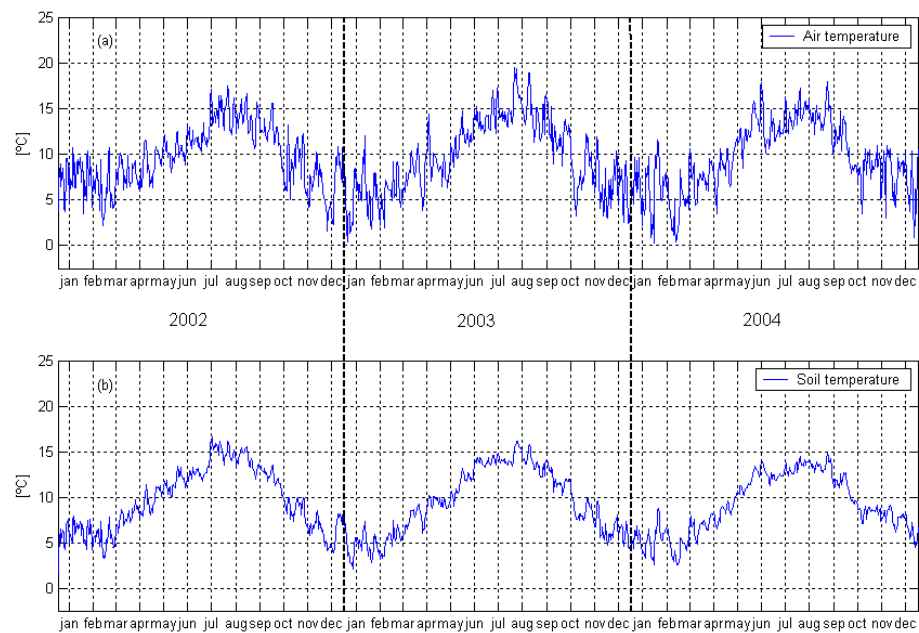


Figure 2.20: Daily (a) air temperature and (b) soil temperature in °C, for 2002, 2003 and 2004.

There are very few days with temperatures under 4°C (the lower threshold temperature for the photosynthetic process).

Chapter 3

Methods

Chapter 3

Methods

3.1 Observations

3.1.1 Eddy covariance method and footprint

The Eddy Covariance or Eddy Correlation (EC) method is a statistical tool, used to analyse time series of high frequency wind and scalar atmospheric data [Baldocchi, 2003], to yields values of fluxes of these properties representing large areas ($\sim 1 \text{ km}^2$, Campbell and Norman, 1998).

The atmosphere near the earth's surface is almost always turbulent, and trace gases are rapidly diffused to (or from) the surface by irregular or random motions generated by wind shear and buoyancy forces [Dabberdt et al., 1993]. The boundary layer defined by Garatt, [1992], is the layer of air directly above the Earth's surface in which the effect of the surface (friction, heating and cooling) are felt directly on time scales less than a day, and in which significant fluxes of momentum, heat or matter are carried by turbulent motions on a scale of the order of the depth of the boundary layer or less.

Transport in the boundary layer of heat, moisture, momentum and pollutants are governed almost entirely by turbulence [Campbell and Norman, 1998]. Using Reynolds decomposition, it is possible to quantify turbulent transport given a high enough sampling rate and fast response instruments [Garatt, 1992]. At the Dripsey flux site, near Cork, two separate EC systems were used for the CO_2 and N_2O flux measurements. All concentrations and wind speeds were logged at 10 Hz and flux values were calculated at 30-minute intervals.

For instance, the flux F_c of carbon dioxide is given by [Webb et al., 1980; Guenther and Hills, 1998; Baldocchi, 2003]:

$$F_c \cong -\overline{w' \rho_c'} \quad \text{Eq. 3.1}$$

where ρ_c' is the density fluctuation of CO_2 gas (mol. m^{-3}), measured with the LI-7500 at 10 Hz, and w' is the vertical wind velocity fluctuation (m. s^{-1}) measured at 10 Hz speed, given by the sonic anemometer (see section 3.1.2).

The EC method depends on turbulence to carry scalar entities (e.g. trace gases) past the measurements sensors and roughly mix the air so that the scalar of interest does not accumulate in the canopy air space [Campbell and Norman, 1998; Dorsey, 2002]. The area of the ground actually sensed in a tower-based flux measurement is known as the sampled footprint [Hsieh et al., 1997; Schmid, 2002]. The fetch is the upwind horizontal distance from

the sensor to the edge of the area contributing to the measured flux [Hsieh et al., 1997; Schmid, 2002; Dorsey, 2002]. Each of these terms, even though slightly different in exact meaning, describes the characteristics of the upwind area, which is expected to influence most of the downwind measurements at a certain height. Hsieh et al. [2000] found that the height to fetch ratio is about 1:100, 1:250, and 1:300 for unstable, neutral, and stable conditions, respectively. The atmospheric conditions that occur the most often are unstable conditions.

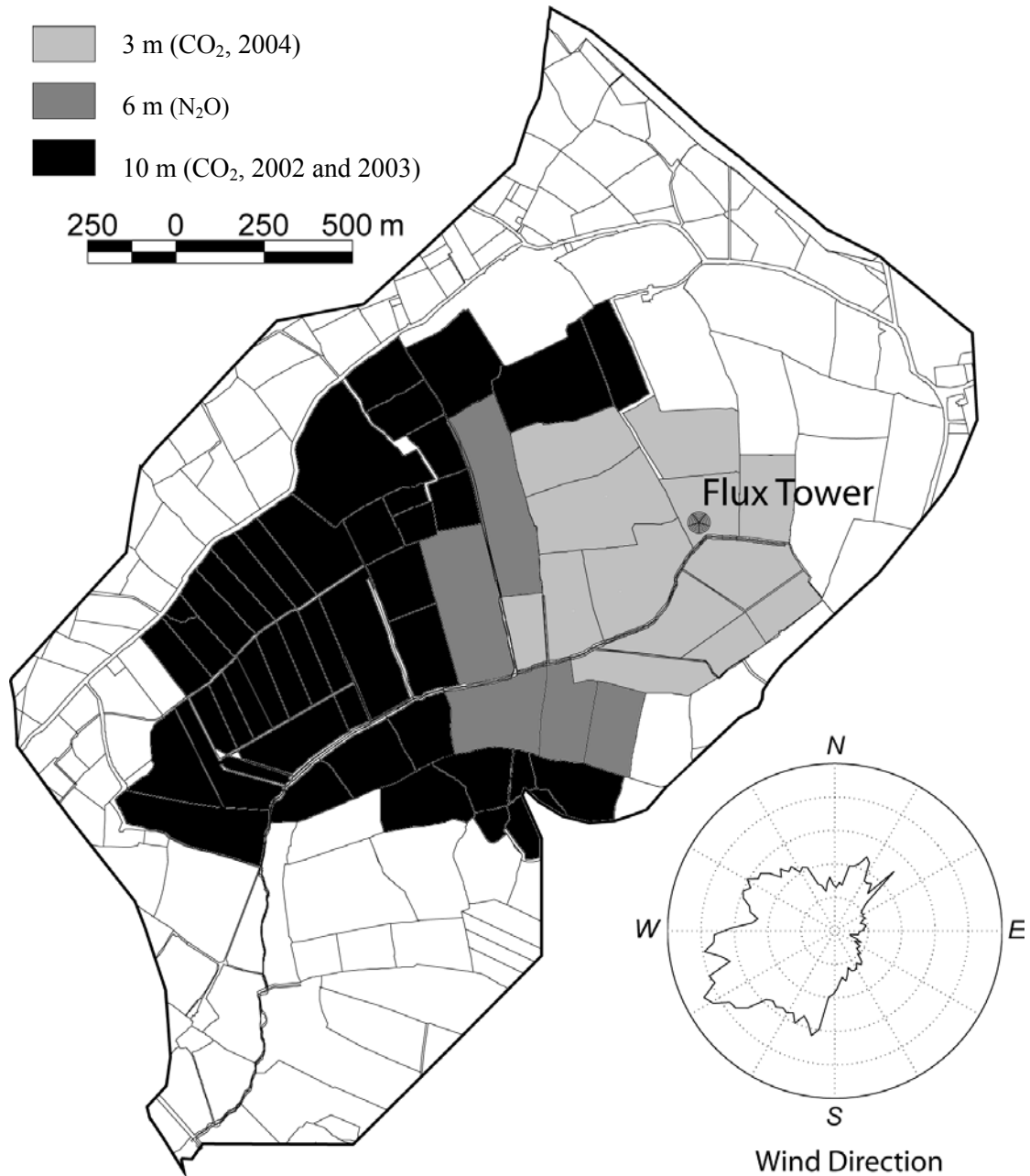


Figure 3.1: Map of the grassland catchment with eddy covariance tower location and the shaded fields indicative of the flux footprint depending on the height of the sensors. There are many small fields in the footprint varying in size from 1 to 5 ha. The prevailing wind direction is from the southwest.

The wind direction histogram changes with the time, so the footprint is shaped according to the wind direction and speed. To calculate the footprint, we applied 1:100 height to fetch ratio, combined with information from the probability density function of the wind direction [Hsieh et al., 2000]. The map of the tower with footprint is shown in Figure 3.1.

The CO₂ / H₂O sensor was mounted at a height of 10 m in 2002 and 2003 and then at 3 m above ground level; and the N₂O sensor intake was mounted 6 m above ground. Although the CO₂ footprint was larger (for 2002 and 2003) and then smaller (for 2004) than the N₂O footprint, the homogeneity of the landscape and the similarity of agricultural management practices across the entire site ensure that comparisons between the two are valid.

3.1.2 Carbon dioxide

Instrumentation

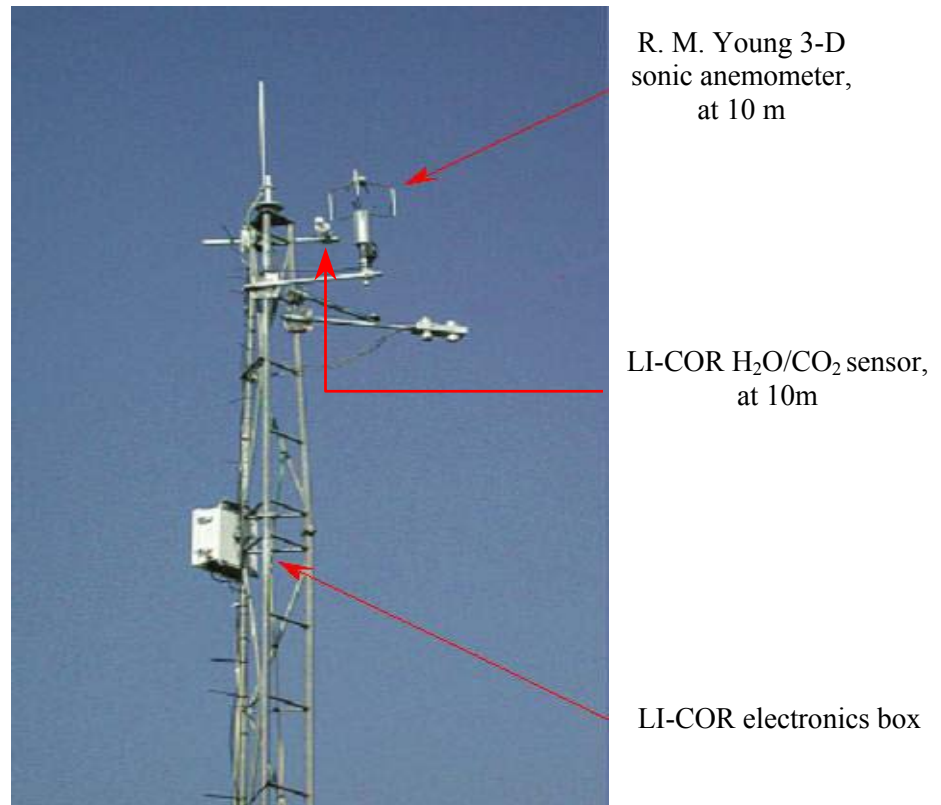


Figure 3.2: Top section of meteorological / EC tower.

The LI-COR CO₂ / H₂O gas analyser and the R. M. Young 3-D sonic anemometer were installed in June 2001 at a height of 10 m. Figure 3.2 shows their position on the tower. On 22nd December 2003 the position of the sonic anemometer and the CO₂ / H₂O sensor were moved from 10 m down to 3 m.

Open path CO₂ / H₂O gas analyser



Figure 3.3: LI-7500 Open path CO₂/ H₂O gas analyser (from LI-COR manual).

Carbon dioxide (CO₂) and water vapour (H₂O) densities in the turbulent air are monitored by a LI-7500 Open Path CO₂ / H₂O non-dispersive, absolute infrared gas analyser from LI-COR (Figure 3.3). In the eddy covariance technique, this data is used in conjunction with sonic anemometer air turbulence data to determine the fluxes of CO₂ and H₂O [LI-COR, 2001]. A high frequency (10 Hz) and high precision analyser such as LI-7500 is needed to correctly sample the turbulent eddies in the lower boundary layer [Garatt, 1992]. The sensor head has a smooth, aerodynamic profile, in order to minimize flow disturbance.

The open path analyser eliminates time delays, pressure drops, and sorption/desorption of water vapour on tubing employed with a closed path analyser [LI-COR, 2001]. The LI-7500 is placed within about 20 cm of the centroid of the air volume measured by the sonic anemometer.

The LI-7500 sensor head has a 12.5 cm open path, with single-pass optics and a large 1 cm diameter optical beam. The LI-7500 operates over a temperature range of -25°C to +50°C. Figure 3.4 shows a cutaway representation of the LI-7500 sensor head [LI-COR, 2001]. The infrared (IR) source emits radiation, which is directed through a chopper filter wheel, focusing lens, and then through the measurement path to a cooled lead selenide detector. Focusing the radiation maximizes the amount of radiation that reaches the detector in order to provide maximum signal sensitivity.

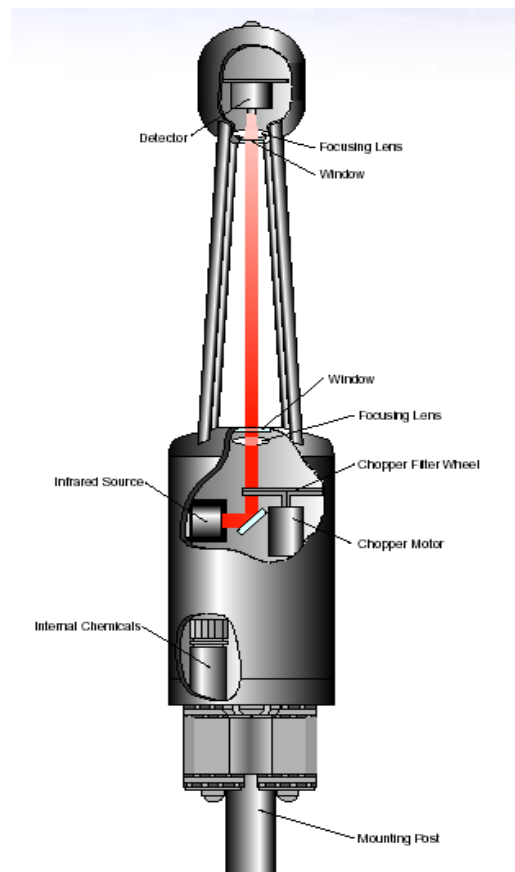


Figure 3.4: Cutaway representation of the LI-COR (from LI-COR manual).

The detector operates approximately as a linear quantum counter; that is, over much of its range the detector signal output is proportional to the number of photons reaching the detector. The existence of certain gas on the IR path reduces the photon flux reaching the other side. Each absorbing gas reacts at a different wavelength of photon. Absorption at wavelengths centred at 4.26 μm and 2.59 μm provide for measurements of CO_2 and water vapour, respectively. Reference filters centred at 3.95 μm and 2.40 μm provide excellent rejection of IR radiation outside the desired band, allowing the analyser to reject the response of other IR absorbing gases. Source and detector lifetimes are greater than 20,000 hours. A brush less chopper motor rotates the chopper wheel at 9000 rpm. The windows at both ends of the optical path are made of sapphire, which is extremely hard and starch resistant, allowing for worry-free of dirt and dust accumulation.

Ultrasonic anemometer (see section 2.3.4)

PAR (Photosynthetic Active Radiation) sensor

The photosynthetic photon flux or photosynthetic active radiation (PAR) is easily calculated with the incoming solar radiation, given some approximations [Campbell and Norman, 1998]:

- the energy content of photons is the same for all wavelengths. It is equal to the energy content of photons at the mean wavelength of the spectrum (green, 0.55 μm) that is $3.6 \times 10^{-19} \text{ J. photon}^{-1}$ ($= 0.217 \text{ J. } \mu\text{mol}^{-1}$).
- about 45% of the incoming solar radiation are in the PAR wavelength.

Then,

$$Q_{PAR} = \frac{0.45 \times E_{(inco\ min\ gsolar)}}{0.217} = \left[\frac{W}{m^2} \times \frac{\mu\text{mol}}{J} \right] = \left[\frac{\mu\text{mol}}{m^2 \times s} \right] \quad \text{Eq. 3.2}$$



Figure 3.5: PAR LITE (Kipp & Zonen).

In order to avoid those approximations, a sensor was used for the photosynthetic flux: PAR LITE from Kipp & Zonen (Figure 3.5). The sensor measures the PAR directly in $\mu\text{mol. m}^{-2}. \text{s}^{-1}$. For the periods when the instrument did not perform well, Q_{par} was approximated as explained above. The PAR Lite is

specifically engineered to measure PAR under naturally occurring daylight. The optical filter of the PAR Lite is designed to deliver a quantum response from 400 to 700 nm [Kipp and Zonen, 2001], which is the same spectral region responsible for stimulating plant photosynthesis [Campbell and Norman, 1998]. PAR LITE uses a photodiode sensor, which creates a voltage output that is proportional to the incoming radiation from the entire hemisphere. An especially optical filter has been designed to provide a quantum response in the PAR (between 0.4 and 0.7 μm).

Filtering and gap-filling

All CO_2 fluxes were adjusted using the Webb correction [Webb et al., 1980]. As eddy covariance performed poorly during rain events, a precipitation filter was used to screen out unsatisfactory flux data. Using an incoming solar radiation threshold of $20 \text{ W} \cdot \text{m}^{-2}$, the data were then partitioned into daytime and nighttime sets. The wind speeds from the sonic anemometer were double rotated such that the mean vertical wind speed was set to zero.

In periods of high atmospheric stability, there is a lack of turbulent mixing near the soil surface and the eddy covariance technique does not always yield reliable results. Nocturnal fluxes corresponding to u_* (frictional velocity) less than $0.2 \text{ m} \cdot \text{s}^{-1}$ were excluded [Pattey et al., 2002; Baldocchi, 2003] and replaced by a regression exponential function of the soil temperature [Jaksic, 2004]. The daytime data was sorted bi-monthly and we further filtered fluxes that exceeded predetermined realistic threshold values for the season. For each two-month period, a different regression relationship was developed between the good daytime CO_2 fluxes and Q_{par} . The regression used the Mysterlich formula [Falge et al., 2001] for the relationship between CO_2 flux and Q_{par} . These relations were then used to gap-fill daytime CO_2 fluxes. After post-processing and filtering of spurious data, 57% of the CO_2 flux data were suitable for analysis. The unsuitable 43% was replaced by modelled (empirical regression) data.

3.1.3 Nitrous Oxide

Instrumentation

The second EC system consisted of a tunable diode laser (TDL) trace gas analyser (TGA100a, Campbell Scientific, USA) to measure high frequency N_2O concentrations and a

3-D sonic anemometer (CSAT-3, Campbell Scientific, USA) to measure high frequency wind speeds.



N₂O intake and CSAT-3
sonic anemometer, at 6 m.

Figure 3.7: Tower, with the N₂O intake and CSAT-3 sonic anemometer, at 6 m.

Closed path TDL trace gas analyser

The principle of a TDL trace gas detection is the absorption of the infrared laser beam through a path containing a gas sample. Molecules possess quantized internal energy levels enabling them to absorb radiation at discrete frequencies. This allows for the detection of the molecule of interest in the gas sample [Edwards et al., 2003].

The total absorption depends on the number of absorbing molecules in the beam and is described by Beer's law:

$$I(\nu_i) = I_0(\nu_i) \exp(-\sigma_\nu NL) \quad \text{Eq. 3.3}$$

where $I(\nu_i)$ is the measured laser intensity at a discrete frequency interval (ν_i) on the absorption line, $I_0(\nu_i)$ the unabsorbed laser intensity, σ_ν is the absorption cross-section ($\text{cm}^2 \cdot \text{molecule}^{-1}$), N the concentration of absorbers ($\text{molecules} \cdot \text{cm}^{-3}$), and L is the path length (cm).

The absorbance $A(\nu_i)$ and the transmittance $T(\nu_i)$ can be defined using Eq. (3.4) as follows:

$$A(\nu_i) = -\ln T(\nu_i) = -\ln \frac{I(\nu_i)}{I_0(\nu_i)} = \sigma_{\nu} N L \quad \text{Eq. 3.4}$$

A linear regression of sample absorbance vs. reference absorbance gives their ratio (D). It is necessary to assume that the temperature and the pressure are the same for the reference and the sample gases; it allows the concentration of the sample (C_S) to be calculated by:

$$C_S = \frac{C_R * L_R * D}{L_S + L_A (1 - D)} \quad \text{Eq. 3.5}$$

where C_R is the concentration of reference gas (ppm), L_R , the length of the short reference cell (cm), L_S , the length of the short sample cell (cm), L_A , the length of the long sample cell (cm). The trace gas concentration is calculated of each scan and then digitally filtered to reduce noise.

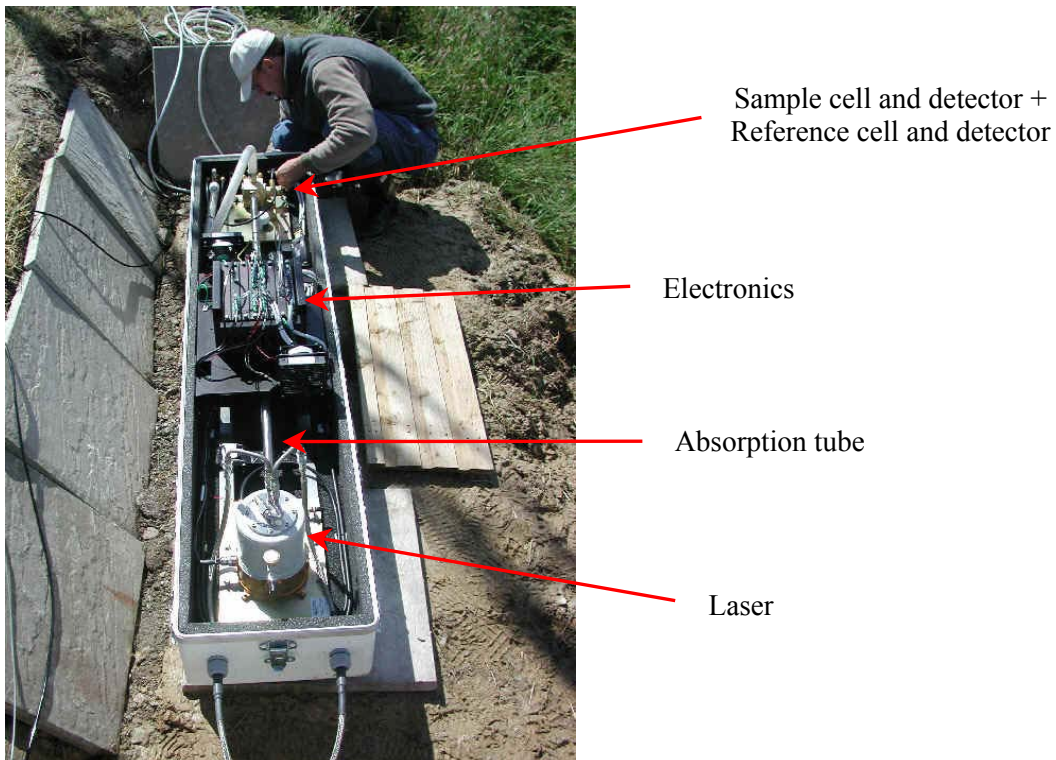


Figure 3.8: Closed path TDL trace gas analyser (TGA100a, Campbell Scientific, USA).

The TGA100a (Campbell Scientific, USA) is composed of a laser system, an optical and gas measurement assembly, and a computer-controlled electronic system, which controls both the laser frequency and data acquisition (see Figure 3.8). It uses a reference gas cell to

maintain its calibration in situ. The air sample intake is mounted on the tower with the sonic anemometer at 6 m above ground. Tubing connects the air sample intake to the inlet of a PD1000 high flow sample air dryer [Campbell, 2005]. The TGA100a analyser is located near the tower to minimize the length of the sample tubing. This minimizes the attenuation of high frequencies in the concentration data caused by tube flow [Campbell, 2005].

The advantage of using tunable diode lasers in infrared absorption spectroscopy is that typical laser emission line widths are small ($\sim 10^{-4} \text{ cm}^{-1}$) relative to typical absorption line widths. Thus, the laser can be tuned over the entire absorption features, allowing the high spectral resolution needed to resolve individual absorption lines at low pressures without interference by other gases [Edwards et al., 2003].

3-D sonic anemometer

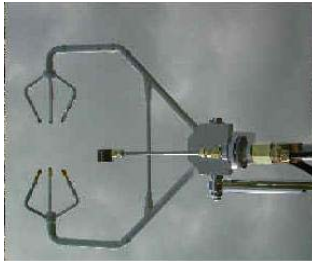


Figure 3.9: CSAT-3, 3-D sonic anemometer.

The 3-D sonic anemometer (CSAT-3, Campbell Scientific, USA), represented in Figure 3.9 [Campbell, 1998] and used in the EC system to measure N_2O fluxes is based on the same principles as the one from R. M. Young used for CO_2 flux measurements.

Filtering and gap-filling

The angular offset of the N_2O anemometer was negligible; therefore co-ordinate rotation was not necessary in this case. The time lag due to the distance travelled by the air sample to the N_2O analyser was determined by calculating the peak correlation between vertical wind speeds and N_2O concentrations [Laville et al., 1999]. A stationarity test based on that of Foken and Wichura, [1996] was used to filter spurious N_2O flux values. N_2O flux values were discarded when the mean of the vertical wind velocity was unsteady within a half-hour period [Leahy et al., 2004]. For the purpose of computing cumulative sums of N_2O flux, gaps of length less than four days were filled by interpolating values from neighbouring days. The two longer gaps (due to instrument downtime) were filled using a 14-day moving average.

3.2 Simulation model

3.2.1 Model description

The model used in this study is PaSim 3.6 (v5) [Riedo et al., 1998; Riedo et al., 1999; Riedo et al., 2000; Riedo et al., 2001; Schmid et al., 2001; Riedo et al., 2002, Vuichard et al., 2005 (manuscript in preparation)]. The first version was described in Riedo et al., [1998]. PaSim is a process-based, meteorologically driven biogeochemical model to simulate fluxes of carbon, nitrogen, energy and water.

Five submodels

The model has five submodels: soil physics; soil biology; plant; microclimate; and animal (Figure 3.10).

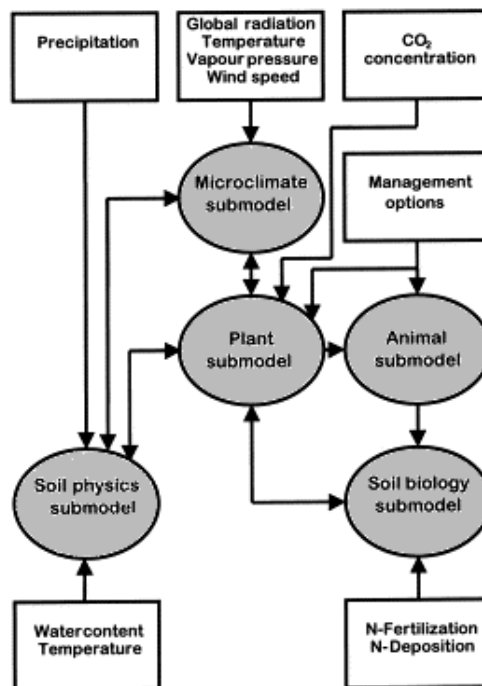


Figure 3.10: PaSim. submodels, driving variables, and internal fluxes of carbon (C), nitrogen (N) and water [Riedo et al., 2000].

The soil physics submodel is used to calculate the water content in different soil layers, which determines photosynthesis and stomatal conductance, soil evaporation, and rates of biological processes, and to calculate soil temperature in the different layers, which influences belowground plant processes, soil heat flux, and soil biological processes.

The soil biology submodel is based on the “soil and decomposition” and “nitrogen” submodels of the CENTURY model [Parton et al., 1987]; the submodel computes the concentration of soil nitrogen (N), as ammonium and nitrate, and the concentration of soil carbon (C) available for the plant. The plant submodel is based on the pasture submodel of the HP-model [Thornley, 1998], which simulates shoot and root growth in relationship to carbon and nitrogen uptake, energy fluxes and soil moisture conditions.

The microclimate submodel is used to calculate the interception of short-wave radiation in the canopy, especially PAR (photosynthetically active radiation) absorbed by the leaves; and to calculate the energy balance of the canopy and of the soil surface (this will set surface conditions for the soil physics submodel and the leaf temperature for the plant submodel). The animal submodel for grazing by dairy cows has been added in PaSim 2.5 [Riedo et al., 2000].

Meteorological input data

This model is driven with hourly meteorological input data for: radiation; air temperature; vapour pressure; wind speed; precipitation and atmospheric concentration of CO₂ and ammonia (NH₃). PaSim integrates the land management practices of grass cuttings, grazing and the nitrogen application of fertilizer and slurry.

All the meteorological input data were measured on site (see Chapter 2 for the description of the instruments), except for the concentration of atmospheric CO₂ and NH₃, which were taken as constants (concentrations of respectively 370 ppm and 2 µg NH₃. m⁻³) from the literature [IPCC, 2001; Seinfeld, 1986]. Actual vapour pressure, in kPa, can be calculated (Equation 3.6) using the relative humidity of the air (RH, that is measured on site) and saturation vapour pressure, calculated as in Equation 3.7 [FAO, 1998]:

$$e_a = \frac{RH \times e_s}{100} \quad \text{Eq. 3.6}$$

The saturation pressure can be calculated [FAO, 1998]:

$$e_s = 0.6108 \times \exp\left(\frac{17.27 \times t_a}{t_a + 237.3}\right) \quad \text{Eq. 3.7}$$

where t_a [°C] is air temperature.

Outputs

The model outputs include the fluxes of CO₂, N₂O and CH₄. The time step of output chosen here is daily. CH₄ and N₂O fluxes are directly computed by PaSim. The model computes gross primary production (GPP) and the total respiration of the ecosystem (R_{tot}), NEE is then the difference between the two. R_{tot} is the sum of respiration of the soil, the plants and the grazing animals. Here soil respiration is defined as microbial respiration only. Other outputs like shoot dry matter, concentrations of carbon or nitrogen in the plant and in the soil are also considered.

3.2.2 Model parameterisation

Site specific parameters

Physical parameters

In Table 3.1 are reminded the physical parameters of Dripsey site, for PaSim model.

Table 3.1: Physical characteristics of the site.

Latitude N	0.907 rad
Slope	0.044 rad
Aspect	0.0 rad
Altitude above sea level	200 m
Soil type	Sandy clay loam

Soil parameters

The majority of the soil parameters need to be defined for each of the soil layers. The number and the thickness of layer from the knowledge of the soil profile can be determinant for achieving sensible model results. The maximum number of layer is six, but we decided to divide the vertical soil profile in three layers: layer 1 from 0 to 2 cm; layer 2 from 2 cm to 20 cm; layer 3 from 20 cm to 60 cm. The soil-rock interface was set at 2 m for modelling purposes. The top layer is very important, as it is the interface between the soil and the atmosphere. It needs to be very thin: 2 cm compared with 18 and 40 cm [Mengelkamp et al., 1999]; its small thickness allows quick responses of energy fluxes to rainfall events for instance [Liang et al., 2003].

Some soil parameters were determined from soil samples taken from the top 20 cm of soil and from 20 to 40 cm within the flux tower footprint. Other soil parameters were adapted from the literature or determined as a result of optimisation of PaSim results and fall within the range of literature values (Table 3.2).

Table 3.2: Soil parameters.

^a Soil pH	5.6
^a Main rooting depth (m)	0.25
^a Sand:Silt:Clay (%)	42:41:17
^a Depth of the 3 layers (m)	0.02; 0.20; 0.60
^a Bulk density (g/cm ³)	1.0; 1.0; 1.7
^a Saturated soil water content (m ³ /m ³)	0.60; 0.43; 0.40
^b Air entry potential (mm)	-50.0; -100.0; -100.0
^b Saturated hydraulic conductivity (mm/day)	188.0; 18.0; 18.0
^c Parameter b	5.4
^a Soil samples; ^b Literature [Dingman, 1994] and model optimisation; ^c Clapp and Hornberger, 1978.	

The dominant grass species is perennial ryegrass, but the model does not take into account the species of grassland; it has been parameterized for perennial grassland. The estimated clover fraction is 25%.

Initial conditions

Initial conditions for organic carbon and nitrogen

The soil biology submodel used in PaSim is derived from the CENTURY model [Parton et al., 1987]. Organic C and N are divided among metabolic and structural pools of plant residue and among three soil organic matter (SOM) pools (active, slow and passive). The metabolic pool is decomposable plant material and the structural pool is resistant plant material. The C and N in the passive pool are physically or biochemically protected with a turnover time of 1000 to 5000 years [Parton et al., 1987]. At the other extreme, more active organic matter cycles more rapidly (6 to 12 months). The material in the slow pool has an intermediate residence time (10 to 50 years). As a simplification, no separation between soil surface and soil plant surface is considered. In addition, no soil profile of the soil carbon and

nitrogen is calculated and only soil carbon and nitrogen in the main rooting depth is considered.

For the first run, we used the values given in Gardiner and Radford, [1980]. Then, to run the model in a steady state, initial condition (IC) values for the concentrations of carbon and nitrogen in the different pools were those obtained at the end of a corresponding equilibrium run (Table 3.3). Equilibrium was reached when the change in C and N levels in the various pools was smaller than a prescribed threshold (here, the convergence criterion was reached when the change in the variables between two cycles was less than 2.5%). There is no initial condition for structural nitrogen in the dead plant matter; it is derived from the metabolic nitrogen in the plant residue and the flow of plant residue according to Parton et al., [1987].

The values at the end of the equilibrium run gave a very good estimation of the CO₂ fluxes, but a poor estimate of the N₂O fluxes. The modelled N₂O fluxes were too small in comparison with the measurements. In order to improve this, we increased the amount of carbon by 15% and multiply the amount of nitrogen by 2.4 (Table 3.3). With this parameterisation, the NEE stayed the same and the N₂O emissions were closer to the observations. With this new set of initial conditions, the model is not run in a steady state, however, because this grassland site is said to be over-fertilised, the soil may not be in equilibrium in terms of carbon and nitrogen.

Table 3.3: Equilibrium run and initial conditions values for organic carbon and nitrogen in various pools.

	End of equilibrium run		Initial conditions	
	Carbon (kgC. m ⁻²)	Nitrogen (kgN. m ⁻²)	Carbon (kgC. m ⁻²)	Nitrogen (kgN. m ⁻²)
^a Wstruct	1.6929	-	1.9468	-
^b Wmetab	0.1094	0.0098	0.1258	0.0235
^c Wactive	0.3045	0.0426	0.3502	0.1022
^d Wslow	5.7013	0.3781	6.5565	0.9074
^e Wpassive	5.0535	0.4548	5.8115	1.0915

^aStructural dead plant material; ^bMetabolic dead plant material; ^cActive SOM; ^dSlow SOM; ^ePassive SOM.

The plant submodel includes C and N variables (Table 3.4); the values are the same as in Riedo et al., [1998].

Table 3.4: Initial conditions for plant carbon and nitrogen.

IC for plant C substrate concentration (kgC. kg ⁻¹)	0.04
IC for plant N substrate concentration (kgN. kg ⁻¹)	0.004
IC for N concentration of structural plant dry matter (kgN. kg ⁻¹)	0.022

Others initial conditions

The initial conditions for the soil water moisture for the different layers and the lower boundary layer were set from the measurements of the soil moisture probes. The parameters for the soil temperature were derived from the measurements of the soil temperature probes. In PaSim, the mineral N pool is split into components for ammonium (NH₄⁺) and nitrate (NO₃⁻) in the soil. Their concentration and atmospheric deposition were those from Jordan, [1997] for Cork Airport. Table 3.5 presents those values. Finally, initial conditions for leaf area index (LAI), shoot and root dry matter (DM) are also given in this table.

Table 3.5: Initial conditions for shoot and root dry matter, LAI, soil water content, soil temperature and ammonium and nitrate.

IC of shoot dry matter (kg. m ⁻²)	0.15
IC of LAI (m ² . m ⁻²)	1.5
IC of root dry matter (kg. m ⁻²)	0.58
IC for soil water content (m ³ . m ⁻³)	0.60; 0.40; 0.40
Water content of lower soil boundary layer in spring (m ³ . m ⁻³)	0.45
Water content of lower soil boundary layer in autumn (m ³ . m ⁻³)	0.28
Average temperature of lower soil boundary layer (K)	281.66
Amplitude of temperature of lower soil boundary layer (K)	4.0
Phase of temperature of lower soil boundary layer (rad)	3.1416
IC for soil ammonium (kgN. m ⁻²)	0.00029
IC for soil nitrate (kgN. m ⁻²)	0.00027
NH ₄ ⁺ deposition other than gaseous NH ₃ (kgN. m ⁻² . day ⁻¹)	1.02*10 ⁻⁶
NO ₃ ⁻ deposition (kgN. m ⁻² . day ⁻¹)	0.95*10 ⁻⁶

Management Data

The footprint area is partitioned into approximately fifty small fields. This implies a degree of heterogeneity (particularly in summer) that cannot easily be addressed directly by the model, even if the management practices described in Chapter 2 are broadly similar across

the whole site. As a consequence, some assumptions were made; first of all, we simplified the modelling exercise by using a single point simulation.

Silage cuts

In the farmers' data log sheets, there is very little information on the timing of the silage cuts; so we determined the dates by comparison with the measurements of the CO₂ fluxes. Linked with the input data for the timing of the silage cuts, the LAI and the shoot dry matter after cutting can be set. If there are different dates for the different years of simulation, only one set of values for LAI and shoot DM is available. Thus, those values are applied to the position of the cut in the year. Furthermore, in order to preserve the fact that usually a field reserved for silage is cut twice a year and to account that the fields are not all the fields are cut at the same time, we applied different LAI and shoot DM after cutting (see Table 3.6).

Table 3.6: LAI and shoot dry matter after cutting and time of the cuttings.

Shoot DM after cutting (kg. m ⁻²)		0.35	0.15	0.40	0.20	0.15
LAI after cutting (m ² . m ⁻²)		3.0	1.0	4.0	1.5	1.5
Time of cut	2002	1 st July	15 th July	23 rd Sept.	30 th Sept.	30 th Dec.
	2003	15 th June	30 th June	8 th Sept.	30 th Sept.	30 th Dec.
	2004	30 th May	19 th July	8 th Sept.	27 th Sept.	30 th Dec.

Moreover, the current version 3.6 (v5) of the model is known to produce too much biomass in winter, even though an additional stress parameter have been included to account for enhanced mortality in autumn and winter [Vuichard et al., 2005 (manuscript in preparation)]. To compensate for this we therefore include an extra cut at the end of each year to reset the biomass and LAI to realistic values.

Grazing

In Chapter 2, we noted that on site, the animal density is 2.2 LU. ha⁻¹ and that there is a rotation of the cows within the paddocks. For modelling purposes, we assumed that the fields were continuously grazed at a constant density of 1.5 LU. ha⁻¹, from March to the end of September in 2002 and 2004 (because the autumn was wet) and from March to the end of October for 2003. 1.5 LU. ha⁻¹ is less than 2.2 LU. ha⁻¹ in order to account that the model only considers dairy cows and not beef cattle (because 1 LU accounts for a cow of 600 kg and beef

cattle is only a fraction of LU). We tried another scenario with periods of 21 days of grazing at a density of 2.2 LU. ha⁻¹ that alternated with 10-day periods of no grazing. The model produced the same results in terms of methane emissions and NEE. However we decided to keep the first assumption.

Nitrogen fertiliser and slurry applications

The timing of the applications of fertiliser and slurry also varies across the average footprint but we are limited by the model to 10 applications days per year. So we reduced the dates and add the amount of nitrogen corresponding. Figure 3.11 compares the monthly data from the farmers with the input for PaSim model. In 2004, the slurry applications are very low; data may be missing in the farmers' data log sheets.

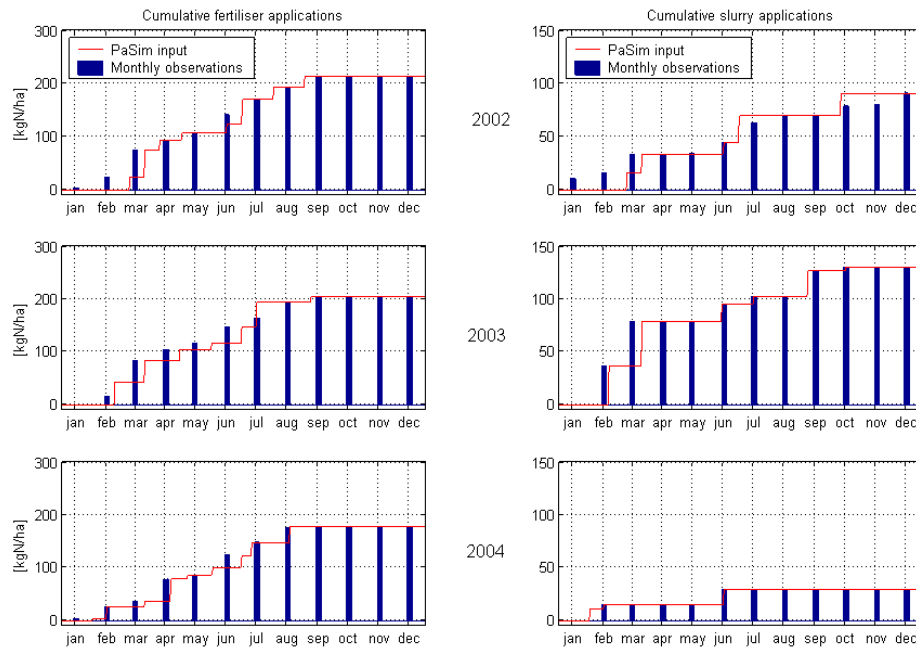


Figure 3.11: Cumulative applications of fertiliser (left column) and of slurry (right column) for 2002, 2003 and 2004. The red curve represents the input for PaSim and the blue bars, the monthly data from the farmers.

For the application of mineral fertilisers, the amount of nitrogen is divided into NH_4^+ NO_3^- . Farmers use different sorts of chemical fertilisers and on average, half of the nitrogen is in ammonia form and the other half in nitrate form. As organic fertilisers, PaSim considers slurry, urea and manure. Here, farmers only apply slurry to the fields. The input data for the fertilisers as well as the other management input data are summarized in Table 3.7.

Table 3.7: Summary of the input data for PaSim for 2002, 2003 and 2004.
The number 500 indicates that nothing is done.

1) tcut – time of the cuttings [julian day]									
182.0	196.0	266.0	273.0	364.0	500.0	500.0	500.0	500.0	500.0
166.0	181.0	251.0	258.0	364.0	500.0	500.0	500.0	500.0	500.0
150.0	200.0	251.0	270.0	364.0	500.0	500.0	500.0	500.0	500.0
2) tfert – time of the application of fertilizers [julian day]									
69.0	84.0	99.0	121.0	166.0	181.0	182.0	213.0	244.0	283.0
51.0	54.0	84.0	119.0	151.0	166.0	181.0	196.0	250.0	288.0
32.0	46.0	84.0	110.0	127.0	152.0	166.0	181.0	191.0	229.0
3) Nfertamm – amount of ammonium for each application of mineral fertilizers [kgN. m⁻²]									
0.00123	0.00248	0.00092	0.00070	0.00086	0.00087	0.00148	0.00115	0.00103	0.00000
0.00000	0.00214	0.00201	0.00109	0.00058	0.00000	0.00159	0.00227	0.00053	0.00000
0.00018	0.00112	0.00049	0.00213	0.00041	0.00072	0.00000	0.00108	0.00125	0.00150
4) Nfertnit – amount of nitrate for each application of mineral fertilizers [kgN. m⁻²]									
0.00123	0.00248	0.00092	0.00070	0.00086	0.00087	0.00148	0.00115	0.00103	0.00000
0.00000	0.00214	0.00201	0.00109	0.00058	0.00000	0.00159	0.00227	0.00053	0.00000
0.00018	0.00112	0.00049	0.00213	0.00041	0.00072	0.00000	0.00108	0.00125	0.00150
5) nanimal – stocking density, or number of livestock units [animal. m⁻²]									
0.00015	0.00000	0.00000	0.00000	0.00000	0.00000	0.00000	0.00000	0.00000	0.00000
0.00015	0.00000	0.00000	0.00000	0.00000	0.00000	0.00000	0.00000	0.00000	0.00000
0.00015	0.00000	0.00000	0.00000	0.00000	0.00000	0.00000	0.00000	0.00000	0.00000
6) tanimal – start of the grazing [julian day]									
60.0	500.0	500.0	500.0	500.0	500.0	500.0	500.0	500.0	500.0
60.0	500.0	500.0	500.0	500.0	500.0	500.0	500.0	500.0	500.0
60.0	500.0	500.0	500.0	500.0	500.0	500.0	500.0	500.0	500.0
7) danimal – duration of the grazing [d]									
214.0	0.0	0.0	0.0	0.0	0.0	0.0	0.0	0.0	0.0
244.0	0.0	0.0	0.0	0.0	0.0	0.0	0.0	0.0	0.0
214.0	0.0	0.0	0.0	0.0	0.0	0.0	0.0	0.0	0.0
8) Nvollquelle – amount of N in slurry [kgN. m⁻²]									
0.00157	0.00180	0.00000	0.00000	0.00105	0.00187	0.00066	0.00000	0.00000	0.00212
0.00362	0.00000	0.00429	0.00000	0.00000	0.00161	0.00000	0.00072	0.00243	0.00036
0.00111	0.00038	0.00000	0.00000	0.00000	0.00000	0.00149	0.00000	0.00000	0.00000
9) Nguellekotarm – amount of N in urea [kgN. m⁻²]									
0.00000	0.00000	0.00000	0.00000	0.00000	0.00000	0.00000	0.00000	0.00000	0.00000
0.00000	0.00000	0.00000	0.00000	0.00000	0.00000	0.00000	0.00000	0.00000	0.00000
0.00000	0.00000	0.00000	0.00000	0.00000	0.00000	0.00000	0.00000	0.00000	0.00000
10) Nmist – amount of N in solid manure [kgN. m⁻²]									
0.00000	0.00000	0.00000	0.00000	0.00000	0.00000	0.00000	0.00000	0.00000	0.00000
0.00000	0.00000	0.00000	0.00000	0.00000	0.00000	0.00000	0.00000	0.00000	0.00000
0.00000	0.00000	0.00000	0.00000	0.00000	0.00000	0.00000	0.00000	0.00000	0.00000

3.2.3 Sensitivity to changes

The uncertainty of the model needs to be estimated by assessing the sensitivity of simulation results to the model parameters and to the initial conditions of the driving variables. This analysis was made in Riedo et al., [1998].

In a first step, the most “sensitive” model parameters were determined. Each parameter was used unchanged or changed by $\pm 25\%$, and for each value a model simulation was carried out using input data from two grassland sites in Switzerland. The parameters were ranked according to the absolute deviation of the simulated annual dry matter yield from the reference simulations, averaged over the two locations and the simulations with $+25$ and -25% of the parameter value. In a second step, the “importance” of the 24 most sensitive parameters was investigated with statistics [Hamby, 1994]. The results are detailed in Riedo et al., [1998] and we will not describe them in here. Indeed, the parameters of the model are written within the codes of the model and we will not change them because the grassland ecosystem in Switzerland (for which the model has been calibrated) is not very different from the grassland in Dripsey and we do not have the knowledge to possibly make the adequate variations in those parameters. Moreover, the major difference between the two sites is climate, and it is defined through the various meteorological input data files.

To investigate the sensitivity of the model to initial conditions, input data which determine the initial values of the state variables of the plant and soil biology submodels were changed by -50 , -25 , $+25$, and $+50\%$. For the plant submodel, the initial values of shoot dry matter and LAI, were changed in parallel, incorporating also the shoot DM and the LAI remaining after each cut. The other initial values for the plant submodel were altered one by one, namely root dry matter, plant C and N substrate concentration and N concentration of structural plant DM. Concerning the soil biology submodel, the initial fractions of the five organic carbon pools in the soil biology submodel were not altered, only a change in their sum (C_{organic}) was assumed. To simulate the sensitivity to different C:N ratios, the initial values of the C:N ratios in the metabolic, active, slow, and passive pools were altered such that the sum of the organic nitrogen associated with changed by approximately -50 , -25 , $+25$, and $+50\%$. In this way, the initial conditions for the state variables for the five organic carbon pools were left unchanged, but the initial values for N metabolic, N active, N slow, and N passive were altered. The soil mineral N pools, for ammonium (N_{amm}) and nitrate (N_{nit}), were altered separately.

Table 3.8: Sensitivity to changes in input data, which determine the initial conditions of state variables of simulated annual yield. ↑ stresses on sensitivity of more than 1% and ↓ stresses on sensitivity of more than 1%.

	- 50%	- 25%	+ 25%	+ 50%
Shoot DM & LAI	↓ -5.7	↓ -1.6	-0.1	-0.5
Root DM	↓ -7.5	↓ -3.5	↑ 3.1	↑ 6.0
Plant C substrate concentration	0.7	0.4	-0.4	-0.8
Plant N substrate concentration	↓ -2.9	↓ -1.4	↑ 1.3	↑ 2.6
N conc. of structural plant DM	↓ -10.6	↓ -4.7	↑ 4.0	↑ 7.5
C _{organic}	↓ -11.3	↓ -5.4	↑ 5.0	↑ 9.6
^a C:N ratio	↑ 28.6	↑ 10.9	↓ -7.4	↓ -12.7
N _{amm}	-0.2	-0.1	0.1	0.2
N _{nit}	-0.2	-0.1	0.1	0.2

^aApproximately -52, -26, 26, 52%

The simulations with altered initial conditions for driving variables of the plant and soil biology submodels revealed a strong influence of the C:N ratio of the soil organic matter on the annual yield (Table 3.8). Other important initial conditions were the total organic carbon in the soil, and the nitrogen concentration of the structural plant biomass. In contrast to all other initial conditions, annual DM yield showed a non-monotonic response to the initial value for the shoot biomass and leaf area index remaining after a cut. A maximum value for annual yield was reached with initial values similar to those determined in the Swiss fields. The uncertainty in the initial value of the living root biomass led to an uncertainty of less than 95% in the annual yield. Considering the large turnover of mineral nitrogen in the soil, the small influence of the initial values of ammonium and nitrate was plausible.

Chapter 4

Greenhouse Gas Balance:

Chapter 4

Greenhouse Gas Balance

4.1 What is a greenhouse gas balance?

The earth's atmosphere contains various trace gases including carbon dioxide (CO₂), methane (CH₄), nitrous oxide (N₂O) and chlorofluorocarbons (CFCs), which absorb infrared radiation emitted from the earth's surface. Higher concentrations of these gases in the atmosphere relate to increased absorption capacity for infrared radiation. Because control of the earth's overall surface temperature depends on a balance between incoming sunlight energy (constant) and re-radiated infrared energy, a net increase in atmospheric absorption of energy causes a net increase in the earth's temperature. This is the cause of the "greenhouse effect" with its associated global warming from additional amounts of greenhouse gases (GHGs).

Some of the GHGs are naturally produced (CO₂ and CH₄) while others (CFCs for instance) are primarily man-made (anthropogenic). In addition to the natural (biogenic) sources of CO₂, N₂O and CH₄, substantial increases of these have occurred over the last century due to anthropogenic sources (especially fossil fuel power plants and man-made management of soils and agricultural lands).

From an agricultural point of view, only CO₂, CH₄ and N₂O will be considered in the greenhouse gas balance. CO₂ is part of the life cycle of the plants; it is fixed through the phenomenon of photosynthesis and is released through the plant's respiration. Depending on the ecosystem, carbon can be fixed or released. Animals contribute through their respiration to a lesser extent to the emissions of CO₂. CH₄ is produced by herbivores as a by-product of enteric fermentation, a digestive process by which carbohydrates are broken down by micro-organisms. CH₄ emissions from soil are not considered in a grassland site, as they are much smaller [CarboEurope-GHG, 2004]. Finally, the soil emits N₂O as a consequence of denitrification and also, to a lesser extent, by nitrification [Trogler, 1999]. The application of slurry and chemical fertilisers increases the supply of reactants for these processes [Leahy et al., 2004]. Figure 4.1 shows the interdependence of GHG fluxes across the ecosystem.

The relative contributions of specific GHGs to global warming also vary. CO₂, N₂O and CH₄ have different radiative forcing. To be able to compare them, their effect is integrated over a period of time and compared to the effect of CO₂, as the latter is the most abundant GHG in the atmosphere. This relative contribution is defined as the global warming potential (GWP). Table 4.1 gives the GWP for CO₂, N₂O and CH₄ over 100-year timescale.

Table 4.1: GWP of CO₂, N₂O and CH₄ for 100-year timescale [IPCC, 2001].

CO ₂	N ₂ O	CH ₄
1	296	23

As a consequence, combining the contribution from each gas over the year to their GWP, the GHG balance for the ecosystem, in CO₂ equivalents (kg CO₂ equiv. m⁻²), can be expressed as:

$$GHG_{Bal} = CO_2 + 296 * N_2O + 23 * CH_4 \quad \text{Eq. 4.1}$$

where CO₂ is in [kg CO₂. m⁻²]; N₂O, [kg N₂O. m⁻²] and CH₄, [kg CH₄. m⁻²].

At present, the greenhouse gas balance arising from grasslands is not known [CarboEurope-GHG, 2004]. In this study, the GHG balance is calculated at the farm scale (~ 50 ha); that is to say, we will not consider: the CH₄ and CO₂ emissions from the cattle when kept indoors, the CH₄ emissions from wastes, the N₂O emissions from leached nitrogen volatilisation and other indirect emissions. A model has been developed for that purpose (FARMSIM, Salètes et al., 2004).

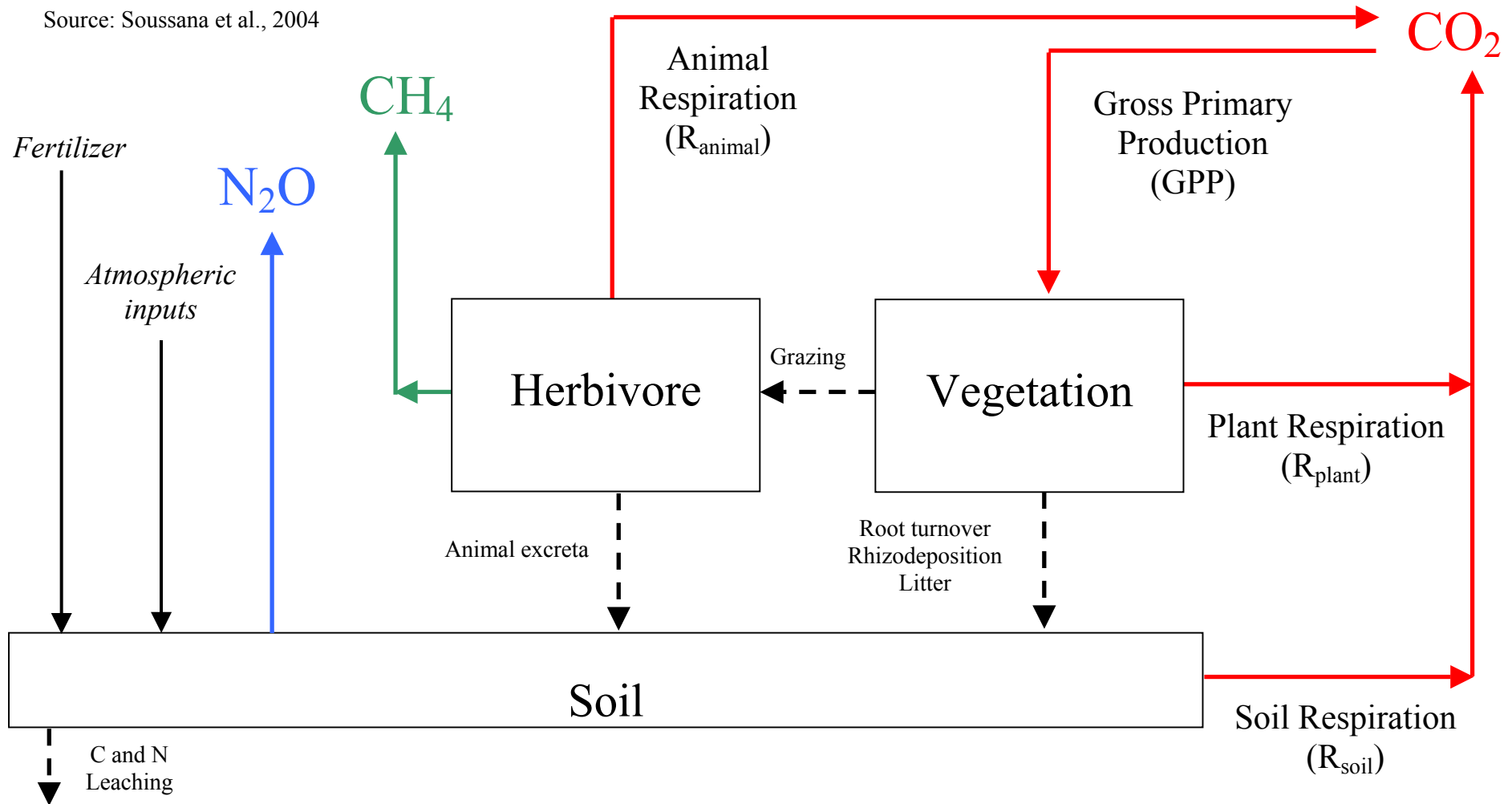


Figure 4.1: Greenhouse gas fluxes and organic matter exchanges for a grassland ecosystem: CO₂ fluxes (red), CH₄ fluxes (green) and N₂O fluxes (blue).

4.2 Carbon dioxide

4.2.1 Comparison of modelled and observed NEE

Figure 4.2 shows the cumulative NEE simulated by PaSim and observed by EC for the three years of study. The vegetation period (roughly April to October) can be divided in an active spring growing phase up to the first major grass cut (see arrow in Figure 4.2), and a less active phase thereafter.

The measured annual uptake is 1.91, 2.59 and 2.95 tC. ha⁻¹ for 2002, 2003, 2004, respectively, whereas the annual uptake computed with PaSim is 2.77, 2.89, 3.71 tC. ha⁻¹ (Table 4.2). Those values fall within the range of values for European grassland (0.5 to 5 tC. ha⁻¹. yr⁻¹, considering the year from June 2002 to June 2003, CarboEurope-GHG, 2004).

For each year of the study, the modelled uptake is higher than the observed. Most of the carbon uptake occurs during the growing season in the months of April, May and June (Figure 4.2). The NEE simulated with PaSim captures the trends during the growing season very well. From June to September, the cumulative NEE shows neither net uptake nor loss, because of land management practices of silage cuttings and intensive grazing. The effects of the silage cuttings are visible as abrupt decreases in the cumulative modelled NEE (see arrows on Figure 2.2). From the end of October to year's end, the cumulative NEE decreases as respiration exceeds photosynthesis.

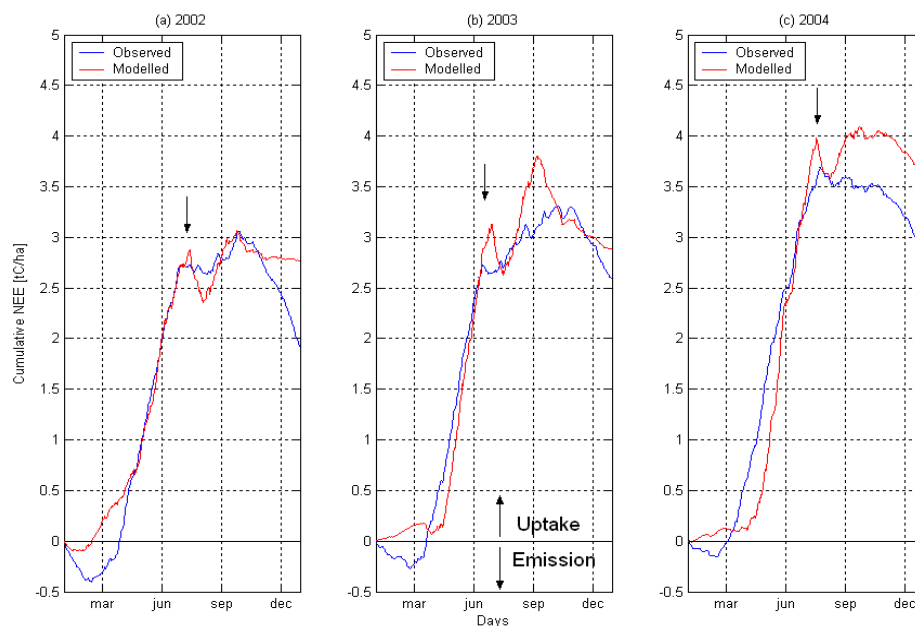


Figure 4.2: Cumulative NEE observed and modelled in tC. ha⁻¹, for: (a) 2002, (b) 2003 and (c) 2004. The arrows represent the first major cut.

Figure 4.2 and Table 4.2 show that the modelled NEE broadly agree with the observations. However, the model overestimates the annual NEE by between 12% and 45%. Better agreement occurs during the growing season, with the rate of change being modelled accurately. PaSim has limitations in the last three months of each year (winter period) where it over predicts the uptake. It is currently acknowledged that PaSim produces too much biomass in winter, and this weakness in the model is currently being investigated [Vuichard et al., 2005 (manuscript in preparation)]. The shape of the curve for the modelled NEE in the first months of 2002 is different from that in 2003 and 2004 (Figure 4.2); this is due to the over-sensitivity of PaSim to initial conditions.

Table 4.2: Comparison of the observed and modelled NEE for 2002, 2003 and 2004.

Annual sum of NEE			
	2002	2003	2004
Observed NEE (tC. ha ⁻¹ . yr ⁻¹)	1.91	2.59	2.95
Modelled NEE (tC. ha ⁻¹ . yr ⁻¹)	2.77	2.89	3.71
% Change	+ 45.0	+ 11.6	+ 25.9
Growing season for observed NEE			
	2002	2003	2004
Starting date (julian day)	79	78	98
Finishing date (julian day)	184	167	204
Length (days)	105	89	106
Gradient (gC. m ⁻² . day ⁻¹)	2.8	3.1	2.7
Growing season for modelled NEE			
	2002	2003	2004
Starting date (julian day)	79	74	74
Finishing date (julian day)	195	180	199
Length (days)	116	106	125
Gradient (gC. m ⁻² . day ⁻¹)	2.1	2.8	3.1

To compare the evolution of NEE during the growing season of each year, it is necessary to define the start and end dates of the season. The start date of the growing season varies within a fifteen-day period from year to year. As there is no standard definition, we choose a growing season start date when the soil temperature at 7.5 cm depth is consistently above 6°C. However, the growth of the grass sometimes may begin before this date (Keane and Collins, 2004). The end of the growing season is defined as the day of the first grass cut. In the observations, the growing season lasts between 89 and 106 days and in the model it is between 112 and 131 days (Table 4.2). The gradient of the cumulative NEE curve represents the rate of change NEE. During the spring growing season, the gradient of uptake for the

cumulative NEE observed is 2.8, 3.1, 2.7 gC. m⁻². day⁻¹ for the three consecutive years of the study. The gradient of uptake for the modeled NEE is similar to the observed (Table 4.2).

The result of our approximation of the spatially and temporally heterogeneous management activities with a single point simulation is that the model captures the cumulative NEE but does not account for the week-to-week variation in NEE. In the autumn and winter period the observations show a decreasing NEE (when respiration process exceeds photosynthesis). The model does capture this trend better in 2003 and 2004 than in 2002.

For both model and observations, there is a year-to-year increase in NEE with the lowest NEE associated with the wettest year. The air temperature, incoming radiation and management practices over the three years were similar. The environmental variable that was most different between the three years was precipitation: 2002 was wetter than average (17% above the long-term annual average); 2003 was drier than average (19% below average); 2004 was 9% drier than average. The decrease in precipitation (from 2002 to 2003) results in an increase in NEE. Some of the observed interannual variation in NEE may be due to the uncertainty inherent in the EC method [Baldocchi, 2003]. The fact that NEE was higher in the dry year by (~ 30%) than in the wet year, suggests that this ecosystem is robust enough to tolerate a wide annual precipitation range (1185 mm to 1835 mm).

4.2.2 Components of NEE

The modelled NEE is the difference between two high fluxes: the gross primary production (GPP) and the total respiration of the ecosystem (R_{tot}):

$$NEE = GPP - R_{tot} \quad \text{Eq. 4.2}$$

Concerning the measurements, the net flux of carbon between the ecosystem and the atmosphere is the sum of the eddy flux (what is measured by the EC technique) and a Δ-storage flux [Hollinger et al., 1994]:

$$NEE = F_{ec} + F_{\Delta} \quad \text{Eq. 4.3}$$

Indeed, this CO₂ storage between the ground and the measurement height can be quite important, especially in forest ecosystems in period of little turbulent mixing at nighttime, as CO₂ molecules are trapped under the canopy. However, for grasslands, the Δ-storage flux can be neglected as many authors did before [Saigusa et al., 1998; Sims and Bradford, 2001; Frank, 2002; Novick et al., 2004].

PaSim simulates GPP and R_{tot}. Figure 4.3 shows the model output of GPP and R_{tot} for the three years of study. The annual GPP increases from 20.7 tC. ha⁻¹. yr⁻¹ (2002) to 22.2 tC. ha⁻¹. yr⁻¹ in 2003 and 2004. The annual R_{tot} increases from 17.9 tC. ha⁻¹. yr⁻¹ (2002) to 19.3 tC. ha⁻¹. yr⁻¹ (2003) and then decreases to 18.5 tC. ha⁻¹. yr⁻¹ (2004). Table 4.3

summarizes the results for GPP, R_{tot} and NEE. The modelled interannual changes of GPP and R_{tot} are less than 7%. However, the modelled interannual change for NEE reaches 29%; as NEE is the difference between GPP and R_{tot} (and is small relative to both), interannual variation in NEE needs to be interpreted with caution.

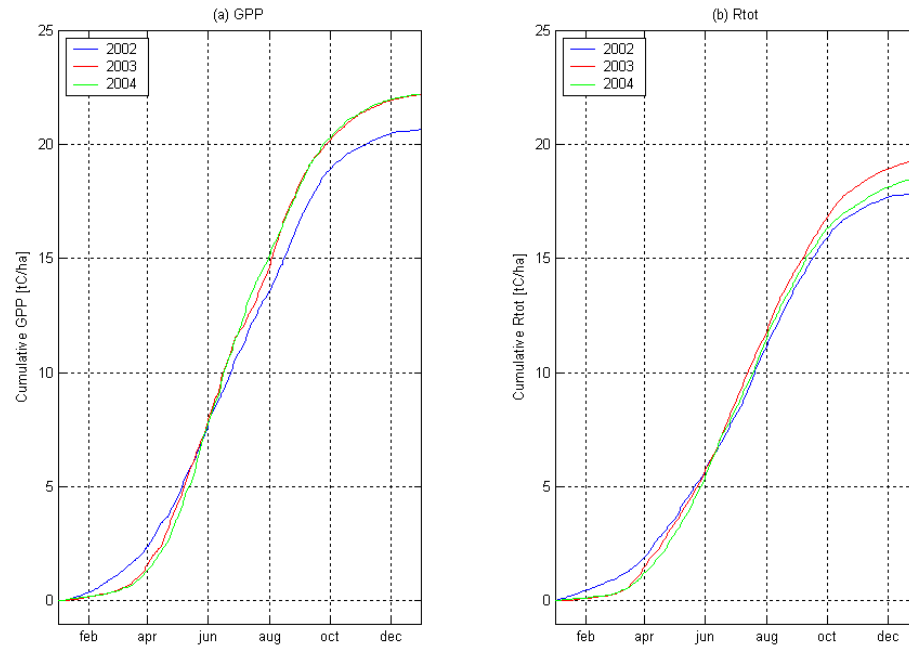


Figure 4.3: Modelled cumulative (a) GPP and (b) R_{tot} , in $tC \cdot ha^{-1}$ for 2002, 2003 and 2004.

We note in Figure 4.3a that the year with lowest GPP ($20.7 tC \cdot ha^{-1} \cdot yr^{-1}$) was the wettest year (1785 mm). We note from Figure 4.3b that the lowest R_{tot} ($17.9 tC \cdot ha^{-1} \cdot yr^{-1}$) was as well in the wettest year. In the wet year, GPP and R_{tot} are lower than in the drier years suggesting that productivity is dependent on a favourable soil moisture status. GPP and R_{tot} are dependent on meteorological, hydrological, soil, vegetation and microbiological conditions; those relationships have been investigated in Lawton et al., [2005, submitted to Glob. Change Biol.].

Table 4.3: Modelled GPP, R_{tot} and NEE, in $tC \cdot ha^{-1} \cdot yr^{-1}$, for 2002, 2003 and 2004.

	GPP	R_{tot}	NEE
2002	20.7	17.9	2.8
2003	22.2	19.3	2.9
2004	22.2	18.5	3.7

We used the model to examine the three components of R_{tot} : the soil respiration (R_{soil}); the plant respiration (R_{plant}) and the animal respiration (R_{animal}):

$$R_{tot} = R_{soil} + R_{plant} + R_{animal} \quad \text{Eq. 4.4}$$

Figure 4.4 shows the modelled partitioning of R_{tot} . On average the soil respiration represents 52%, plants 43% and grazing animals 5%. Research projects focused on ecosystem respiration [Flanagan and Johnson, 2005] or soil efflux (sum of microbial respiration and root respiration) [Franzuebbers et al., 2002; Leiros et al., 1999]; but, there are few field scale studies partitioning respiration into its autotrophic (R_{plant}) and heterotrophic (R_{soil}) components for grassland ecosystems [Hanson et al., 2000]. In laboratory analysis, Tu, [2001] found that, for a grassland, the plant respiration accounted for ~ 66% of the ecosystem respiration. In forests, plant respiration is considered to account for ~ 75% of total respiration [Arneeth et al., 1998; Kinerson et al., 1977].

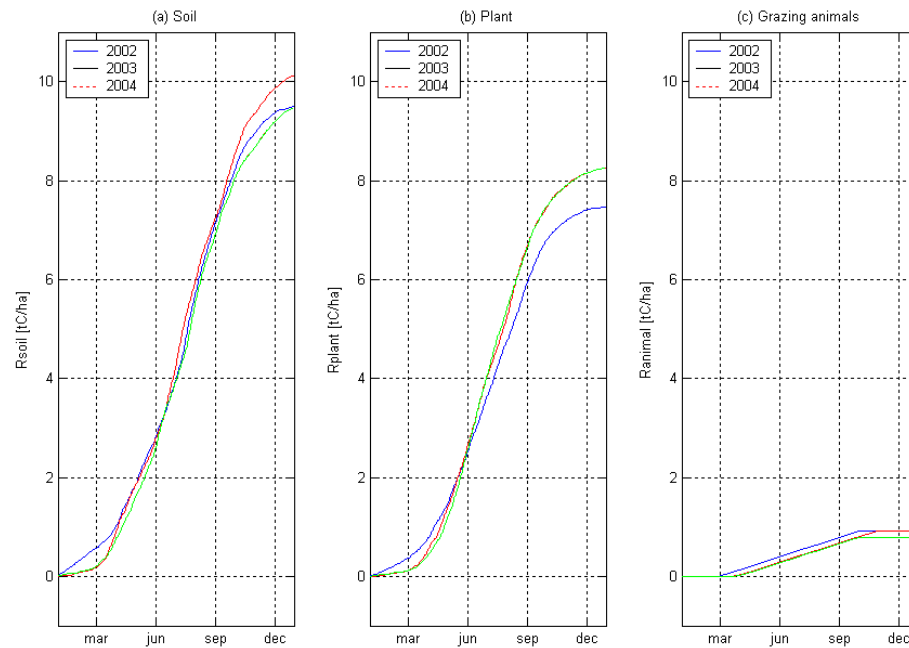


Figure 4.4: The three components of modelled total respiration: (a) soil, (b) plant, (c) grazing animals, in $tC \cdot ha^{-1}$, for 2002, 2003 and 2004.

4.3 Nitrous oxide

There are no on-site measurements of N_2O in 2002. Figure 4.5 shows the cumulative emissions of nitrous oxide. The observed emissions are $11.6 \text{ kg } N_2O\text{-N} \cdot ha^{-1} \cdot yr^{-1}$ for 2003

and 3.6 kg N₂O-N. ha⁻¹. yr⁻¹ for 2004. The modelled emissions are 7.6, 9.6 and 8.3 kg N₂O-N. ha⁻¹. yr⁻¹ respectively for 2002, 2003 and 2004. In the GreenGrass project, seven of the eleven European sites measured nitrous oxide for grasslands and the annual emissions varied from 0.3 to 18.6 kg N₂O- N. ha⁻¹. yr⁻¹ [CarboEurope-GHG, 2004]. The results fall as well within the range of measurements of nitrous oxide for comparable applications of nitrogen in Great Britain [Dobbie and Smith, 2003].

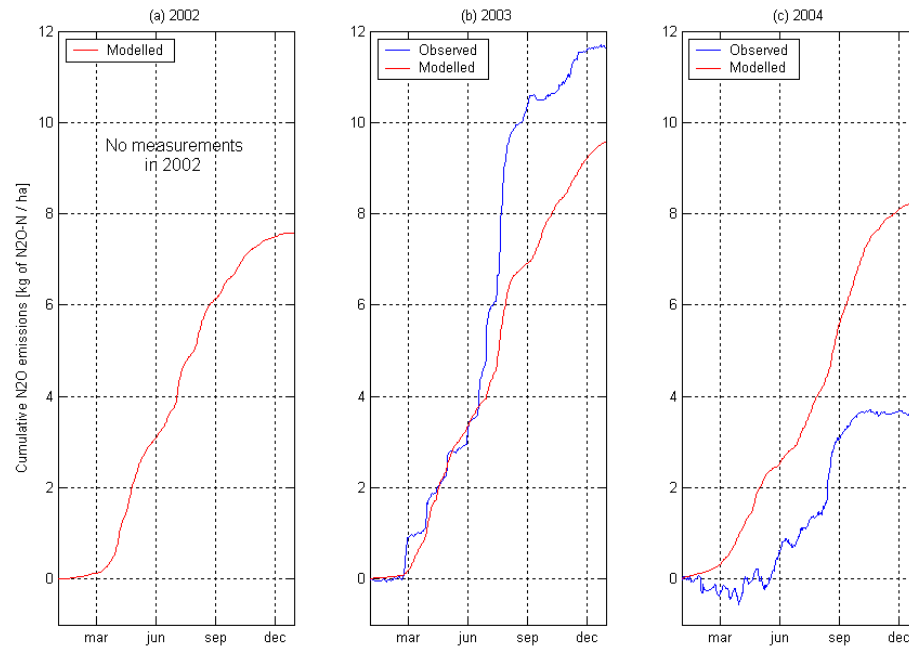


Figure 4.5: Cumulative N₂O emissions observed and modelled, in kg of N₂O- N. ha⁻¹, for: (a) 2002, (b) 2003 and (c) 2004. There was no record of N₂O emissions site in 2002.

The model underestimates the measurements by 17% in 2003 and overestimates them by 132% in 2004. Spatial variability of soil parameters within the flux tower footprint and the temporal variability of the footprint itself due to fluctuations in wind direction and speed may account for some of this discrepancy. In 2003, PaSim does not catch the typical pulses of increase of N₂O following heavy rainfall [Leahy et al., 2004]; however, PaSim models quite well for the first 6 months of 2003 (Figure 4.5b). In 2004, the modelled curve (Figure 4.5c) is quite dissimilar to the observations both concerning the seasonal trends and the annual emissions. PaSim does not especially catch the small uptake of nitrous oxide during the winter and the spring. Concerning this uptake, it can be noticed that, on a daily basis (Figure 4.6 and 4.7), there are no negative modelled fluxes of nitrous oxide; these negative fluxes especially happen in 2004. Indeed, the uptake of nitrous oxide is a very complex phenomenon not yet explained, but it is often observed [Ryden, 1981].

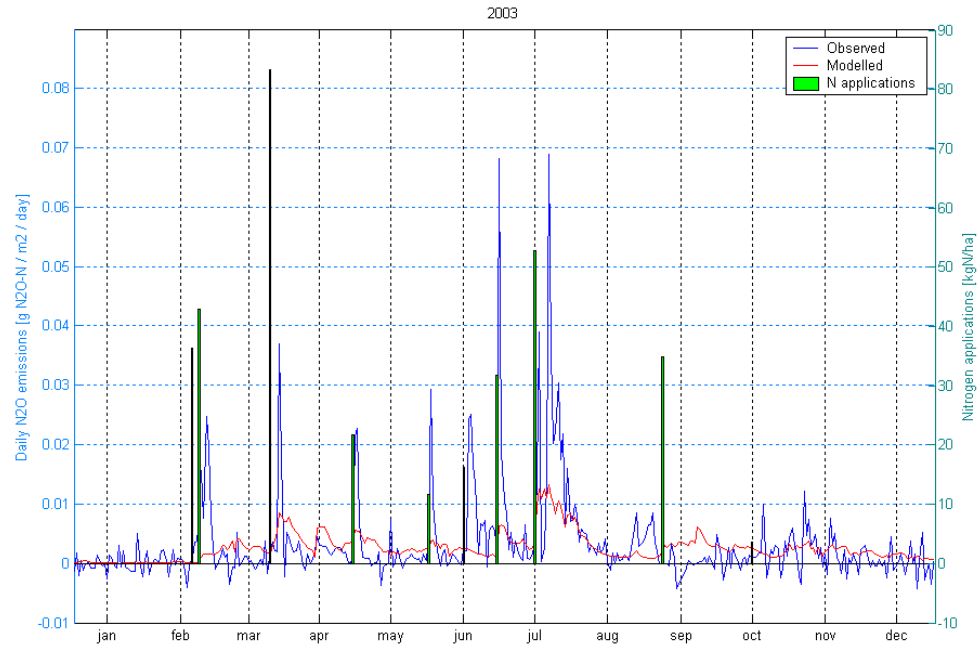


Figure 4.6: Daily N_2O emissions observed and modelled, in g of $\text{N}_2\text{O}-\text{N} \cdot \text{m}^{-2} \cdot \text{day}^{-1}$ for 2003 and nitrogen applications (fertiliser + slurry) for PaSim in $\text{kgN} \cdot \text{ha}^{-1}$.

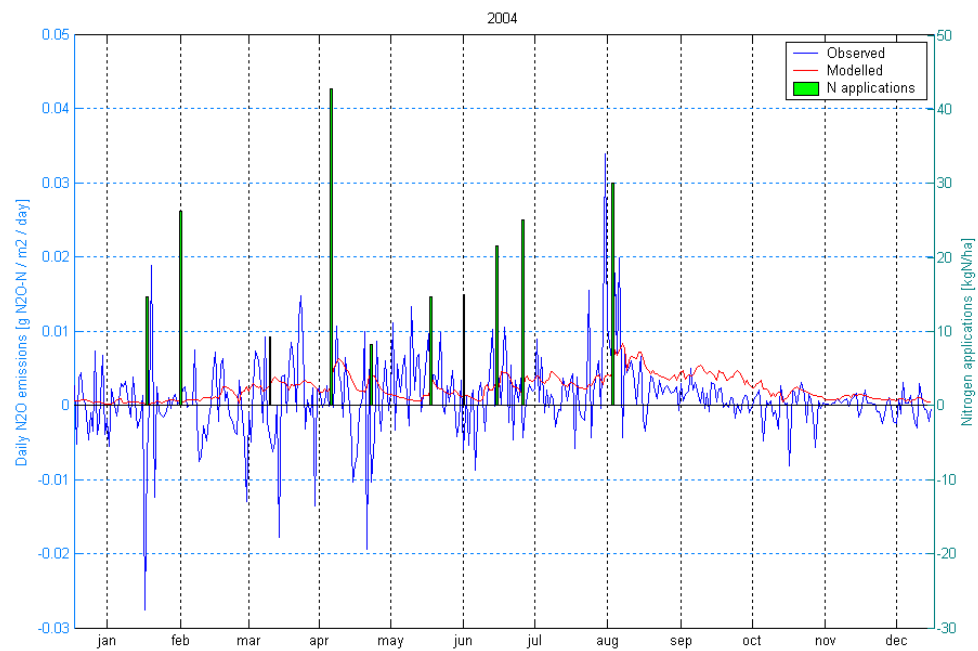


Figure 4.7: Daily N_2O emissions observed and modelled in g of $\text{N}_2\text{O}-\text{N} \cdot \text{m}^{-2} \cdot \text{day}^{-1}$ for 2004 and nitrogen applications (fertiliser + slurry) for PaSim in $\text{kgN} \cdot \text{ha}^{-1}$.

For 2003, PaSim modelled the overall emissions of N_2O . However, if we look at the daily fluxes (Figure 4.6 and 4.7), the modelled maximal values are much lower than the

observed; still some local maximal of the model curve correspond with measurements (March 29th, July 21st 2003). But, sometimes the trends are opposite (September and October 2003).

On Figure 4.6 and 4.7, the timing and amount of nitrogen spread was superimposed on the daily fluxes. N₂O emissions are closely related to nitrogen applications and as well as to soil WFPS (water filled spore space) and rainfall [Dobbie et al., 1999]. This implies that the timing of applications is very important, but because the data log sheet from the farmers are not very precise and the model limits the applications of fertiliser and slurry to 10 dates, the fluxes of N₂O cannot be very close to the measurements. We tried to run the model injecting a major rain event 7 days and 20 days after a day of application of fertilisers, but it did not make a major difference. However, some peaks follow applications of fertilisers (e.g. April and August 2004).

The total amount of fertilisers spread (i.e. chemical fertilisers and slurry) was 305 kgN. ha⁻¹, 334 kgN. ha⁻¹ and 207 kgN. ha⁻¹. The emissions are supposed to be linked with the amount of fertilisers [Ryden, 1981; IPCC, 1997], however, the modelled emissions in 2004 were 10% higher than in 2002 whereas the applications decreased by 32%; it may be a consequence of the build up of nitrogen in the soil due to the high applications in 2003. The observed and modelled emission factor (percentage of applied N fertiliser lost as N₂O) are summarised in Table 4.4. All the emission factors are smaller than the IPCC guideline value of 1.25 ± 1.0 % [IPCC, 1997] of applied N, except for the modelled emission factor in 2004 (but it is may be because of the uncertainty of the amount of slurry spread), but still fall within the range given by the IPCC guideline (emission factors are: 3.8 ± 3.0 %, 4.2 ± 3.3 % and 2.6 ± 2.1 % respectively for 2002, 2003 and 2004).

Table 4.4: Summary of observed and modelled N applications, N₂O emissions and emission factor for 2002, 2003 and 2004.

	Total N application (kgN. ha ⁻¹)		N ₂ O emission (kgN. ha ⁻¹)		Emission factor (%)	
	Observed	Modelled	Observed	Modelled	Observed	Modelled
2002	305	305	-	7.6	-	2.5
2003	334	334	11.6	9.6	3.5	2.9
2004	207	207	3.6	8.3	1.7	4.0

4.4 Methane

Methane is not measured on site. However, according to the IPCC guidelines, we estimate the emissions of methane based on knowledge of animal type and number. The annual emissions from enteric digestion in Western Europe are 100 kg CH₄. head⁻¹. yr⁻¹ for dairy cattle and 48 kg CH₄. head⁻¹. yr⁻¹ for non-dairy cattle [IPCC, 1997]. Given that half of the cattle grazing are dairy cows and the other half are beef cattle, it represents 74 kg CH₄. head⁻¹. yr⁻¹, or 0.203 kg CH₄. head⁻¹. day⁻¹. Combining that figure with a density of 2.2 LU. ha⁻¹ and using the same grazing periods as in the management input data, we obtain the estimated emissions in Figure 4.8.

Figure 4.8 presents as well PaSim modelled emissions of methane for 2002, 2003 and 2004. In 2002, the total modelled emissions are 66 kgC. ha⁻¹. yr⁻¹, 69 kgC. ha⁻¹. yr⁻¹ in 2003 and 60 kgC. ha⁻¹. yr⁻¹ in 2004 (Table 4.5). On annual methane emissions, the IPCC estimations are less than 17% higher and they do not take in account changes in the diet of the animals. Here methane only originates from enteric digestion. The straight line is due to the assumption that the fields are continuously grazed.

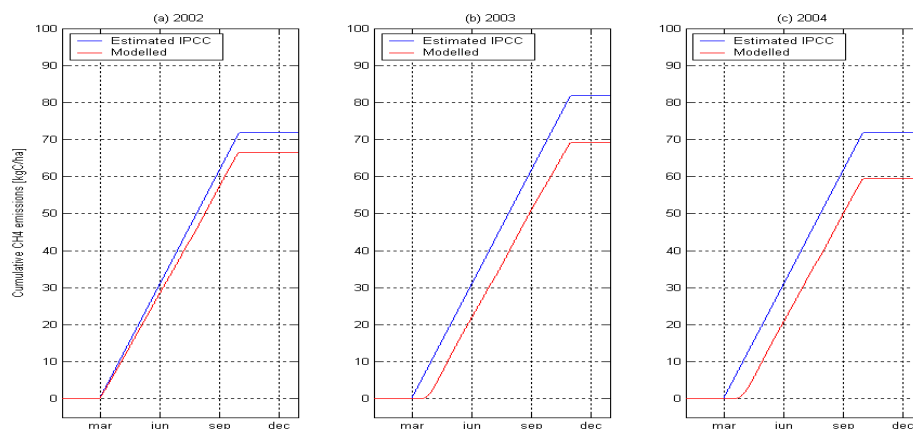


Figure 4.8: Cumulative CH₄ emissions estimated and modelled in kgC. ha⁻¹, for: (a) 2002, (b) 2003 and (c) 2004. There is no CH₄ record for the site.

Combining the curve gradient and the livestock density, we obtain that PaSim predicts an average of 0.265 kg CH₄. head⁻¹. day⁻¹ (see Table 4.5 for details). Those figures are closest to dairy cow emissions, as the values are: 0.274 kg CH₄. head⁻¹. day⁻¹ for dairy cows and 0.131 kg CH₄. day⁻¹. yr⁻¹ for non-dairy cows. This is expected as the model only considers dairy cows. But, on an annual basis the emissions are quite close because we introduced a cattle density of only 1.5 LU. ha⁻¹ in the inputs of the model (see section 3.2.2 for the model parameterisation).

Table 4.5: Summary of IPCC estimated and PaSim modelled annual CH₄ emissions and gradient for 2002, 2003 and 2004.

	Annual emissions (kgC. ha ⁻¹ . yr ⁻¹)		Gradient (kg CH ₄ . head ⁻¹ . day ⁻¹)	
	IPCC	PaSim	IPCC	PaSim
2002	72	66	0.203	0.275
2003	81	69	0.203	0.258
2004	72	60	0.203	0.261

For the three years, it is considered that the cattle start to graze on March 1st. However, we can note that there is a lag of 16 days in 2003 and 13 days in 2004. This is because methane emissions depend on the animal's diet (quantity and quality) and the dry matter modelled was too small at the beginning of March 2003 and 2004 (see dotted line on Figure 4.9b and 4.9c). Enteric digestion emissions reach their full capacity when the shoot dry matter exceeds 0.2 kg. m⁻². Figure 4.9 underlines this characteristic. The major decrease in the methane emissions after a cutting event is also representative of it.

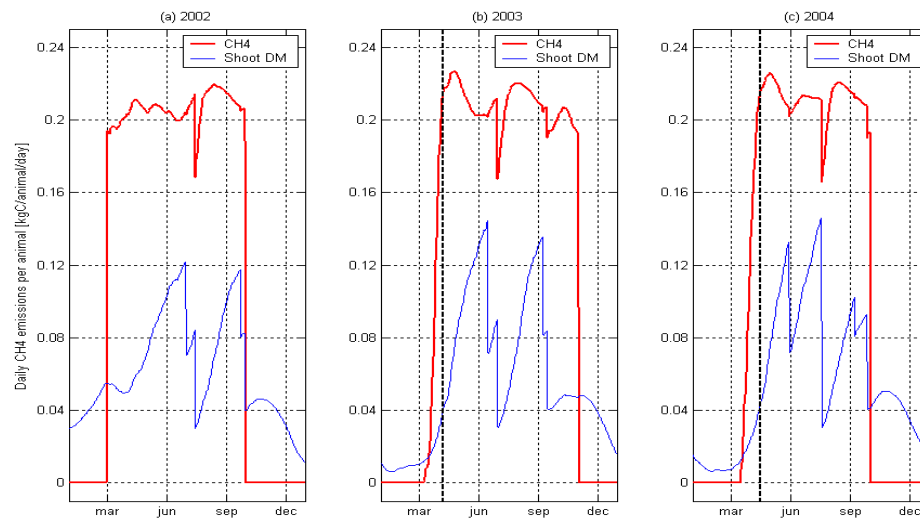


Figure 4.9: Daily CH₄ emissions modelled per animal in kgC. animal⁻¹. day⁻¹ and modelled shoot dry matter, in kg. m⁻², reduced to 20% of its value for: (a) 2002, (b) 2003 and (c) 2004. The dotted vertical line shows the threshold after which the methane emissions get normal values; the threshold is 0.2 kg. m⁻² (0.04 on the figure).

Because those results are based on a simplification of the effective management practices and cannot be verified by on-site measurements, those results should be taken with extreme care.

4.5 Greenhouse gas balance

4.5.1 Modelled vs. observed GHG balance

Figure 4.10 is a summary of the comparison of the observed versus the modelled greenhouse gases and the GHG balance itself. The GHG balance in 2002 is not shown as there are no observations of nitrous oxide and methane is only estimated. Positive values are representative of an uptake by the grassland, however N₂O and CH₄ emissions are represented on the positive axis for more legibility. For the three years, an uptake is observed. The amplitude of the GHG sink is summed up in Table 4.6.

Table 4.6: Observed and modelled GHG balance in T of CO₂ equiv. ha⁻¹. yr⁻¹.

	2002	2003	2004
Observed	-	1.6	6.9
Modelled	4.6	4.0	7.9

The GreenGrass project calculated the net balance for GHG for seven European grassland ecosystems and found a range from a sink of 18 T of CO₂ equiv. ha⁻¹. yr⁻¹, for sown grass in Denmark, to emissions of 5.5 T of CO₂ equiv. ha⁻¹. yr⁻¹, for the site in France that is continuously grazed and intensively managed [CarboEurope-GHG, 2004]. The Irish site in Carlow (South West of Dublin) that is extensively cut and grazed provides a sink of approximately 11 T of CO₂ equiv. ha⁻¹. yr⁻¹ [CarboEurope-GHG, 2004].

Table 4.7: Modelled percentage of the CO₂ uptake counteracted by N₂O and CH₄.

	2002	2003	2004
N ₂ O	34.7 %	42.1 %	28.4 %
CH ₄	20.1 %	20.1 %	13.4 %

In Table 4.7 can be found the modelled percentage of carbon dioxide uptake that is counteracted by nitrous oxide and methane. In average for the three years, modelled N₂O accounts for 35% and modelled CH₄ for 18%. Thus, nitrous oxide has the worst effect on the carbon uptake from plants in the GHG balance. Observed N₂O counteracts 56.8% of the observed NEE in 2003, that is quite comparable with the model results. In 2004, unlike the model results, IPCC estimated methane cancels 20.4% of the observed CO₂ uptake whereas, observed N₂O emissions counteracts only 15.4%.

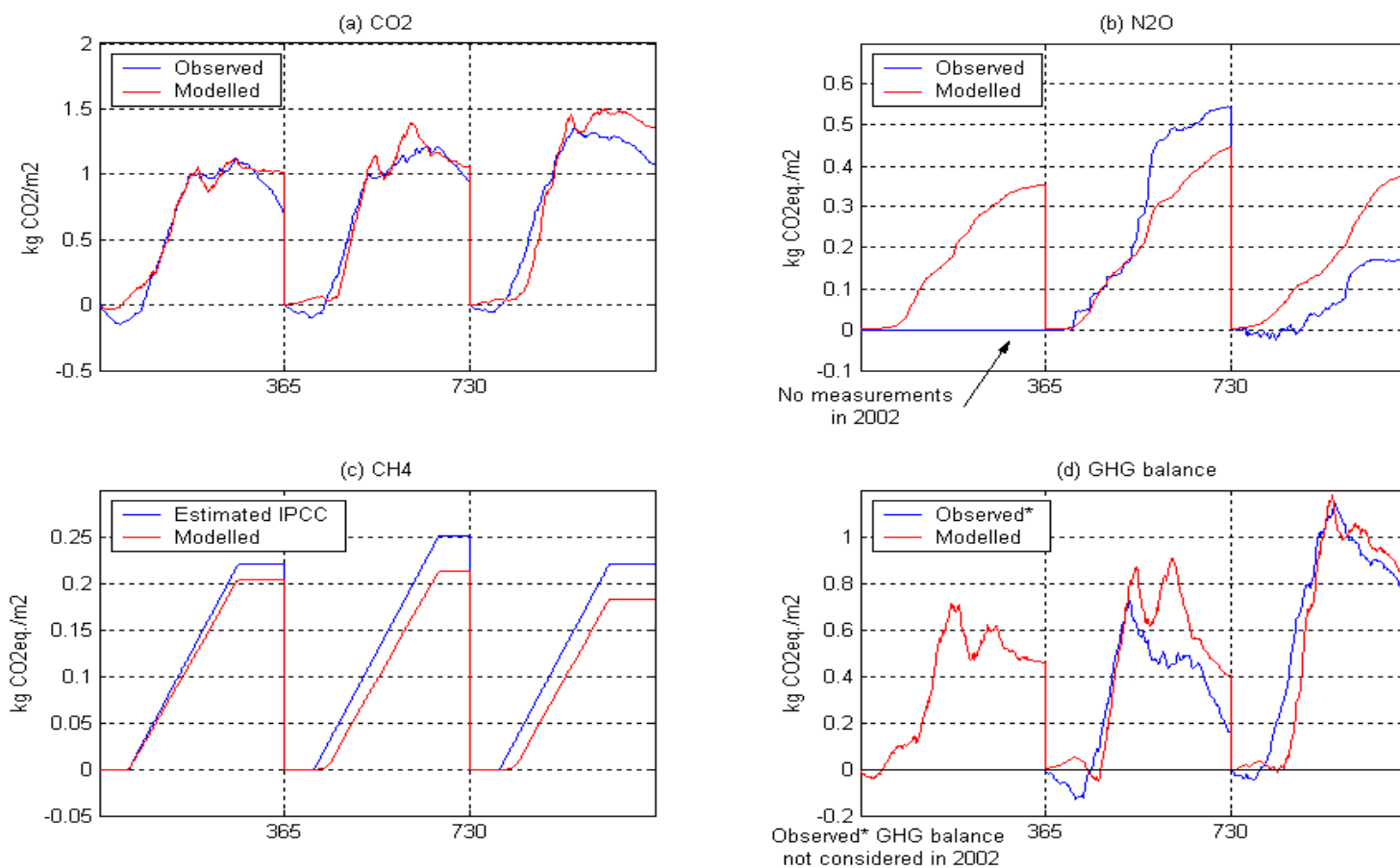


Figure 4.10: (a) CO₂ observed and modelled; (b) N₂O observed and modelled; (c) CH₄ IPCC estimated and modelled; and (d) GHG balance observed and modelled for 2002, 2003 and 2004, in kg CO₂ equiv. m⁻². The observed* GHG balance is calculated with the IPCC estimation of methane. *Note:* there are no N₂O measurements in 2002 so the observed GHG balance is not considered. N₂O and CH₄ emissions are shown on the positive axis for more legibility.

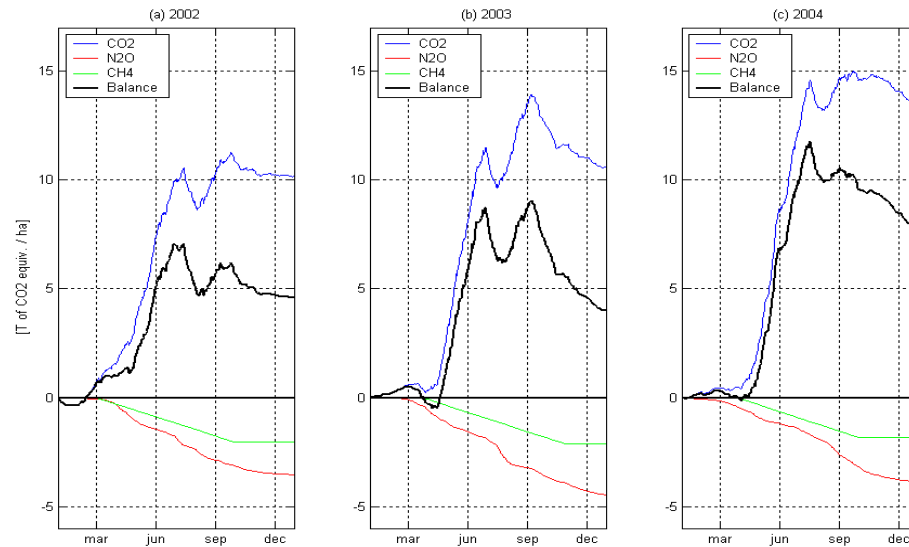


Figure 4.11: Modelled CO_2 , N_2O , CH_4 emissions and GHG balance in T of CO_2 equiv. ha^{-1} , for (a) 2002, (b) 2003 and (c) 2004.

Figure 4.11 shows the modelled greenhouse gas balance and its three components (CO_2 , N_2O and CH_4). The modelled GHG balance curve (bold black) mainly follows the variations of CO_2 uptake; emissions of GHG are strong after each cutting event like it is for NEE. The CO_2 curve and the GHG balance curve get detached in March when the N_2O emissions start to be significant and cattle start grazing out. The year 2004 has the highest uptake because of the very high CO_2 uptake.

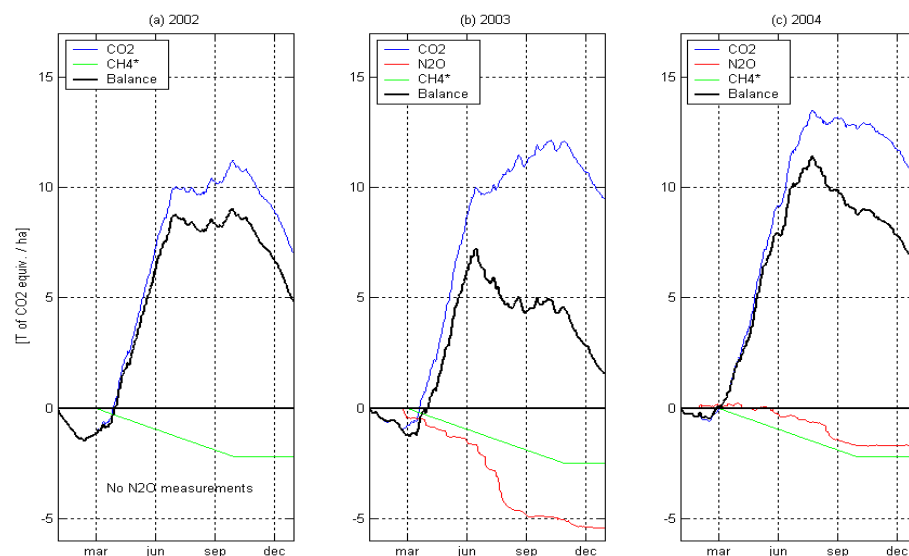


Figure 4.12: Observed CO_2 , CH_4 emissions and GHG balance in T of CO_2 equiv. ha^{-1} , for: (a) 2002, (b) 2003 and (c) 2004. CH_4^* has been estimated with the IPCC guidelines. Note: there are no N_2O measurements in 2002.

In Figure 4.12a, the observed GHG balance is represented even if there are no N₂O measurements in 2002 and the methane is only estimated according to the IPCC guidelines. In 2003 (Figure 4.12b), the observed CO₂ uptake is counteracted mainly by the emissions of N₂O. It is much less the case in 2004 (Figure 4.12c) as the N₂O emissions are reduced by 70%. In addition, the N₂O sink at the beginning of the year improves the GHG sink. The observed curves in 2003 and 2004 have the same characteristics as the modelled curves.

The modelled GHG balance in 2003 is higher than the observed one; this is due to the combination of higher modelled NEE and smaller modelled N₂O emissions in comparison with the observations. In 2004, the observed and modelled GHG balances are very similar. However, this is because the balance is the difference between NEE and (N₂O + CH₄) emissions. So even if the GHG balance is about the same, it may be due to different values of the components. That is to say, in 2004, the two NEE are similar, however for the observations, CH₄ counteracts the CO₂ uptake more than N₂O does (Figure 4.12c) whereas, for the modelling, N₂O counteracts the CO₂ uptake more than CH₄ does (Figure 4.11c).

4.5.2 GHG balance modelled

Figure 4.13 represents the modelled greenhouse gas balance for 2002, 2003 and 2004 in T of CO₂ equiv. ha⁻¹. There is an uptake of 4.6 T of CO₂ equiv. ha⁻¹. yr⁻¹ in 2002; then in 2003, the GHG balance decreases a little (4.0 T of CO₂ equiv. ha⁻¹. yr⁻¹), and it ends with a strong uptake of 7.9 T of CO₂ equiv. ha⁻¹. yr⁻¹ for 2004.

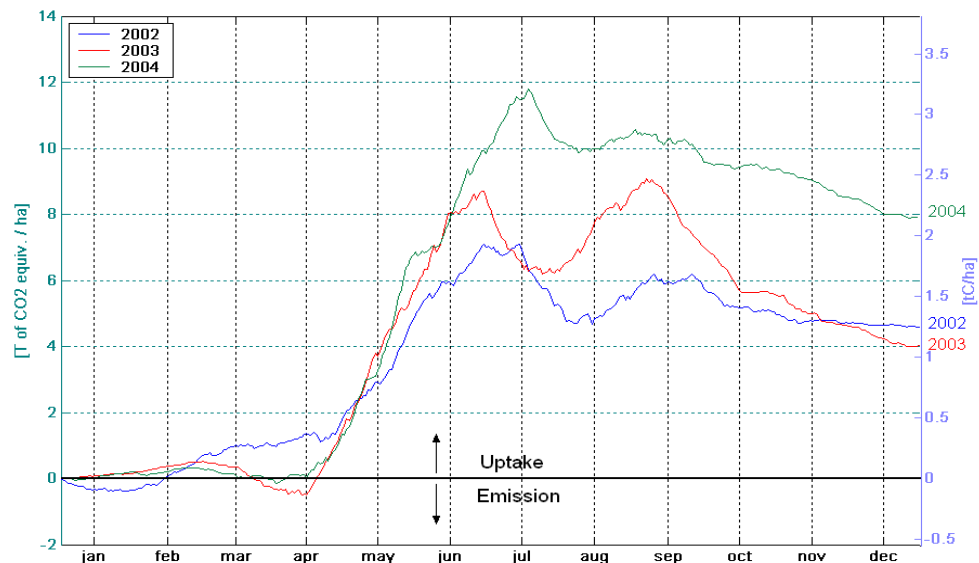


Figure 4.13: Modelled greenhouse gas balance in T of CO₂ equiv. ha⁻¹, for 2002, 2003 and 2004.

The bulk of the fixation of carbon dioxide (reducing the GHG effect) starts in April and ends in August (see Figure 4.14 for the monthly average of the modelled GHG balance). Nonetheless, emissions of greenhouse gases are indicated in July 2002 and 2003. Again, it reflects the impact of silage cuts.

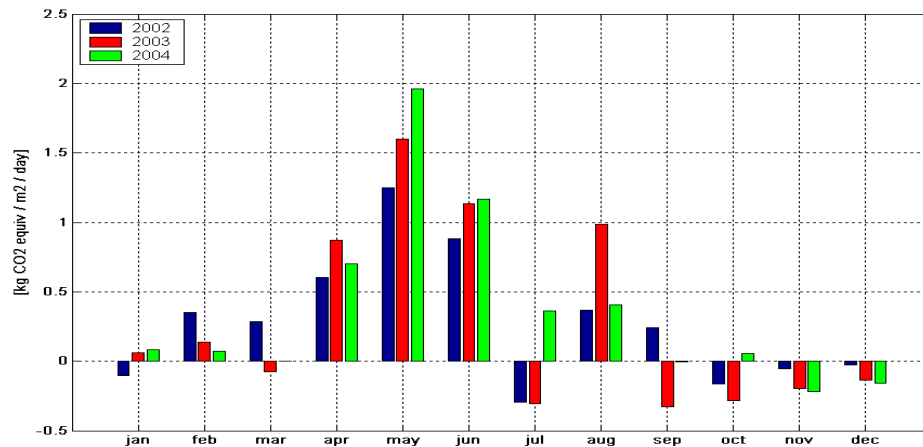


Figure 4.14: Monthly average of the modelled GHG balance in kg CO₂ equiv. m⁻². day⁻¹, for 2002, 2003 and 2004.

In a nutshell, PaSim is quite accurate while modelling CO₂ fluxes, however, the results are less satisfying for N₂O emissions. CH₄ emissions seem to be in agreement with the IPCC estimations. So this study shows that the process oriented biogeochemical model for carbon cycling in this temperate humid grassland simulates well the greenhouse gases over the three-year study period.

The model's results confirm that this grassland acts as a small greenhouse gas sink under the current climate. However, GHG emissions are closely linked with management practices; nitrous oxide has the worst effect on the balance and should be tackled by government policies, prior to methane. The parameterisation of this simulation will be taken as a reference for the following chapter that considers different scenarios.

Chapter 5

Climate Change Scenarios

Chapter 5 **Climate Change Scenarios**

5.1 Definition of the scenarios

Running the model with modifying the meteorological input data as well as the management data can give an idea of how the ecosystem will respond to such changes. In this project, we decided to consider a climate change scenario combined with elevated CO₂ (which is commonly referred as a doubled concentration, CO₂*2) and a reduction in the application of nitrogen fertiliser according to the Irish Rural Environment Protection Scheme (REPS) 2000.

5.1.1 Climate change scenario and elevated CO₂

Here as a climate change scenario, we consider changes only in temperature and precipitation, like other authors did [Hunt et al., 1991; Chen et al., 1996]. We do not change the input files for incoming radiation or relative humidity because significant changes in the greenhouse gases can already be observed. However in a more detailed study, it would be relevant to consider the changes in the incoming radiation, relative humidity and the wind speed.

We base our calculations on the HadCM3 model. This is a coupled atmosphere-ocean general circulation model (AOGCM) developed in 1998 at the Hadley Centre and described by Gordon et al., [2000] and Pope et al., [2000]. AOGCMs are the most complex models in use, consisting of an AGCM coupled to an OGCM. They can be used to predict the future rate of climate change. They are also used to study the variability and physical processes of the coupled climate system. Global climate models typically have a resolution of a few hundred kilometres.

The HadCM3 model has been run under the scenario IS92a. The IS92 (IS92a to f) scenarios were published in the 1992 Supplementary Report to the IPCC Assessment [Leggett et al., 1992]. These scenarios embodied a wide array of assumptions affecting how future greenhouse gas emissions might evolve in the absence of climate policies beyond those already adopted. The different worlds that the scenarios imply, in terms of economic, social and environmental conditions, vary widely and the resulting range of possible greenhouse gas futures spans almost an order of magnitude. IS92a has been widely adopted as a standard scenario for use in impact assessments. It is a middle of the range (“business as usual”)

scenario in which population rises to 11.3 billion by 2100, economic growth averages 2.3% per year between 1990 and 2100 and a mix of conventional and renewable energy sources are used. Only those emission controls internationally agreed upon and national policies enacted into law, e.g., London Amendments to the Montreal Protocol, are included. It is the baseline for numerous GCMs. It can be noted that in 1995, the IPCC 1992 scenarios were evaluated and the evaluation recommended that changes should be addressed. The IPCC 2001 defined a new set of emissions scenarios in the SRES (Special Report on Emissions Scenarios, IPCC, 2000) to replace the IS92 scenarios. However, some models still use the IS92 scenarios.

Table 5.1 gives the temperature and precipitation perturbations under the IS92a scenario for the HadCM3 model, in southern Ireland, for the period 2070-2100.

Table 5.1: Climate perturbations for seasonal precipitation and temperature under HadCM3 model (IS92a scenario) for southern Ireland.

Season	Change in precipitation (mm/day)	Change in temperature (°C)
December-February (DJF)	+ 0.75	+ 2.5
March-May (MAM)	0	+ 2.0
June-August (JJA)	- 0.75	+ 2.5
September- November (SON)	0	+ 2.5

In 2002, the atmospheric concentration of CO₂ is approximately 370 ppm (parties per million) [IPCC, 2001]. Atmospheric CO₂ concentrations are increasing and according to the Bern-CC model [Joos et al., 1996], the concentration is expected to reach 703 ppm by 2100. The other model cited in the IPCC 2001 report is the ISAM model [Jain et al., 1994] and the value predicted is quite close to the one of the Bern-CC model, namely 723 ppm, but we won't consider this hypothesis.

Climate change and elevated CO₂ are coupled. However, in order to understand the influence and the relative importance of each scenario, we will first study the impacts of the changes in the temperature and precipitation only, then, focus on the influence of the CO₂*2, before considering the effects of climate change combined with elevated CO₂, like it has been done in other modelling studies [Chen et al., 1996; Coughenour and Chen, 1997].

5.1.2 REPS 2000

The Irish Rural Environment Protection Scheme (REPS) 2000 is a measure included in the CAP Rural Development Plan, co-funded under the National development plan 2000-2006 and the European Agricultural Guidance and Guarantee Fund of the European Union in

the implementation of Council Regulations (EC) 1257/1999. REPS is not a law, the farmers voluntarily agree to the scheme and are rewarded for carrying out their farming activities in an environmentally friendly manner [REPS, 2002]. This scheme is a step toward the EU Nitrates Directive (91/676/EEC) that is not fully implemented in Ireland yet.

For grasslands, REPS sets an upper limit of total nitrogen (N) of 260 kg. ha⁻¹ (total nitrogen includes chemical fertiliser, animal's waste while grazing, and other wastes, i.e. slurry, manure or urea) and the permitted level of N from animal and other wastes on the same area shall not exceed 170 kg. ha⁻¹. Then, the maximum level of chemical nitrogen that can be applied to grassland can never be greater than the planned level of N from animal and other wastes applied on the same area.

5.2 Climate change scenario

5.2.1 Definition of the scenario in terms of meteorological data

The seasonal climate perturbations were given in Table 5.1. The precipitation changes are given in mm. day⁻¹; nonetheless, in order to conserve the alternation of sunny days and rain events, we calculated the predicted total amount of precipitation for each season, and then calculated the percentage of change in the total in order to apply this percentage to the hourly values.

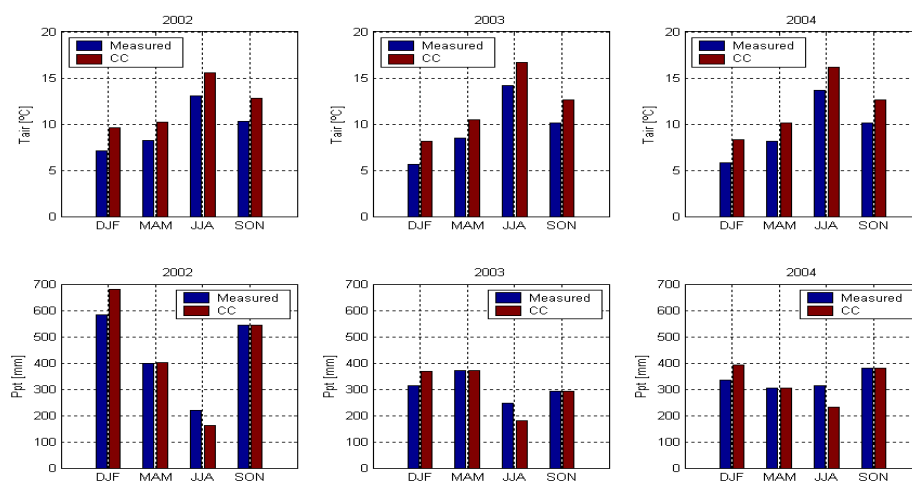


Figure 5.1: Seasonal air temperature and precipitation from measurements under ambient climate and in a changed climate. DJF stands for December-January-February, MAM for March-April-May, JJA for June-July-August and SON for November-December-January.

Concerning temperature perturbations, the method was easier; we just had to add 2.0 or 2.5°C (according to the season) to the hourly data. Figure 5.1 shows the comparison between the observed seasonal average and the modelled seasonal averages for air temperature and precipitation.

All the other input files (other meteorological input data files, initial conditions file, site specific parameter file and management input data file) are kept as in the reference simulation (from Chapter 4).

5.2.2 Results and analysis

Figure 5.2 presents the comparison of a simulation with climate perturbations for air temperature and precipitation with the simulation of reference, for CO₂, N₂O and CH₄. The last graph represents the greenhouse gas balance, where positive values indicate a GHG sink.

CO₂ fluxes

Concerning CO₂ fluxes, climate perturbations have a negative effect on the sink activity of the grassland. For the three years of simulation, the annual uptake is smaller in comparison with the reference simulation (Figure 5.2a).

When looking at the components of the NEE, gross primary production (GPP) increased on average by 6% whereas the total respiration (R_{tot}) increased by 10%. Because warmer temperatures improve the plant growth, the GPP (result of the photosynthesis) is enhanced like the net primary productivity (NPP, that represents the net augmentation of plant biomass) but the latter in a smaller percentage. The CENTURY model predicted an increase of the NPP under the CCC (Canadian Climate Change) scenario [Ojima et al., 1993], while, under ambient CO₂ and increased temperatures of 3°C, the GRASS-CSOM model predicted a decrease of the NPP by 15.6% [Coughenour and Chen, 1997].

Among the three components of R_{tot}, it was the soil respiration that had the biggest increase. The higher soil respiration may be due to the augmentation of microbial activity, as more organic matter is available to decompose. It can also be explained by the fact that the organic matter may be the same but the microbial activity is boosted by the increase in temperature.

Compared to the reference simulation, the growing season starts slightly earlier (4, 20 and 2 days earlier according to the definition given in section 4.2.1); this is mainly due to the warmer air temperature that causes warmer soil temperature and thus, an earlier start of the growth of the plants.

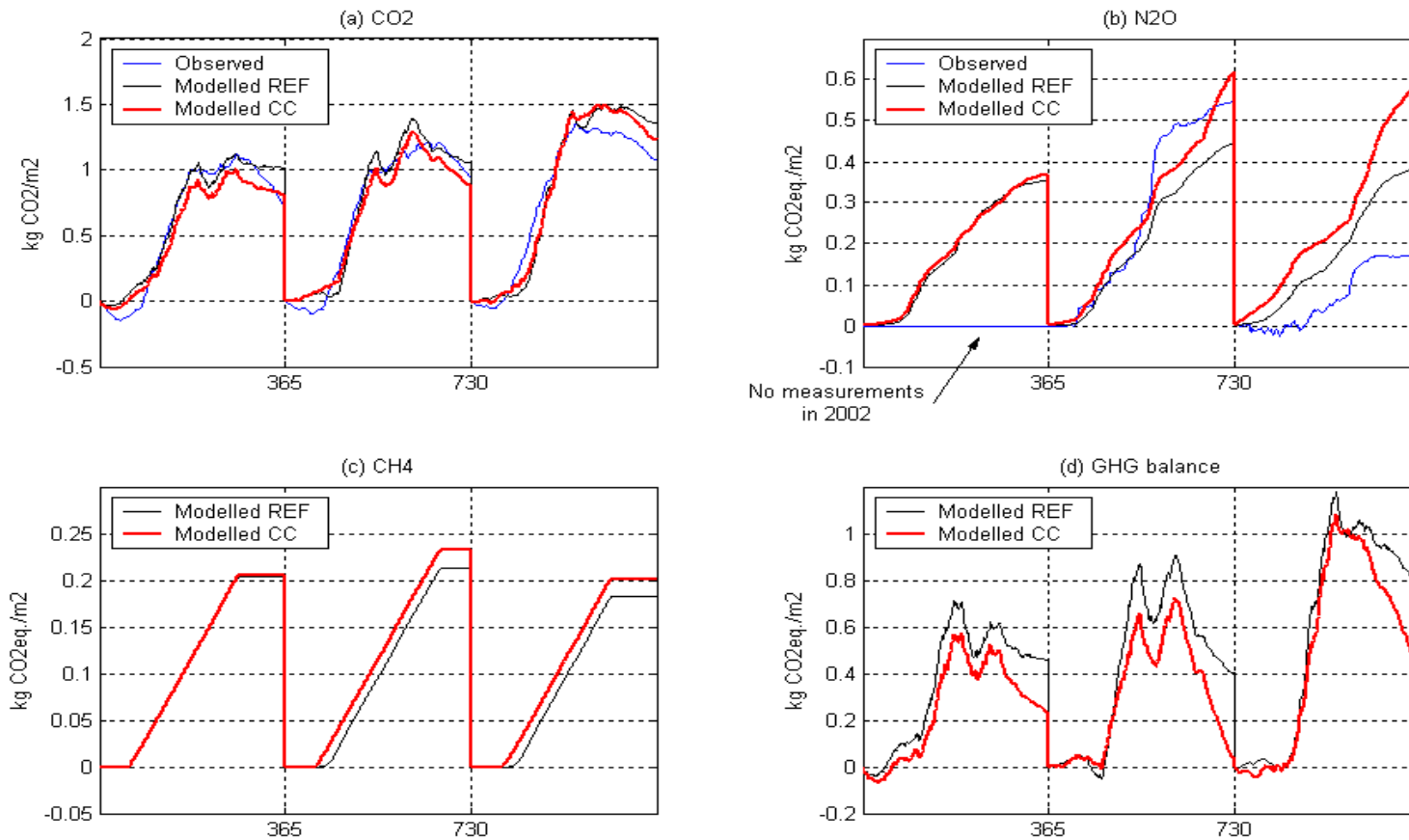


Figure 5.2: (a) CO₂ observed, reference modelled and modelled with climate change perturbations; (b) N₂O observed, reference modelled and modelled with climate change perturbations; (c) CH₄ reference modelled and modelled with climate change perturbations; and (d) GHG balance reference modelled and modelled climate change perturbations for 2002, 2003, 2004, in kg CO₂ equiv. m⁻². N₂O and CH₄ emissions are shown on the positive axis for more legibility.

On a seasonal basis (Figure 5.3), the CO₂ fluxes are smaller for every season except the summer (JJA) 2002 and 2004. We remind that, for the whole year, there is a rise of the air temperature of 2.5°C (except for MAM, where the change is only of 2.0°C). Concerning the precipitation, spring (MAM) and autumn (SON) do not see any change whereas winter (DJF) experiences an increase of rainfall and summer a decrease.

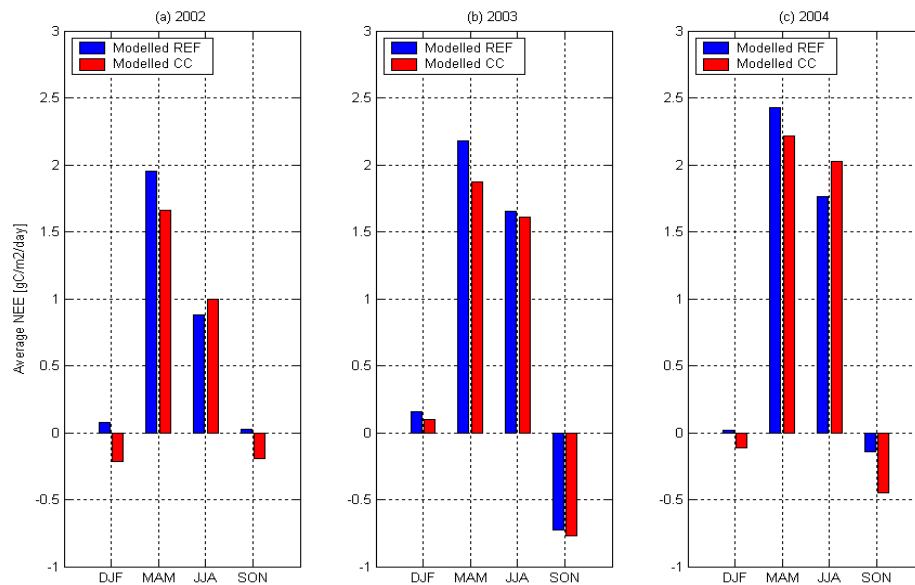


Figure 5.3: Daily NEE averaged on a seasonally basis for the reference simulation and the climate change simulation, in $\text{gC} \cdot \text{m}^{-2} \cdot \text{day}^{-1}$, for (a) 2002, (b) 2003 and (c) 2004.

During winter, the decrease in uptake or even emissions of CO₂ may be due to a limited uptake, which is in turn unable to compensate for emissions (especially from heterotrophic respiration augmented by wetter conditions and warmer temperatures). This can be confirmed by the fact that the only uptake is observed in 2003, the driest year. During spring, the average daily flux is smaller with the climate perturbations, supposedly because warmer temperatures enhance the soil respiration. In summer, the fluxes are higher in 2002 and 2004, but smaller in 2003. The summer in the climate change scenario is drier, so this has a good effect on the CO₂ fluxes when the year is wetter (like it was for 2002 and 2004 compared to 2003). Finally, the NEE is smaller during the autumn; it may be explained as a consequence of the drier summer.

N₂O fluxes

The IS92a climate change scenario (Table 5.1) results in increased nitrous oxide emissions (Figure 5.2b). Other models found the same results (e.g. DNDC, Hsieh et al.,

2005). This is mainly due to the temperature increase that favours the reactions of nitrification and denitrification [Barnard et al., 2005]. However, in 2002 under the CC scenario, the model shows an increase of only 4.5% in relation to the reference simulation (compared to 38.9% and 55.1% for 2003 and 2004); this may be explained by the sensitivity of the model to initial condition.

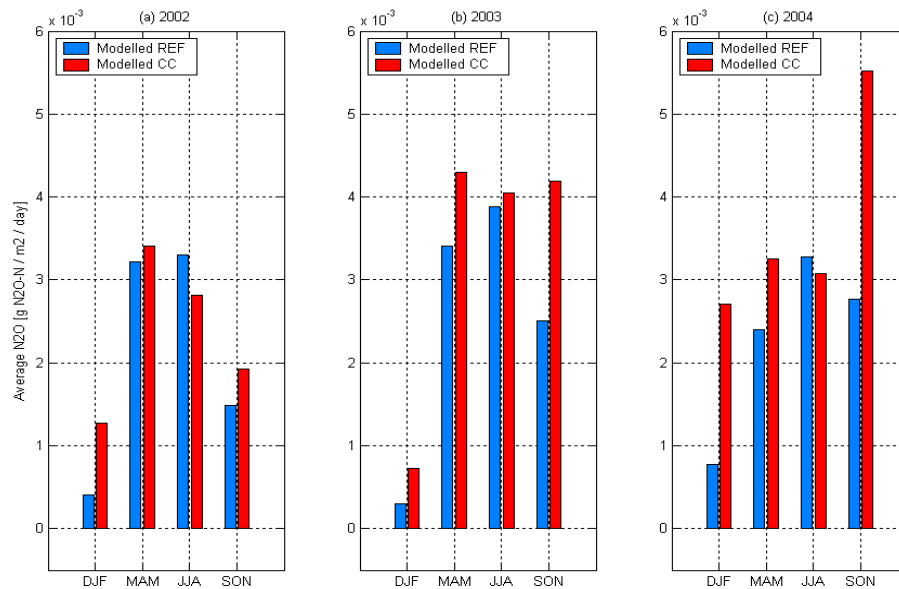


Figure 5.4: Daily N₂O emissions averaged on a seasonally basis for the reference simulation and the climate change simulation, in gN₂O-N. m⁻². day⁻¹, for (a) 2002, (b) 2003 and (c) 2004.

On average per season (Figure 5.4), N₂O emissions are higher under climate perturbations, except for JJA 2002 and JJA 2004. DJF has the biggest increase for the three years. JJA is the only season with smaller rainfall and DJF, the only season with higher rainfall. This confirms the close relationship between N₂O emissions and rainfall.

The daily N₂O fluxes are not shown here, but, if the annual emissions increased significantly, the maximum daily fluxes under the climate change scenario did not increase in the same extent. The augmentation of nitrous emissions comes mostly from a general rise of daily mean values (i.e. background).

CH₄ fluxes

Methane emissions under CC scenario start as soon as cattle are brought to the fields in March of each year, whereas there is a time lag for the reference simulation in 2003 and 2004. This is due to the slightly earlier start of the growing season that provides a better grass earlier. It results in a rise of the annual emissions of respectively 0.6, 9.3, and 10.4%.

GHG balance

Under the IS92a climate change scenario, the role of the grassland as a sink for GHG is less pronounced, even null in 2003. This due to the combination of a reduced CO₂ sink and higher emissions of N₂O.

5.3 Elevated CO₂ scenario

In comparison with the reference simulation in Chapter 4, we only changed the atmospheric concentration of carbon dioxide. CO₂ was increased in a single step from 370 ppm to 703 ppm (estimated concentration in 2100, IPCC, 2001). The results obtained are shown in Figure 5.5. With elevated CO₂, there is a major increase in the NEE. In parallel to the carbon uptake, there is a reduction in the emissions of nitrous oxide. Thus, the combination of the increased uptake of CO₂ and decreased emissions of N₂O increases the GHG sink significantly.

CO₂ fluxes

CO₂ uptake through plant fixation increases by at least 50% under elevated CO₂. GPP increases much more than R_{tot}, this is the reason of the increase in NEE. Ecosystem responses to increased CO₂ are often constrained by nutrient limitation [Rastetter et al., 1997]; however, this is not normally the case for this Irish grassland because of the large amount of nitrogen applied in the past and in the present.

The Grassland Ecosystem Model (GEM) predicted increased productivity and C storage in plant residue and soil organic matter in response to doubled CO₂ [Hunt et al., 1991]. Thornley and Cannell, [1997] underlined the same conclusions with the HP-model. Coughenour and Chen, [1997] pointed out an increase in the productivity as well and described the consequences of doubled CO₂ as a positive feedback loop that amplifies the positive responses of plants, thus increased NPP provides more organic matter to decomposers, thus increasing microbial activity, which increases the nitrogen in the soil, and then NPP.

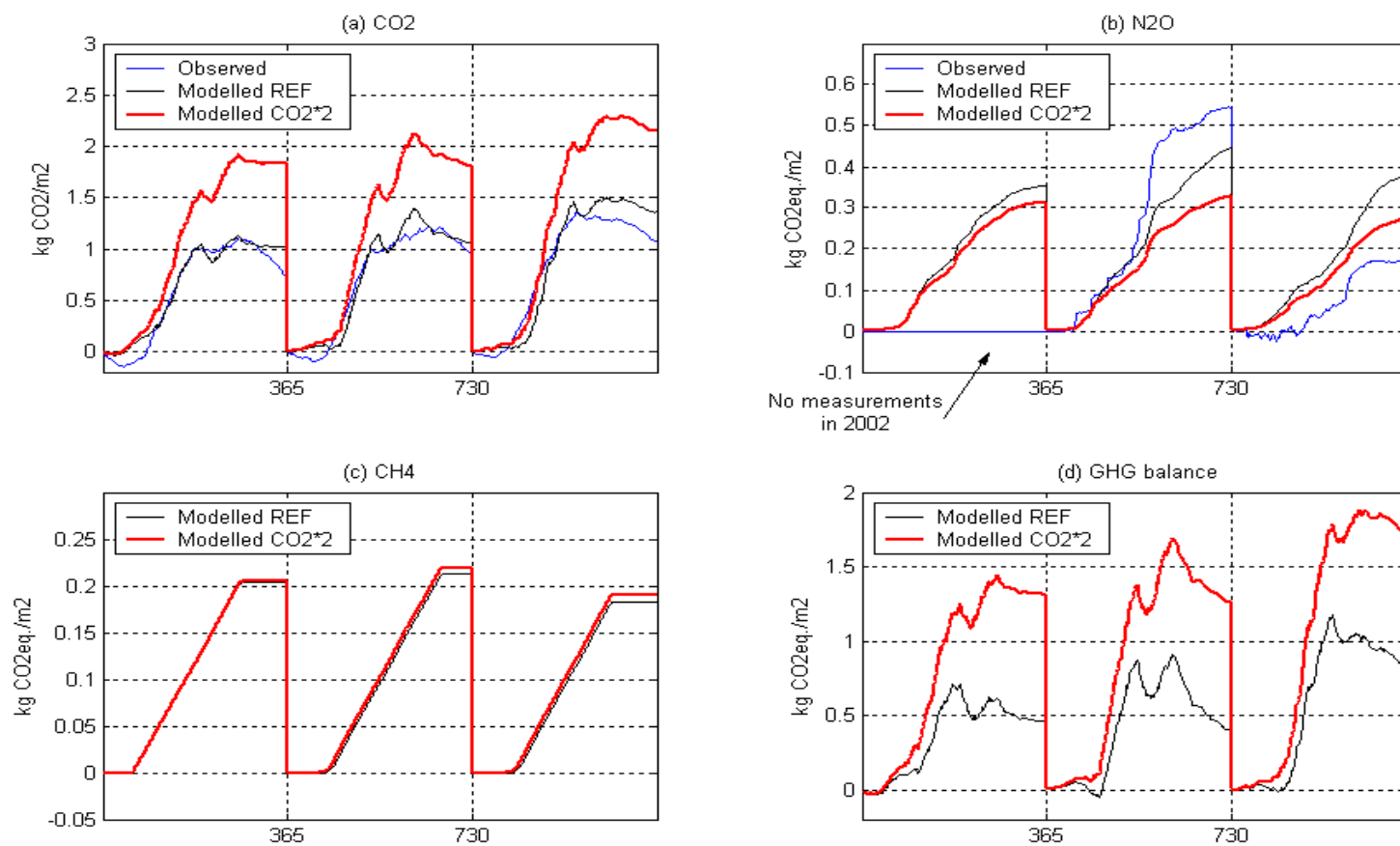


Figure 5.5: (a) CO₂ observed, reference modelled and modelled with CO₂*2; (b) N₂O observed, reference modelled and modelled with CO₂*2; (c) CH₄ reference modelled and modelled with CO₂*2; and (d) GHG balance reference modelled and modelled with CO₂*2, for 2002, 2003 and 2004, in kg CO₂ equiv.m⁻². N₂O and CH₄ emissions are shown on the positive axis for more legibility.

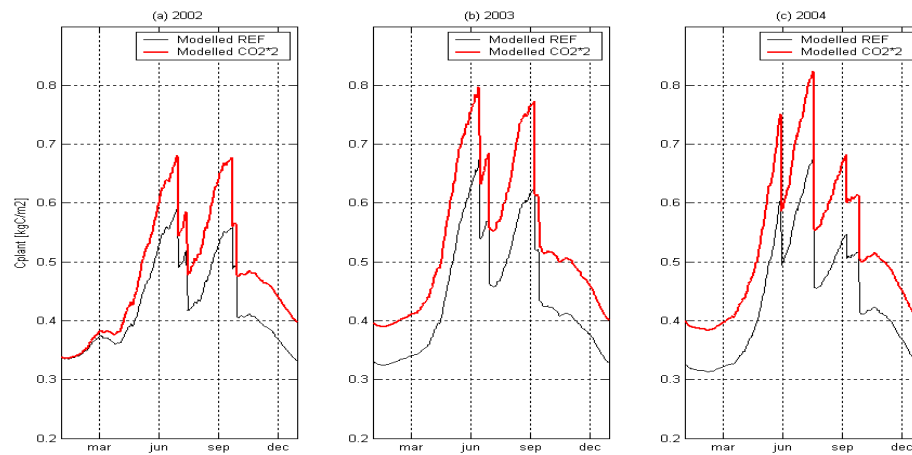


Figure 5.6: Concentration of carbon in the plant based on the reference simulation and the elevated CO₂ simulation, in kgC. m⁻², for (a) 2002, (b) 2003 and (c) 2004.

The increase of the CO₂ uptake may be explained by the fact that more carbon is available for the plant to be fixed (CO₂ is not limitant anymore). Indeed, shoot dry matter production is enhanced (not shown here) and the concentration of carbon in the plant is higher under elevated CO₂ (Figure 5.6). The response of modelled plant production to doubled CO₂ is consistent with field experiments [Picon-Cochard et al., 2004].

N₂O fluxes

The emissions of nitrogen are reduced significantly (between 11% and 27%). Like with the CC scenario, the annual emissions of N₂O for 2002 are quite close to the reference simulation. This may be as well due to the sensitivity of the model to initial conditions.

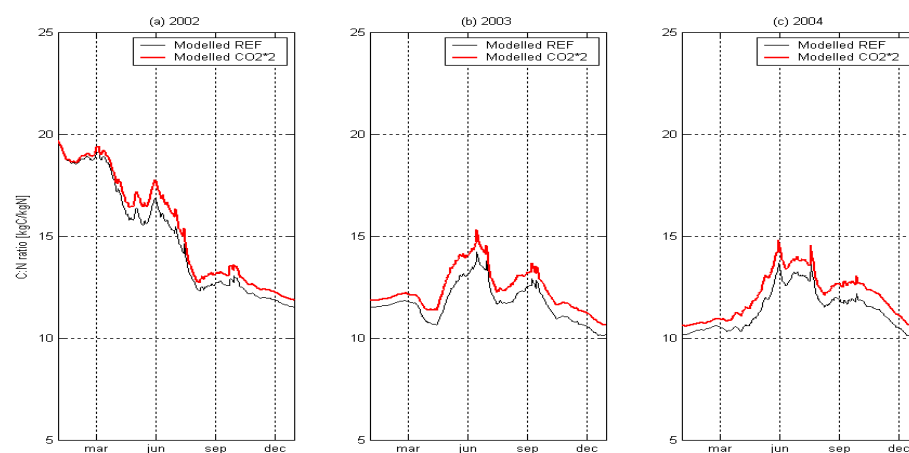


Figure 5.7: C:N ratio for plants for the reference simulation and the elevated CO₂ simulation, in kgC. kgN⁻¹, for (a) 2002, (b) 2003 and (c) 2004.

While the N₂O emissions decrease, the concentration of nitrogen in the plant increases (not shown). That is to say that grass is more efficient at fixing nitrogen and the ecosystem enters in the positive feedback described by Coughenour and Chen, [1997]. In parallel to the increase in the N concentration in the plant, the concentration of carbon in the plant augments (not shown). In addition, the C:N ratio in the plant increases in comparison with the reference simulation (Figure 5.7), so the ecosystem may use the extra carbon fixed under elevated CO₂ to acquire and retain nutrients [Cannell and Thornley, 1998].

CH₄ fluxes

Methane emissions start earlier under CO₂*2 because the gross primary production (and thus shoot DM available for the cattle, see Figure 5.6) is enhanced, but it does not make a big difference in the annual budget (less than 5% change).

GHG balance

The GHG balance under elevated CO₂ is much higher than under ambient conditions because the uptake of carbon dioxide by the plants is higher and the emissions of nitrous oxide are reduced at the same time.

5.4 Climate change and elevated CO₂ scenario

Here we simulate at the same time climate change and elevated CO₂ (CC + CO₂*2), a scenario that is more likely to happen. Figure 5.8 displays the summary of the three GHG budgets and the GHG balance. The curves are very similar to the one of the simulation under CO₂*2 only, however, when looking closer, the effect of elevated CO₂ is mitigated by the changes in temperature and precipitation.

CO₂ fluxes

NEE under CC + CO₂*2 scenario increase on average by 56% in relation to the reference simulation, whereas under elevated CO₂ scenario without CC, it increases by 70% in relation to the reference simulation (see Table 5.2 for the details). The overall increase is due to the CO₂ fertilisation effect and the slight decrease is due to the climate change.

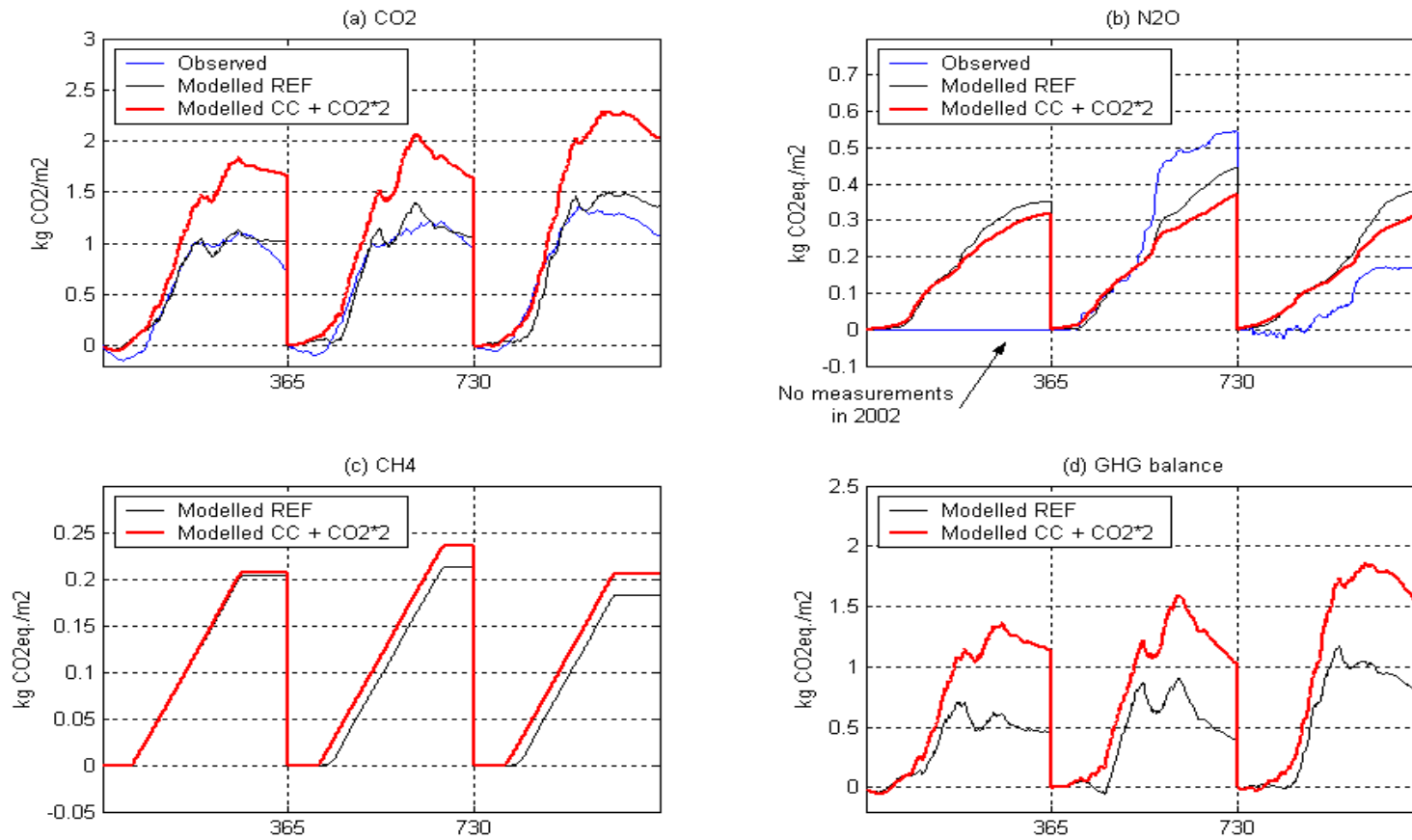


Figure 5.8: (a) CO₂ observed, reference modelled and modelled with CC + CO₂*2; (b) N₂O observed, reference modelled and modelled with CC + CO₂*2; (c) CH₄ reference modelled and modelled with CC + CO₂*2; and (d) GHG balance reference modelled and modelled with CC + CO₂*2 for 2002, 2003 and 2004, in kg CO₂ equiv. m⁻². N₂O and CH₄ emissions are shown on the positive axis for more legibility.

However, the GPP has the highest increase of the three scenarios (Table 5.2), thus, there is a cumulative positive effect of elevated CO₂ and climate change on the productivity of the plants. Coughenour and Chen, [1997] using linked plant-soil process models found that under doubled CO₂ and CC, the net primary production for C3 species increased by 25.8%. We find the same results with an increase of 26.3% in average for the three years.

Table 5.2: Comparison between the CC scenario, the CO₂*2 scenario and the CC + CO₂*2 scenario, expressed as a percentage of the reference simulation, for NEE, GPP and Rtot. Negative change is presented in red.

	2002			2003			2004		
	NEE	GPP	Rtot	NEE	GPP	Rtot	NEE	GPP	Rtot
CC	-21.2	5.0	9.0	-16.3	6.5	10.0	-9.3	6.9	10.2
CO ₂ *2	80.0	17.6	8.0	70.7	19.8	12.2	57.9	20.6	13.2
CC + CO ₂ *2	62.8	25.0	19.2	54.4	28.7	24.9	49.3	30.1	16.3

Rtot increases also more when combining the first two scenarios. Here as well, it is because of the combination of the two scenarios has a strong effect on the soil respiration (increased decomposition rates) and doubled CO₂ influences plants' respiration (higher productivity).

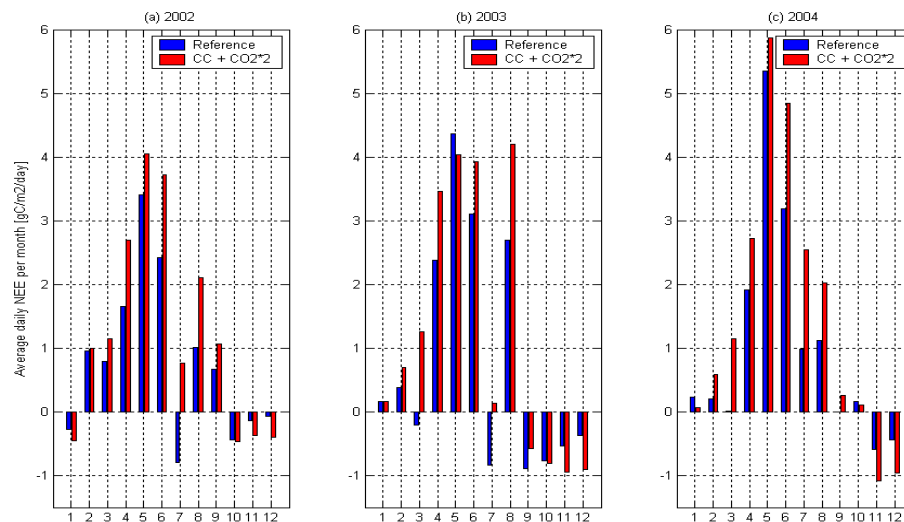


Figure 5.9: Daily NEE averaged on a monthly basis for the reference simulation and the CC + CO₂*2 simulation, in gC. m⁻². day⁻¹, for (a) 2002, (b) 2003 and (c) 2004.

Monthly fluxes presented in Figure 5.9 reflect the global increase of the CO₂ uptake, especially during the growing season and the summer. Only January and the last months of each year (plus May 2003) are smaller than the reference simulation, supposedly because of high heterotrophic respiration in relation to the high productivity during spring and summer.

N₂O fluxes

Annual emissions of nitrous oxide decreased by 9.8%, 16.8% and 16.9% respectively for 2002, 2003 and 2004 (Table 5.3). The decrease is smaller for the combination of the CC and the CO₂*2 scenarios than for elevated CO₂ only. Like the comment made for the NEE, the decrease caused by CO₂*2 may be partially counteracted by the negative effect of climate change.

Table 5.3: Comparison between the CC scenario, the CO₂*2 scenario and the CC + CO₂*2 scenario, expressed as a percentage of the reference simulation, for CO₂, N₂O and CH₄. Negative change is presented in red.

	2002			2003			2004		
	CO ₂	N ₂ O	CH ₄	CO ₂	N ₂ O	CH ₄	CO ₂	N ₂ O	CH ₄
CC	-21.2	4.5	0.6	-16.3	38.9	9.3	-9.3	55.1	10.4
CO ₂ *2	80.0	-11.1	0.7	70.7	-26.3	3.4	57.9	-27.5	4.1
CC + CO ₂ *2	62.8	-9.8	1.3	54.4	-16.8	10.9	49.3	-16.9	12.5

The cumulative curve of N₂O emissions (Figure 5.8b) for the reference simulation and for the CC + CO₂*2 get disconnected by mid-April in 2002, by mid-March for 2003 and from the very beginning of the year in 2004. The dissimilarity of the fluxes may come from an adaptation of the system to the environmental changes.

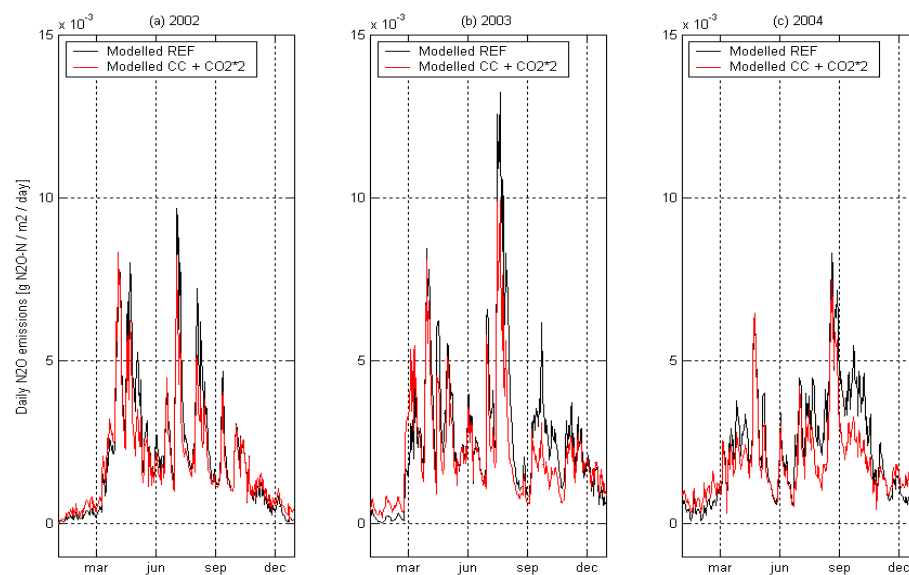


Figure 5.10: Daily N₂O emissions for the reference simulation and the CC + CO₂*2 simulation, in g N₂O-N. m⁻². day⁻¹, for (a) 2002, (b) 2003 and (c) 2004.

For the first half of the year, when slurry and fertilisers have not been spread yet, the daily emissions are similar (Figure 5.10). Emissions of nitrous oxide are reduced at the end of the summer because plants fix a lot of nitrogen during the summer through photosynthesis. 2004 was the year of highest CO₂ uptake and so, of the highest nutrient utilisation, thus, of more reduced N₂O emissions.

Table 5.4: Summary of total N applications, N₂O emissions and emission factor for the reference simulation and the CC + CO₂*2 simulation, for 2002, 2003 and 2004.

	N application (kgN. ha ⁻¹)	N ₂ O emission (kgN. ha ⁻¹)		Emission factor (%)	
	Modelled	REF	CC + CO ₂ *2	REF	CC + CO ₂ *2
2002	305	7.6	6.8	2.5	2.3
2003	334	9.6	8.0	2.9	2.4
2004	207	8.3	6.9	4.0	3.3

Table 5.4 presents the comparison between the emission factors for the reference and the CC + CO₂*2 simulations. The emission factors obtained for the new simulation are still within the range given in the IPCC [IPCC, 1997], see section 4.3.

CH₄ fluxes

Methane fluxes under the combination of the two previous scenarios are a little higher than under the reference scenario. They are even higher than under each scenario taken separately (Table 5.3), unlike to CO₂ and N₂O fluxes for which there is mitigation between the effects of the two scenarios. As those emissions are highly dependant on the quality and quantity of forage, there seems to be a positive combination of climate change and elevated CO₂ on the grass production. This is a confirmation of what was previously concluded about the GPP.

GHG balance

As a consequence of the higher uptake of CO₂ and reduced emissions of N₂O, the role of the grassland as a greenhouse gas sink is enhanced under climate change and elevated CO₂. The grassland uptakes 11.3, 10.3 and 15.0 kg CO₂ equiv. ha⁻¹. yr⁻¹ respectively for the three years of simulation, that is to say, is almost triple for 2002 and 2003 and double for 2004, in comparison with the simulation under ambient conditions.

5.5 REPS scenario

5.5.1 Definition of the scenario in terms of management data

For this scenario, all the sources of nitrogen added to the ecosystem must be considered. REPS discusses about nitrogen from animals and other wastes (that is to say urine and faeces of cattle grazing on the field), and about slurry that is produced by cattle when housed indoors (in winter). There is no application of manure or urea for the Dripsey site. Table 5.5 presents a summary of the actual amount of nitrogen spread on the fields.

Table 5.5: Nitrogen in kgN. ha⁻¹ received by the fields. * PaSim models those values.

	Fertilisers	Slurry	Urine*	Faeces*	Animals' Total	TOTAL N
2002	214	91	68	45	204	418
2003	204	130	89	60	279	483
2004	177	30	76	50	156	333

REPS requires that the total nitrogen from animals and wastes should be less than 170 kgN. ha⁻¹ (this does not account for chemical fertiliser). Only the year 2004 complies with this recommendation. And even if we have doubts concerning the validity of the slurry amount in 2004, there can be a margin of 14 kgN. ha⁻¹. The surplus will be subtracted from the applications of slurry (and not by reducing the grazing period or the density of cows because it can affect the farmers economical balance).

Table 5.6: Application of chemical fertilisers and slurry, in kgN. ha⁻¹, under actual management and REPS scenario. * this may be underestimated.

	Actual		REPS		% Change	
	Fert.	Slurry	Fert.	Slurry	Fert.	Slurry
2002	214	91	90	58	- 58%	- 36%
2003	204	130	90	20	- 56%	- 85%
2004	177	30*	104	30	- 41%	-

The total of nitrogen (i.e. chemical fertiliser, animals' waste and other wastes, e.g. slurry) should be inferior to 260 kgN. ha⁻¹. Neither of the years complies with it. The surplus, once the condition about nitrogen from animals and wastes is respected, will be taken out

from the applications of fertilisers. The reductions in the fertilisers and slurry applications to comply with REPS are shown in Table 5.6. Concerning the management input file, the timing of the applications of nitrogen remains the same and the amount of nitrogen spread is reduced with the calculated percentage (Table 5.6).

5.5.2 Results and analysis

Figure 5.11 shows the results of the simulation injecting the application rates recommended by the REPS. In a nutshell, the uptake of CO₂ remains about the same, the emissions of N₂O are considerably increased, methane emissions remain the same, and as a result, the uptake of GHG is more pronounced (Table 5.7).

CO₂ fluxes

There is little variation in the overall uptake of carbon dioxide (Table 5.7) and even smaller variation in the shoot dry matter (not shown here). We observe a decrease of the gross primary productivity smaller than 1%. It means that the reduction in the amount of nitrogen does not affect much the yield of the plants and thus, it can be concluded that too much nitrogen is spread compared to the needs of the grassland.

N₂O fluxes

The emissions of nitrous oxide decrease by 37.2%, 49.3% and 38.0% respectively for the three years of simulation (Table 5.7) while the total amount of nitrogen spread has been reduced by respectively 51.5%, 67.1% and 35.3%.

Table 5.7: Percentage of change between the reference simulation and the REPS simulation for the GHG balance, CO₂, N₂O and total nitrogen applications.

	2002	2003	2004
GHG sink	+ 21.8%	+ 62.6%	+ 17.3%
CO ₂	- 3.1%	+ 2.9%	- 0.7%
N ₂ O	- 37.2%	- 49.3%	- 38.0%
N applications	- 51.5 %	- 67.1%	- 35.3%

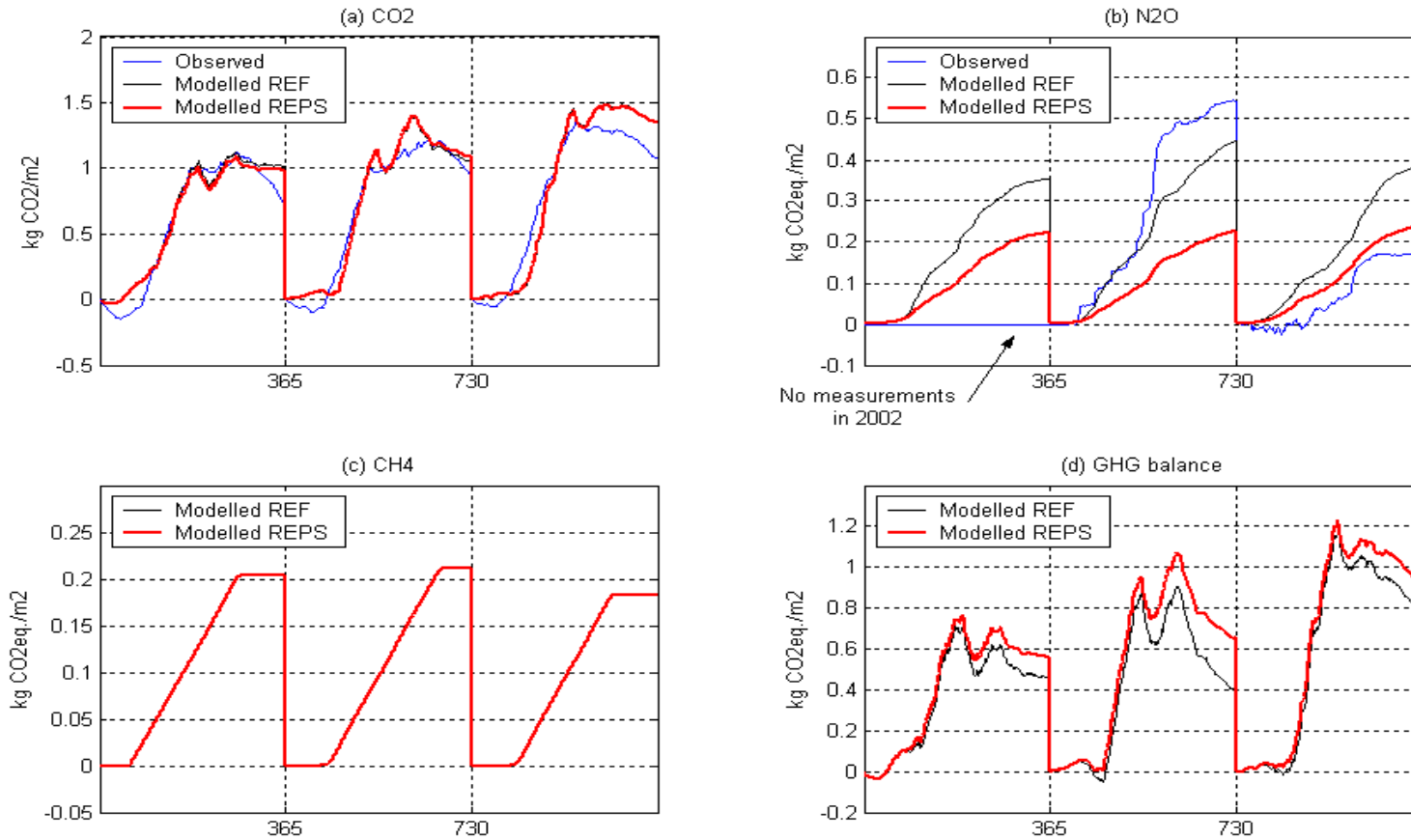


Figure 5.11: (a) CO₂ observed, reference modelled and modelled with REPS; (b) N₂O observed, reference modelled and modelled with REPS; (c) CH₄ reference modelled and modelled with REPS; and (d) GHG balance reference modelled and modelled with REPS for 2002, 2003 and 2004, in kg CO₂ equiv. m⁻². N₂O and CH₄ emissions are shown on the positive axis for more legibility.

The minimal daily N₂O fluxes (Figure 5.12) with reduction in fertilisers' applications are slightly smaller, whereas the peaks of emissions decrease a lot.

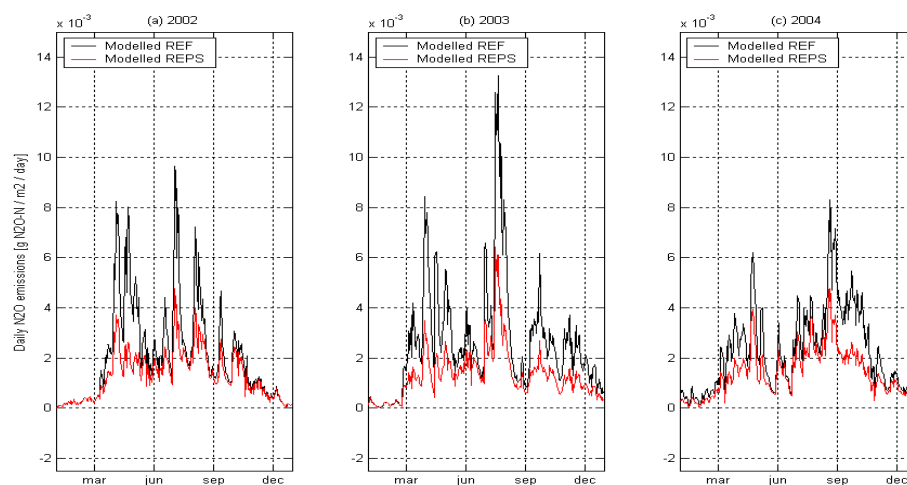


Figure 5.12: Daily N₂O emissions for the reference simulation and the REPS scenario, in g N₂O-N. m⁻². day⁻¹, for (a) 2002, (b) 2003 and (c) 2004.

The emissions factors (Table 5.8) when respecting the REPS recommendations are well under the values given by the IPCC guideline (that is to say respectively 3.8, 4.2 and 2.6%), except for 2004 (because of the uncertainty about the slurry applications).

Table 5.8: Summary of observed and measured N applications, N₂O emissions and emission factor for 2002, 2003 and 2004.

	Total N application (kgN. ha ⁻¹)		N ₂ O emission (kgN. ha ⁻¹)		Emission factor (%)	
	Reference	REPS	Reference	REPS	Reference	REPS
2002	305	148	7.6	4.8	2.5	1.6
2003	334	110	9.6	4.9	2.9	1.5
2004	207	134	8.3	5.2	4.0	2.5

CH₄ fluxes

As the dry matter yield is not changed, the cattle have the same quality and quantity of grass and so the emissions of methane remain the same. The percentage change between the REPS simulation and the reference simulation does not exceed 1%.

GHG balance

For the three years, the GHG balance is improved by at least 17% (Table 5.7). In 2003, there is a 63% increase in the sink activity of the ecosystem (the year of highest decrease of N applications). To conclude, a reduction of nitrogen application: does not decrease the uptake of carbon dioxide; does not decrease the dry matter yield; and brings the nitrous oxide emissions significantly down. In addition, farmers will save money on fertiliser and the water quality of the surrounding streams will be improved. In other words, there seems to be many significant advantages in reducing the total amount of nitrogen spread on the fields. Furthermore, the grassland could even be a larger GHG sink if recommendations about cattle density were introduced as cattle add a considerable amount of nitrogen through faeces and urine and emit a huge volume of methane. However, because the model has been run only for three years, this may be a transient period where the ecosystem relies on the high soil content of nutrient that has been built during the twenty years of intensive management.

Chapter 6

Conclusion

Chapter 6

Conclusion

6.1 Conclusion

PaSim is a complex biogeochemical model driven by hourly meteorological data. We parameterised the model using measurements, literature values and model optimisation (from the comparison of the observations of CO₂ and N₂O measured by an eddy covariance systems).

The model provides a good estimate of the CO₂ fluxes, especially during the growing season. The cumulative end of year CO₂ fluxes are about 28% higher for the model than those of the observations over the three years. The N₂O fluxes modelled by PaSim are not as accurate as those for CO₂; the daily maximum modelled N₂O fluxes are lower than the measured fluxes and the model does not always simulate the sudden emission after the spreading of fertilisers. For CH₄ emissions, we do not have measurements to compare with, but PaSim seems to give a good estimation (by comparison with IPCC estimates). Once all the greenhouse gases were modelled, we combined them using their global warming potential, and so calculated the GHG balance, in CO₂ equivalents. For modelled GHGs, the grassland site is a sink of 4.6, 4.0 and 7.9 T of CO₂ equiv. ha⁻¹ respectively for 2002, 2003 and 2004. For observed GHGs, considering that methane emissions have been estimated by the IPCC guideline, there is a sink of 1.6 only T of CO₂ equiv. ha⁻¹ in 2003, and of 6.9 T of CO₂ equiv. ha⁻¹, which is very close to the modelled GHG balance. The GHG balance for 2002 is not calculated as there are no N₂O measurements and CH₄ is only estimated.

As regard model scenarios, we firstly run the model under an IS92a climate change scenario for temperature and precipitation. The uptake of CO₂ decreased (as the soil respiration due to high decomposing rate increased more than the gross primary production). The N₂O emissions increased as the reactions of nitrification and denitrification are more likely to happen when the temperature increases. These two trends accounted for the reduction of the GHG balance.

Secondly, we run the model under elevated CO₂ only. As a consequence, the CO₂ uptake increased in a great extent because of the enhanced gross primary production. The N₂O emissions were reduced significantly as the plants use nitrogen more efficiently. These two results tend to increase the CO₂ sink greatly.

We gain understanding of the mechanisms of the reaction of the ecosystem by decomposing the CC + CO₂*2 scenario into two scenarios: IS92a CC scenario only and

CO₂*2 scenario only; and finally, we run the model under the combination of the two previous scenarios (i.e. CC + CO₂*2). We found that the carbon sink strength of the grassland is enhanced by a factor of two or three. This is a consequence of enhanced CO₂ uptake and reduced N₂O emissions (same pattern as under the CO₂*2 scenario only). The GHG balance under the combination of CC + CO₂*2 is smaller than the one under CO₂*2 only, and higher than the one under CC only. So we could conclude that the C sink increased due to elevated CO₂, but part of the CO₂ sink was counteracted by the negative effect of the climate change.

Under a reduction of nitrogen applications according to the recommendations of the Irish REPS, the GHG balance is improved (i.e. sink enhanced). The uptake of CO₂ by the plants as well as their productivity is not reduced (as expected!), and the N₂O emissions are reduced. This is an important finding that can be help to convince farmers of the benefits of reducing the N applications. A parallel consequence is that the surrounding environment (e.g. rivers and streams) will receive less nutrients (nitrogen, phosphorus, potassium).

Research groups (Swiss Federal Station for Agroecology and Agriculture; Laboratoire des Sciences du Climat et de l'Environnement CEA-CNRS, France; Unité d'Agronomie INRA, France) have been improving PaSim for over ten years now. Nonetheless, during this study, some limits of the model were identified such as the overestimation of the CO₂ fluxes in winter when it produces too much biomass (this fault is being investigated, by Calanca et al., 2005). Moreover, the model was unable to model the N₂O fluxes accurately. Some of the uncertainty is due to fact that the farmers' data log sheets are not always very precise and there seems to be some missing data, so the input data for nitrogen applications may not be precisely what was applied to the land. In addition, the C and N pools, that cannot be easily measured, have a strong influence on the results of the model, especially for the first year of modelling.

Finally, we have to keep in mind that even if the model is comparable with observations under today's conditions, this comparison may not imply precision of the model under changed conditions [Hanninen, 1995]; absolute values are not to be taken into consideration; only the relative change can give an idea of the trend of the model's response.

6.2 Suggestion for further investigation

We underlined that the modelling of the management practices was difficult as there were numerous fields within the footprint with different management in each. Additional work to improve the modelling can be done by running the model for each field separately

with the exact management practices, and then aggregating the results of the multiple runs. The aggregation can be based on a weighted-area average.

This study focused on the GHG balance at the ecosystem scale (~ 50 ha), this could be enlarged to the catchment or regional scale. CO₂ emissions of agricultural machines, GHG emissions for the use of electricity, emissions from the production of fertilisers, etc could also be considered.

While considering a climate change scenario, we only took into account the perturbations in temperature and in precipitation. The use of General Circulation Models (GCMs) generating data for incoming radiation and relative humidity may strengthen the results of the simulation. Moreover, we changed in a single step the input data for temperature, precipitation and atmospheric CO₂, so the ecosystem was not in equilibrium anymore and we studied the transient response of the grassland. But, these individual changes will occur progressively. To improve the modelling of the grassland responses to climate change, perturbation data files introduced at a defined step, equilibrium run and acclimation factors (changes in the photosynthesis processes or alterations in the community structure) can be considered.

We also have three years of continuous CO₂ measurements and precise management data for a grassland in Wexford (south-east of Ireland) and it could be interesting to use PaSim to model those fluxes and study the sensitivity of the model to another site with slightly different soil parameters and a more moderate climate (less rainfall, higher temperature).

Finally, we can exploit other outputs of the model such as the simulation of the carbon in the different pools of the soil, so the carbon sequestration could be investigated as C uptake by ecosystems may compensate for some emissions of greenhouse gases [IPCC, 2001]. It would require more field measurements, particularly soil organic carbon (SOC), and a better understanding of the carbon dynamics in soil in relation with the plants.

References

References

- Arneeth, A., Kelliher, F.M., McSeveny, T.M. and Byers, J.N. (1998). Net ecosystem productivity, net primary productivity and ecosystem carbon sequestration in a *Pinus radiata* plantation subject to soil water deficit. *Tree Physiology*, 18, 785-793.
- Baldocchi, D.D. (2003). Assessing the eddy covariance technique for evaluating carbon dioxide exchange rates of ecosystems: past, present and future. *Glob. Change Biol.*, 9, 479-492.
- Baldocchi, D.D., Vogel, C.A. and Hall, B. (1997). Seasonal variation of carbon dioxide exchange rates above and below a boreal jack pine forest. *Agri. For. Meteorol.*, 83, 147-170.
- Baldocchi, D. (1992). A Lagrangian random-walk model for simulating water vapor, CO₂ sensible heat densities and scalar profiles over and within a soybean canopy. *Boundary-Layer Meteorol.*, 61, 113-144.
- Barnard, R., Leadley, P.W. and Hungate, B.A. (2005). Global change, nitrification, and denitrification: A review. *Glob. Biogeochem. Cycles*, 19, doi:10.1029/2004GB002282.
- Bowling, D.R., Tans, P.P. and Monson, R.K. (2001). Partitioning net ecosystem carbon exchange with isotopic fluxes of CO₂. *Glob. Change Biol.*, 7, 127-145.
- Brown, J.F. (1998). *Mapping global grassland ecosystem: a comparison of four data sets*. Proceedings of the IEEE International Geoscience and Remote Sensing Symposium Proceedings, Seattle, Washington.
- Brutsaert, W. (1991). *Evaporation into the Atmosphere: Theory, History, and Applications*. Kluwer Academic Publishers, Boston.
- Calanca, P. (2005). *Personal communication*. Swiss Federal Research Station for Agroecology and Agriculture.
- Campbell, S.G. and Norman, J.M. (1998). *An introduction to environmental Biophysics, second edition*. Springer-Verlag, New York.
- Campbell (2003a). Model HMP45C temperature and relative humidity probe instruction manual. *Campbell Scientific, Inc.*, USA. <http://www.campbellsci.co.uk>.
- Campbell (2000). Tipping bucket rain gauges, ARG100. *Campbell Scientific, Inc.*, USA. <http://www.campbellsci.co.uk>.
- Campbell (2003b). Model 107 & 107B temperature probes instruction manual. *Campbell Scientific, Inc.*, USA. <http://www.campbellsci.co.uk>.
- Campbell (2005). TGA100A trace gas analyser overview. *Campbell Scientific, Inc.*, USA. http://www.campbellsci.com/documents/manuals/tga100a_ov.pdf.
- Campbell (1998). CSAT3 three dimensional sonic anemometer instruction manual. *Campbell Scientific, Inc.*, USA. <http://www.campbellsci.com/documents/manuals/csat3.pdf>.
- Campbell (2002). CS616 water content reflectometer. *Campbell Scientific, Inc.*, USA. www.campbellsci.co.uk/products/sensors/cs616.htm.

References

- Cannell, M.G.R. and Thornley, J.M.H. (1998). N-poor ecosystem may respond more to elevated [CO₂] than N-rich ones in long term. A model analysis of grassland. *Glob. Change Biol.*, 4, 431-442.
- Cao, M. and Woodward, I. (1998). Net primary and ecosystem production and carbon stocks of terrestrial ecosystems and their response to climate change. *Glob. Change Biol.*, 4, 185-198.
- CarboEurope-GHG (2004). Greenhouse Gas Emissions from European Grasslands. <http://gaia.agraria.unitus.it/ceuroghg/ReportSS3.pdf>.
- Chen, D.-X., Hunt, H.W. and Morgan, J.A. (1996). Responses of a C₃ and C₄ perennial grass to CO₂ enrichment and climate change: Comparison between model predictions and experimental data. *Ecol. Model.*, 96, 11-27.
- Clapp, R.B. and Hornberger, G.M. (1978). Empirical equations for some hydraulic properties. *Water Resources Research*, 14, 601-604.
- Coughenour, M.B. and Chen, D.-X. (1997). Assessment of grassland and ecosystem responses to atmospheric change using linked plant-soil process models. *Ecol. Appl.*, 7, 802-827.
- Dabberdt, W.F., Lenschow, D.H., Horst, T.W., Zimmerman, P.R., Oncley, S.P. and Delany, A.C. (1993). Atmosphere-surface exchange measurements. *Science*, 260, 1472-1481.
- Daly, K. (1999). *An Environmental appraisal of the phosphorous of the Irish grassland soils*. PhD. Thesis, Trinity College, Dublin.
- DeRamus, H.A., Clement, T.C., Giampola, D.D. and Dickison, P.C. (2003). Methane emissions of beef cattle on forages. *Journal of Environmental Quality*, 32, 269-277.
- Dingman, S.L. (1994). *Physical Hydrology*. Macmillan Publishing Company, New York.
- Dobbie, K.E., McTaggart, I.P. and Smith, K.A. (1999). Nitrous oxide emissions from intensive agricultural systems: Variations between crops and seasons, key driving variables, and mean emission factors. *J. Geophys. Res.*, 104, 26,891-26,899.
- Dobbie, K.E. and Smith, K.A. (2003). Nitrous oxide emission factors for agricultural soils in Great Britain: the impact of soil water-filled pore space and other controlling variables. *Glob. Change Biol.*, 9, 204-218.
- Dorsey, J. (2002). UMIST, Atmospheric Physics Research Group, Introduction to the eddy covariance method. Manchester, UK. <http://cloudbase.phy.umist.ac.uk/people/dorsey/Edco.htm>.
- Edwards, G.C., Thurtell, G.C., Kidd, G.E., Dias, G.M. and Wagner-Riddle, C. (2003). A diode laser based gas monitor suitable for measurement of trace gas exchange using micrometeorological techniques. *Agri. For. Meteorol.*, 115, 71-89.
- EncyclopediaBritannica (2002).
- EnvironmentalMediaService (2003). Pentagon Report Describes Global Warming Dangers. http://www.ems.org/climate/pentagon_climate_change.html#report.

References

- EPA (2000). *Ireland's environment, chapter 4: Emissions to air, A Millennium Report*. Edited by Michael McGettigan
- EPA (2003). *National Inventory Report 2003, Greenhouse gas emissions 1990-2001 reported to the United Nations framework convention on climate change*. Edited by Michael McGettigan and Paul Duffy
- Falge, E., Baldocchi, D., Olson, R., Athoni, P., Aubinet, M., Bernhofer, C., Burba, G., Ceulemans, R., Clement, R., Dolman, H., Granier, A., Gross, P., Grünward, T., Hollinger, D., Jensen, N.-O., Katul, G., Keronen, P., Kowalski, A., Lai, C.T., Law, B.E., Meyers, T., Moncrieff, J., Moors, E., Munger, J.W., K., P., Rannik, Ü., Rebmann, C., Suyker, A., Tenhunen, J., Tu, K., Verma, S., Vesala, T., Wilson, K. and Wofsy, S. (2001). Gap filling strategies for defensible annual sums of net ecosystem exchange. *Agri. For. Meteorol.*, 107, 43-69.
- Falge, E., Baldocchi, D., Tenhunen, J., Aubinet, M., Bakwin, P., Berbigier, P., Bernhofer, C., Burba, G., Clement, R. and Davis, K.J. (2002). Seasonality of ecosystem respiration and gross primary production as derived from FLUXNET measurements. *Agri. For. Meteorol.*, 113, 53-74.
- FAO (1998). *Crop evapotranspiration - Guidelines for computing crop water requirements - FAO Irrigation and drainage paper 56*. Food and Agriculture Organisation of the United Nations, Rome.
- FAO (1988). *Milk and dairy products: production and processing costs - FAO Animal production and health paper 62*. Food and Agriculture Organisation of the United Nations
- Flanagan, L.B., Wever, L.A. and Carlson, P.J. (2002). Seasonal and interannual variation in carbon dioxide exchange and carbon balance in a northern temperate grassland. *Glob. Change Biol.*, 8, 599-615.
- Flanagan, L.B. and Johnson, B.G. (2005). Interacting effects of temperature, soil moisture and plant biomass production on ecosystem respiration in a northern temperate grassland. *Agri. For. Meteorol.*, 130, 237-253.
- Foken, T. and Wichura, B. (1996). Tools for quality assessment of surface-based flux measurements. *Agri. For. Meteorol.*, 78, 83-85.
- Follett, R.F., Paul, E.A., Leavitt, S.W., Halvorson, A.D., Lyon, D. and Peterson, G.A. (1997). Carbon isotope ratios of Great Plains and in wheat-fallow systems. *Soil Sci. Soc. Am. J.*(61), 1068-1077.
- Foy, J.K., Teague, W.R. and Hanson, J.D. (1999). Evaluation of the upgraded SPUR model (SPUR2.4). *Ecol. Model.*, 118, 149-165.
- Frank, B.A. and Dugas, A.W. (2001). Carbon dioxide fluxes over a northern, semiarid, mixed-grass prairie. *Agri. For. Meteorol.*, 108, 317-326.
- Frank, A.B. (2002). Carbon dioxide fluxes over a grazed prairie and seeded pasture in the Northern Great Plains. *Environmental Pollution*, 116, 397-403.
- Franzluebbers, K., Franzluebbers, A.J. and Jawson, M.D. (2002). Environmental controls on soil and whole-ecosystem respiration from a tallgrass prairie. *Soil Sci. Soc. Am. J.*, 66, 254-262.

References

- Frolking, S., Roulet, N.T., Moore, T.R., Lafleur, P.M., Bubier, J.L. and Crill, P.M. (2002). Modelling seasonal to annual carbon balance of Mer Bleue Bog, Ontario, Canada. *Glob. Biogeochem. Cycles*, 16, 10.1029/2001GB001457.
- Garatt, J.R. (1992). *The Atmospheric Boundary Layer*. Cambridge University Press, Cambridge.
- Gardiner, M.J. and Radford, T. (1980). *Soil Associations of Ireland and Their Land Use Potential*. An Foras Talúntais, Dublin.
- Gordon, C., Cooper, C., Senior, C.A., Banks, H., Gregory, J.M., Johns, T.C., J.F.B., M. and Wood, R.A. (2000). The simulation of SST, sea ice extents and ocean heat transports in a version of the Hadley Centre coupled model without flux adjustments. *Climate Dynamics*, 16, 147-168.
- Guenther, B.A. and Hills, A.J. (1998). Eddy covariance measurement of isoprene fluxes. *J. Geophys. Res.*, 103, doi: 10.1029/97JD03283.
- Hamby, D.M. (1994). A review of techniques for parameter sensitivity analysis of environmental models. *Environ. Monit. Ass.*, 32, 135-154.
- Hanninen, H. (1995). Assessing ecological implications of climatic change: can we rely on our simulation results? *Clim. Change*, 31(1-4).
- Hanson, P.J., Edwards, N.T., Garten, C.T. and Andrews, J.A. (2000). Separating root and soil microbial contributions to soil respiration: A review of methods and observations. *Biogeochemistry*, 48, 115-146.
- Hollinger, D.Y., Kelliher, F.M., Byers, J.N., Hunt, J.E., McSeveny, T.M. and Weir, P.L. (1994). Carbon dioxide exchange between an undisturbed old-growth temperate forest and the atmosphere. *Ecology*, 75, 134-150.
- Hsieh, C.-I., Katul, G.G., Schieldge, J., Sigmon, J.T. and Knoerr, K.K. (1997). The Lagrangian stochastic model for fetch and latent heat flux estimation above uniform and non-uniform terrain. *Water Resources Res.*, 33, 427-438.
- Hsieh, C.-I., Katul, G.G. and Chi, T.-W. (2000). An approximate analytical model for footprint estimation of scalar fluxes in thermally stratified atmospheric flows. *Advances in Water Resources*, 23, 765-772.
- Hsieh, C.-I., Leahy, P., Kiely, G. and Li, C. (2005). The effect of future climate perturbations on N₂O emissions from a fertilised humid grassland. *Nutrient Cycling in Agroecosystems*, Submitted.
- Hunt, H.W., Trlica, M.J., Redente, E.F., Moore, J.C., Detling, J.K., Kittel, T.G.F., Walter, D.E., Fowler, M.C., Klein, D.A. and Elliott, E.T. (1991). Simulation model for the effects of climate change on temperate grassland ecosystems. *Ecol. Model.*, 53, 205-246.
- IPCC (2001). *Climate Change 2001: The Scientific Basis*. Intergovernmental Panel on Climate Change; D. J.T. Houghton, Y. , Griggs, D.J., Noguera, M., van der Linden, P.J., Dai, X., Johnson, C.A., Maskell, K., eds.; Cambridge University Press, Cambridge, U.K.

References

- IPCC (1996). *Climate Change 1995: The Science of Climate Change*. Contribution of Working Group 1 to the second assessment report of the Intergovernmental Panel on Climate Change; J. T. Houghton, Meira Filho, L.G., Callander, B.A., Harris, N., Kattenberg, A. and Maskell, K., eds.; Cambridge University Press, Cambridge, UK.
- IPCC (1997). Revised 1996 IPCC Guidelines for National Greenhouse Gas Inventories. <http://www.ipcc-nggip.iges.or.jp/public/gl/invs1.htm>.
- IPCC (2000). *Special Report on Emissions Scenarios*. Nakicenovic, N., J. Alcamo, G. Davis, B. de Vries, J. Fenhann, S. Gaffin, K. Gregory, A. Grübler, T. Yong Jung, T. Kram, E.L. La Rovere, L. Michaelis, S. Mori, T. Morita, W. Pepper, H. Pitcher, L. Price, K. Riahi, A. Roehrl, H.-H. Rogner, A. Sankovski, M. Schlesinger, P. Shukla, S. Smith, R. Swart, S. van Rooijen, N. Victor and Z. Dadi (eds.). A Special Report of Working Group III of the intergovernmental Panel on Climate Change, Cambridge University Press, Cambridge, UK.
- Ito, A. and Oikawa, T. (2002). A simulation model of the carbon cycle in land ecosystems (Sim-CYCLE): a description based on dry-matter production theory and plot-scale validation. *Ecol. Model.*, 151, 143-176.
- Jain, A.K., Kheshgi, H.S. and Wuebbles, D.J. (1994). Integrated Science Model for Assessment of Climate Change. *Lawrence Livermore National Laboratory*, UCRL-JC-116526.
- Jaksic, V. (2004). *Observations and modelling of carbon dioxide and energy fluxes from an Irish grassland for a two year campaign*. M.Eng.Sc. Thesis, University College, Cork, Ireland.
- Johnson, K.A. and Johnson, D.E. (1995). Methane Emissions from Cattle. *J. Anim. Sci.*, 73, 2483-2492.
- Joos, F., Bruno, M., Fink, R., Siegenthaler, U. and Stocker, T.F. (1996). An efficient and accurate representation of complex oceanic and biospheric models of anthropogenic carbon uptake. *Tellus*, 48B, 397-417.
- Jordan, C. (1997). *Mapping of rainfall chemistry in Ireland 1972-94*. Biology and Environment: Proceedings of the Royal Irish Academy.
- Keane, T. and Collins, J.F. (2004). *Climate, Weather and Irish Agriculture*. AGMET, Dublin.
- Kiely, G. (1997). Global climate change-greenhouse gases. In *Environmental Engineering*. McGraw-Hill Publishing Company, UK, pp. 358-362.
- Kinerson, R.S., Ralston, C.W. and Wells, C.G. (1977). Carbon cycling in a loblolly pine plantation. *Oecologia*, 29, 1-10.
- Kipp and Zonen (2000). CNR1 Net-Radiometer instruction manual. *Kipp & Zonen*, Delft, Netherlands. http://www.campbellsci.ca/CampbellScientific/Catalogue/CNR1_Br.pdf.
- Kipp and Zonen (2001). PAR LITE Sensor for photosynthetic photon flux. *Kipp & Zonen*, Delft, Netherlands. http://www.campbellsci.ca/CampbellScientific/Catalogue/PAR_Lite_Br.pdf.

References

- Kirschbaum, M.U.F., Eamus, D., Gifford, R.M., Roxburgh, S.H. and Sands, P.J. Definitions of Some ecological terms commonly used in carbon accounting. http://svc237.bne113v.server-web.com/crc/ecarbon/publications/nee/chapter_definitions.pdf.
- KyotoProtocol (1997). The text of the Kyoto Protocol is available at: www.unfccc.de.
- Laville, P., Jambert, C., Cellier, P. and Delmas, R. (1999). Nitrous oxide fluxes from a fertilised maize crop using micrometeorological and chamber methods. *Agri. For. Meteorol.*, 96, 19-38.
- Lawton, D., Leahy, P., Kiely, G., Byrne, K. and Calanca, P. (2005). Observations and process-based modeling of the net ecosystem exchange and its components for a humid grassland ecosystem. *Glob. Change Biol.*, submitted.
- Le Bris, C. (2002). *Observations and modelling of carbon dioxide flux from an Irish Grassland for a one year campaign*. M.Eng.Sc. Thesis, University College, Cork, Ireland.
- Leahy, P., Kiely, G. and Scanlon, T.M. (2004). Managed grasslands: A greenhouse gas sink or source? *Geophysical Research Letters*, 31, doi:10.1029/2004GL021161.
- Leggett, J., Pepper, W.J., Swart, R.J., Edmonds, J., Meira Filho, L.G., Mintzer, I., Wang, M.X. and Watson, J. (1992). Emissions Scenarios for the IPCC: an Update. In *Climate Change 1992: The Supplementary Report to The IPCC Scientific Assessment*. Cambridge University Press, UK, pp. 68-95.
- Leiros, M.C., Trasar-Cepeda, C., Seoane, S. and Gil-Sotres, F. (1999). Dependence of mineralization of soil organic matter on temperature and moisture. *Soil Biol. Biochem.*, 31, 327-335.
- Lewis, C. (2003). *Phosphorus, nitrogen and suspended sediment loss from soil to water from agricultural grassland*. M.Eng.Sc. Thesis, University College, Cork, Ireland.
- Li, C., Frohling, S. and Harriss, R. (1994). Modeling carbon biogeochemistry in agricultural soils. *Global Biogeochem. Cycles*, 8, 237-254.
- Liang, X., Xie, Z. and Huang, M. (2003). A new parameterization for surface and groundwater interactions and its impact on water budgets with the variable infiltration capacity (VIC) land surface model. *Journal of Geophysical Research*, 108, doi:10.1029/2002JD003090.
- LI-COR (2001). LI-7500 Product Information. *LI-COR, Inc*, USA. <http://www.licor.com>.
- Mengelkamp, H.T., Warrach, K. and Raschke, E. (1999). SEWAB – a parameterization of the Surface Energy and Water Balance for atmospheric and hydrologic models. *Advances in Water Resources*, 23, 165-175.
- Mosier, A.R., Duxbury, J.M., Freney, J.R., Heinemeyer, O. and Minami, K. (1996). Nitrous oxide emissions from agricultural fields: Assessment, measurement and mitigation. *Plant and Soil*, 181, 95-108.
- Novick, K.A., Stoy, P.C., Katul, G.G., Ellsworth, D.S., Siquiera, M.B.S., Juang, J. and Oren, R. (2004). Carbon dioxide and water vapour exchange in a warm temperate grassland. *Oecologia*, 138, 259-274.

References

- Ojima, D.S., Dirks, B.O.M., Glen, E., Owensby, V.C. and Scurlock, J.M.O. (1993). Assessment of C budget for grasslands and drylands of the world. *Water, Air and Soil Pollution*, 70, 95-109.
- Parton, W.J., Schimel, D.S., Cole, C.V. and Ojima, D.S. (1987). Analysis of factors controlling soil organic matter levels in Great Plains grasslands. *Soil Sci. Soc. Am. J.*, 51, 1173-1179.
- Parton, W.J., Scurlock, J.M.O., Ojima, D.S., Schimel, D.S. and Hall, D.O., Scopegram Group Members (1995). Impact of climate change on grassland production and soil carbon worldwide. *Glob. Change Biol.*, 1, 13-22.
- Pattey, E., Strachan, I.B., Desjardins, R.L. and Massheder, J. (2002). Measuring nighttime CO₂ flux over terrestrial ecosystems using eddy covariance and nocturnal boundary layer methods. *Agri. For. Meteorol.*, 113, 145-158.
- Picon-Cochard, C., Teyssonneyre, F., Besle, J.M. and Soussana, J.-F. (2004). Effects of elevated CO₂ and cutting frequency on the productivity and herbage quality of a semi-natural grassland. *Europ. J. Agronomy*, 20, 363-377.
- Pope, V.D., Gallani, M.L., R., R.P. and Stratton, R.A. (2000). The impact of new physical parametrizations in the Hadley Centre climate model -- HadAM3. *Climate Dynamics*, 16, 123-146.
- Rasse, D.P., François, L., Aubinet, M., Kowalski, A.S., Vande Walle, I., Laitat, E. and Gérard, J.C. (2001). Modelling short-term CO₂ fluxes and long-term tree growth in temperate forests with ASPECTS. *Ecol. Model.*, 141, 35-52.
- Rastetter, E.B., Agren, G.I. and Shaver, G.R. (1997). Responses of N-limited ecosystems to increased CO₂: a balanced-nutrition, coupled element-cycles model. *Ecol. Appl.*, 7, 444-460.
- Rastetter, E.B. and Shaver, G.R. (1992). A model of multiple-element limitation for acclimating vegetation. *Ecology*, 73, 1154-1174.
- REPS (2002). *Agri-Environmental Specifications For REPS 2000*. Departement of Agriculture, Food and Rural Development.
- Riedo, M., Grub, A., Rosset, M. and Fuhrer, J. (1998). A pasture simulation model for dry matter production, and fluxes of carbon, nitrogen, water and energy. *Ecol. Model.*, 105, 141-183.
- Riedo, M., Gyalistras, D., Fischlin, A. and Fuhrer, J. (1999). Using an ecosystem model linked to GCM-derived local weather scenarios to analyse effects of climate change and elevated CO₂ on dry matter production and partitioning, and water use in temperate managed grasslands. *Glob. Change Biol.*, 5, 213-223.
- Riedo, M., Gyalistras, D. and Fuhrer, J. (2000). Net primary production and carbon stocks in differently managed grasslands: simulation of a site-specific sensitivity to an increase in atmospheric CO₂ and to climate change. *Ecol. Model.*, 134, 207-227.
- Riedo, M., Gyalistras, D. and Fuhrer, J. (2001). Pasture responses to elevated temperature and doubled CO₂ concentration: assessing the spatial pattern across an alpine landscape. *Clim. Res.*, 17, 19-31.

References

- Riedo, M., Milfort, C., Schmid, M. and Sutton, M.A. (2002). Coupling soil-plant-atmosphere exchange of ammonia with ecosystem functioning in grasslands. *Ecol. Model.*, 158, 83-110.
- Ruimy, A., Dedieu, G. and Saugier, B. (1996). TURC: A diagnostic model of continental gross primary productivity and net primary productivity. *Glob. Biogeochem. Cycles*, 10, 269-285.
- Ryden, J.C. (1981). N₂O exchange between a grassland soil and the atmosphere. *Nature*, 292, 235-236.
- Saigusa, N., Oikawa, T. and Liu, S. (1998). Seasonal variations of the exchange of CO₂ and H₂O between a grassland and the atmosphere: An experimental study. *Agri. For. Meteorol.*, 89, 131-139.
- Salètes, S., Fiorelli, J.L., Vuichard, N., Cmahou, J., Olesen, J.E., Hacala, S., Sutton, M.A., Fuhrer, J. and Soussana, J.F. (2004). *Proceedings of the International Conference "Greenhouse gas emissions from agriculture - Mitigation options and strategies"*, Leipzig, 10-12th February 2004.
- Sarmiento, J.L. and Gruber, N. (2002). Sinks for anthropogenic carbon. *Physics Today*, 55, 30-36.
- Scanlon, T.M., Kiely, G. and Xie, Q. (2004). A nested catchment approach for defining the hydrological controls on non-point phosphorus transport. *Journal of Hydrology*, 291, 218-231.
- Scanlon, T.M. and Kiely, G. (2003). Ecosystem-scale measurements of nitrous oxide fluxes for an intensely grazed, fertilized grassland. *Geophysical Research Letters*, 30, doi:10.1029/2003GL017454.
- Schmid, M., Neftel, A., Riedo, M. and Fuhrer, J. (2001). Process-based modelling of nitrous oxide emissions from different nitrogen sources in mown grassland. *Nutrient Cycling in Agroecosystems*, 60, 177-187.
- Schmid, P.H. (2002). Footprint modelling for vegetation atmosphere exchange studies: a review and perspective. *Agri. For. Meteorol.*, 113, 159-183.
- Seinfeld, J. (1986). *Atmospheric Chemistry and Physics of Air Pollution*. John Wiley, New-York.
- Sims, P.L. and Bradford, J.A. (2001). Carbon dioxide fluxes in a southern plains prairie. *Agri. For. Meteorol.*, 109, 117-134.
- Soussana, J.-F., Loiseau, P., Vuichard, N., Ceschia, E., Balesdent, J., Chevallier, T. and Arrouays, D. (2004). Carbon cycling and sequestration opportunities in temperate grasslands. *Soil Use and Management*, 20, Special Issue 1, 219-230.
- Thornley, J.M.H. and Cannell, M.G.R. (1997). Temperate grassland responses to climate change: an analysis using the Hurley Pasture Model. *Annals of Botany*, 80, 205-221.
- Thornley, J.M.H. (1998). *Grassland Dynamics. An Ecosystem Simulation Model*. CAB International, Oxon.

References

- Trogler, W.C. (1999). Physical properties and mechanisms of formation of nitrous oxide. *Coord. Chem. Rev.*, 187, 303-327.
- Tu, K.P. (2001). *Partitioning ecosystem respiration using stable carbon isotopes in a mixed C3 annual grassland*. American Geophysical Union, Fall Meeting 2001, San Francisco, Ca.
- UNFCCC (1992). United Nations Framework Convention on Climate Change. <http://unfccc.int/resource/docs/convkp/conveng.pdf>.
- Volpe Horii, C., Zahniser, M.S., Nelson, D.D.J., McManus, J.B. and Wofsy, S.C. (1999). Nitric acid and nitrogen dioxide flux measurements: a new application of tunable diode laser absorption spectroscopy. *SPIE*, 3758, 152-161.
- Vuichard, N., Ciais, P., Viovy, N., Ammann, C., Calanca, P., Clifton-Brown, J., Fuhrer, J., Jones, M., Martin, C. and Soussana, J.-F. (2005). Estimating the greenhouse gas fluxes of European grasslands with a process driven model: Part 1. Model evaluation from in-situ measurements. *in preparation*.
- Warnant, P., François, L., Strivay, D. and Gerard, J.-C. (1994). CARAIB: A global model of terrestrial biological productivity. *Glob. Biogeochem. Cycles*, 8, 255-270.
- Webb, E.K., Pearman, G.I. and Leuning, R. (1980). Correction of flux measurements for density effects due to heat and water vapor transfer. *Q.J.R. Met. Soc.*, 106, 85-100.
- Williams, D.L., Ineson, P. and Coward, P.A. (1999). Temporal variations in nitrous oxide fluxes from urine-affected grassland. *Soil Biol. Biochem.*, 31, 779-788.
- Wohlfahrt, G., Anfang, C., Bahn, M., Haslwanter, A., Newesely, C., Schmitt, M., Drosler, M., Pfadenhauer, J. and Cernusca, A. (2005). Quantifying nighttime ecosystem respiration of a meadow using eddy covariance, chambers and modeling. *Agri. For. Meteorol.*, 128, 141-162.
- Xu, L. and Baldocchi, D.D. (2004). Seasonal variation in carbon dioxide exchange over a Mediterranean annual grassland in California. *Agri. For. Meteorol.*, 123, 79-96.
- Young (2001). Model 81000 Ultrasonic anemometer, manual PN 81000-90. *RM Young Company*, Michigan, USA. <http://www.youngusa.com/81000.pdf>.

Appendix 1
Glossary of terms

Air entry potential: It is the point of inflexion in the relationship between pressure head and water content (in cm). The absolute value of the air-entry potential equals the height of the tension-saturated zone.

Autotrophic respiration (Ra): Plants fix carbon by photosynthesis. The word “photosynthesis” is used here to denote the carbon fixed by gross photosynthesis minus the carbon lost by photorespiration. Some of that photosynthetically fixed carbon is lost by internal plant metabolism. This loss is termed autotrophic respiration and typically amounts to about half the carbon fixed by plants.

Bulk density: It is the mass of soil (dry) divided by the total soil volume (soil + water + air), in g. cm⁻³.

Climate Change (CC): The term ‘climate change’ is sometimes used to refer to all forms of climatic inconsistency, but because the earth's climate is never static, the term is more properly used to imply a significant change from one climatic condition to another. Under the United Nation Framework Convention on Climate Change (UNFCCC, 1992), the definition of climate change is “a change of climate which is attributed directly or indirectly to human activity that alters the composition of the global atmosphere and which is in addition to natural climate variability observed over comparable time periods.” In some cases, ‘climate change’ has been used synonymously with the term, ‘global warming’.

Eddy covariance (EC): Also called eddy correlation, see section 3.1.1.

Emission factor (EF): It is the percentage of applied nitrogen fertiliser lost as N₂O.

Enteric fermentation: Enteric fermentation is fermentation that takes place in the digestive systems of animals. In particular, ruminant animals have a large "fore-stomach," or rumen, within which microbial fermentation breaks down food into soluble products that can be utilized by the animal. The microbial fermentation that occurs in the rumen enables ruminant animals to digest coarse plant material that monogastric animals cannot digest. Methane is produced in the rumen by bacteria as a by-product of the fermentation process. This CH₄ is exhaled or belched by the animal and accounts for the majority of emissions from ruminants. Methane also is produced in the large intestines of ruminants and is expelled.

Global warming potential (GWP): The concept of global warming potential (GWP) was invented to allow comparisons of the total cumulative warming effects of different GHGs over a specified time period. A GWP is a measure of relative contribution to radiative forcing. GWPs are used to convert emissions of non-CO₂ gases into their CO₂ warming equivalents. The warming effect of CO₂ is assigned a value of 1, and the warming effects of other gases are calculated as multiples of this value. The CO₂ equivalent of a non-CO₂ gas is calculated by multiplying the mass of the emissions of the non-CO₂ gas by its GWP.

Greenhouse gas (GHG): GHG are gaseous components of the atmosphere that contribute to the greenhouse effect. GHG are transparent to certain wavelengths of the sun's radiant energy, allowing them to penetrate deep into the atmosphere or all the way to the earth's surface. GHG and clouds prevent some of infrared radiation from escaping, trapping the heat near the earth's surface where it warms the lower atmosphere (greenhouse effect). Alteration of this natural barrier of atmospheric gases can raise or lower the mean global temperature of the earth.

Greenhouse effect: The earth naturally absorbs and reflects incoming solar radiation and emits longer wavelength terrestrial (thermal) radiation back into space. On average, the absorbed solar radiation is balanced by the outgoing terrestrial radiation emitted to space. A portion of this terrestrial radiation, though, is itself absorbed by gases in the atmosphere. The energy from this absorbed terrestrial radiation warms the earth's surface and atmosphere, creating what is known as the “natural greenhouse effect.”

Gross primary productivity (GPP): GPP refers to the total amount of carbon fixed in the process of photosynthesis by plants in an ecosystem.

Heterotrophic respiration (Rh): Heterotrophic respiration refers to the carbon lost by organisms in ecosystems other than the plants, the primary producers, themselves. It constitutes the respiration by animals that live aboveground, which tends to be a minor component, but most importantly, by all those organisms (flora and fauna) that live in the soil and the litter layer and decompose organic matter that has reached the soil by litter fall, root turn-over, root exudation, dead organisms and faecal matter.

Hydraulic conductivity: The hydraulic conductivity (or permeability) is the rate at which water moves through a porous medium under a unit potential energy gradient (in cm. s⁻¹).

Leaf area index (LAI): LAI is the total surface area of leaves of plants in a given area divided by the area of ground covered by the plants (in $\text{m}^2 \cdot \text{m}^{-2}$). In an area of dense vegetation, such as a forest, the LAI will be high.

Net ecosystem exchange (NEE): NEE is the measurement of CO_2 fluxes by an EC technique. In this study, it is considered that $\text{NEE} = \text{NEP} = \text{GPP} - (\text{Ra} + \text{Rh})$. NEP and NEE are used somewhat interchangeably, but to be more precise, $\text{NEE} = \text{NEP} - \text{carbon run-off}$.

Net ecosystem production (NEP): NEP refers to net primary production minus carbon losses in heterotrophic respiration, Rh : $\text{NEP} = \text{NPP} - \text{Rh}$.

Net primary production (NPP): NPP refers to the net production of organic carbon by plants in an ecosystem usually measured over a period of a year or more. It is GPP minus the amount of carbon respired by plants themselves in autotrophic respiration, Ra : $\text{NPP} = \text{GPP} - \text{Ra}$.

Radiative forcing: Radiative forcing is the change in the balance between radiation coming into the atmosphere and radiation going out. A positive radiative forcing tends on average to warm the surface of the earth, and negative forcing tends on average to cool the surface.

Respiration of the ecosystem (R_{tot}): R_{tot} is the total respiration of the ecosystem; it includes autotrophic respiration (plants) and heterotrophic respiration (soil micro-organisms and animals).

Water content: It is the ratio of water volume to soil volume. The water content can vary both in time and space. The theoretical range is from 0 (completely dry) to saturation, but the range in natural soil is much less than this.

Appendix 2
Paper submitted to
Global Change Biology

Observations and process-based modeling of the net ecosystem exchange and its components for a humid grassland ecosystem

Delphine Lawton¹, Paul Leahy¹, Ger Kiely¹, Kenneth A. Byrne¹ and Pierluigi Calanca²

¹Department of Civil and Environmental Engineering, University College Cork, Cork, Ireland.

²Swiss Federal Research Station for Agroecology and Agriculture, Zurich, Switzerland.

Running title: Grassland NEE observations and modeling

Submitted to: Global Change Biology

Date submitted: June 23, 2005.

Date received:

Corresponding Author:

Gerard Kiely

Department of Civil and Environmental Engineering,

University College Cork,

Cork, Ireland.

Phone: 353-21-4902965

Fax: 353-21-4276648

Email: g.kiely@ucc.ie

Abstract

Temperate grasslands are one of the most widespread ecosystems in the world and cover approximately 45% of the area of Ireland. We measured the net ecosystem exchange (NEE) of an intensively grazed humid grassland in South West Ireland during the period 2002 to 2004 using an eddy covariance (EC) system. A process based biogeochemical model (PaSim) was used to simulate the carbon dynamics of the ecosystem. PaSim incorporates land management practices such as grass cuttings (forage), grazing and the application of fertilizers. The model outputs include gross primary production (GPP) and the respiration components from soil, plants and grazing animals. The PaSim simulation captures most of the seasonal variation in NEE with especially good agreement with the EC observations during the growing season. The sums of annual NEE derived from EC and PaSim are similar. The fact that the NEE was ~ 30% higher in the driest of the three years than in the wettest year suggests that this ecosystem is robust enough to tolerate a wide precipitation range. The performance of PaSim on this ecosystem indicates that it will prove a useful tool for upscaling flux measurements and predicting responses of grasslands to climate change.

1. Introduction

Grasslands cover between 12% and 27% of the total land area of the world (Brown, 1998) and are the dominant ecosystem in Ireland, representing 90% of agricultural land and 45% of the total land area (Gardiner and Radford, 1980). They play a key role in the carbon cycle through photosynthetic and respiratory processes. The study of carbon fluxes between vegetation and the atmosphere is important as carbon uptake by ecosystems may compensate for some emissions of greenhouse gases (IPCC, 2001). Long-term measurements of carbon dioxide (CO₂) fluxes are necessary to determine the seasonal and interannual variability of net ecosystem exchange (NEE). CO₂ fluxes between the atmosphere and grasslands in the Great Plains of the USA have been extensively measured with eddy covariance (EC, Flanagan et al., 2002; Frank, 2002; Frank and Dugas, 2001; Sims and Bradford, 2001), but few long-term studies have been made of grasslands in more temperate humid climates (Saigusa et al., 1998; Novick et al., 2004).

Eddy covariance studies, while valuable, can only measure the NEE. Ecosystem respiration is usually estimated from a combination of: an extrapolation of night-time fluxes under strong turbulence (Falge et al., 2002) and an empirical regression model of night-time fluxes with soil temperature (Xu and Baldocchi, 2004; Jaksic, 2004). The exceptions include a few studies, in which direct estimates of the respiration have been obtained by locating the EC instruments below the canopy of a forest (Baldocchi et al., 1997) or using isotopic flux measurements of ¹³CO₂ (Bowling et al., 2001). The variations in soil and ecosystem respiration are commonly linked with soil temperature and soil water content. Some relationships have also been found with soil organic carbon and plant growth rate (Franzluebbers et al., 2002).

Biogeochemical models used to study the carbon cycle of different ecosystems include: HP (Thornley, 1998); CENTURY (Parton et al., 1987); SPUR (Foy et al., 1999); DNDC (Li et al., 1994) or MEL (Rastetter and Shaver, 1992) and the Pasture Simulation (PaSim) model (Riedo et al., 1998). Models can provide an improved understanding of the seasonal and interannual trends in the NEE and can be used to examine scenarios (e.g.,

climate change scenarios) through the computation of the two components of the NEE: the gross primary production (GPP) and the total respiration of the ecosystem (R_{tot}). Models are also useful in upscaling flux measurements to regional or larger scales. The Pasture Simulation (PaSim) model (Riedo et al., 1998) is a process-based biogeochemical model for grasslands. It simulates the carbon and nitrogen dynamics and the energy and water fluxes of the ecosystem. It has been modified by Riedo et al., 2000) to include grazing in addition to other management input data such as grass cutting (forage) and fertilization. PaSim also computes (individually) the soil, plant and animal respiration.

The purpose of this study was to examine the effectiveness of PaSim in simulating the seasonal and interannual variability of NEE, GPP and R_{tot}. We also used PaSim to investigate the impact of fluctuations in environmental variables (e.g., precipitation) on GPP and R_{tot} over a three-year flux measurement period.

2. Experiments and Methods

Site

Eddy correlation measurements of the NEE were carried out in managed, intensively grazed and fertilised grassland in County Cork in southern Ireland (Latitude: 52.14° N, Longitude: 8.66° W). The site has an average elevation of 200 m above sea level. The dominant soil type is sandy clay loam. The climate is temperate maritime with an average rainfall of 1470 mm year⁻¹ and an annual daily mean temperature of 9.6°C. The number of days when the air temperature is above 5°C varies between 317 and 320 for each of the three years of the study (2002, 2003 and 2004). Frost occurs on less than 10 days per year. Some physical and climatic characteristics of the site are reported in Table 1.

For each of the three years, the site received applications of approximately 200 kg of synthetic N ha⁻¹ (mainly as NH₄NO₃) and approximately 130 kg organic N ha⁻¹ (as farmyard slurry). The site was intensively grazed by dairy and beef cattle at a density of 2.2 LU ha⁻¹ (livestock units per ha) between April and October. Cattle were housed for the remainder of the year. Approximately 50% of the fields were cut for silage, twice a year, typically in June

and September. The dominant grass species is perennial ryegrass (*Lolium perenne*). The site is in managed grassland for approximately 20 years.

The average flux footprint was estimated based on a fetch to sensor height ratio of 100:1 combined with the probability density distribution of the wind direction. Most of the site is well drained with a small area prone to seasonal waterlogging. The footprint area is partitioned into approximately fifty small fields (or paddocks) to facilitate rotation of grazing cattle. Some of the fields are reserved for silage cutting to provide winter feed. Management practices are broadly similar across the whole site but the timing of fertilizer applications and grass cuttings varies. This implies a degree of heterogeneity (particularly in summer) that cannot easily be addressed directly by the model. We simplified the modeling exercise by using a single point simulation and representing each major succession of cutting events taking place in the field with two cuts separated by seven days in the model. In the model, the net effect of the cuts is to set the LAI to $1.5 \text{ m}^2 \text{ m}^{-2}$ and the shoot dry matter to 0.15 kg m^{-2} . We also assume that all the fields were continuously grazed during the summer time.

Instrumentation

The CO₂ concentration is monitored by an LI-7500 Open Path CO₂ non-dispersive, infrared gas analyzer (LI-COR, USA). In the eddy covariance technique, this data was used in conjunction with wind speed data from a 3-D sonic anemometer (Model 81000, R. M. Young, USA) to determine the fluxes of CO₂. Concentrations of CO₂ and wind speeds were logged at 10 Hz and CO₂ flux values were calculated at 30-minute intervals. The CO₂ sensor intake was mounted 10 m above ground for 2002 and 2003, and at 3 m for 2004.

Precipitation was measured using a tipping bucket rain gauge (ARG100, Environmental Measurements Ltd, UK). A net radiometer (CNR1) was used to measure the solar irradiance (Kipp and Zonen, Netherlands). Photosynthetic photon flux density Q_{ppfd} (or photosynthetic active radiation Q_{par}) was measured using a PAR LITE sensor (Kipp and Zonen, Netherlands). Air temperature and humidity were monitored using a HMP45C

temperature and humidity probe (Campbell Scientific, UK) mounted 3 m above ground and were recorded at 30-minute intervals.

All CO₂ fluxes were adjusted using the Webb correction (Webb et al., 1980). As eddy covariance performed poorly during rain events, a precipitation filter was used to screen out unsatisfactory flux data. Using an incoming solar radiation threshold of 20 W.m⁻² the data were then partitioned into daytime and night-time sets. The wind speeds from the sonic anemometer were double rotated such that the mean vertical wind speed was set to zero. In periods of high atmospheric stability, there is a lack of turbulent mixing near the soil surface and the eddy covariance technique does not always yield reliable results. Nocturnal fluxes corresponding to u^* (frictional velocity) less than 0.2 m s⁻¹ were excluded (Pattey et al., 2002; Baldocchi, 2003) and replaced by a regression exponential function of the soil temperature (Jaksic, 2004). The daytime data was sorted bi-monthly and for each two-month period a different regression relationship was developed between the good daytime CO₂ fluxes and the photosynthetic photon flux density Q_{ppfd} (photosynthetic active radiation Q_{par}). The regression used the Mysterlich formula (Falge et al., 2001) for the relationship between CO₂ flux and Q_{ppfd} . These relations were then used to gap-fill daytime CO₂ fluxes. As discussed in Jaksic (2004), an upper threshold (for daytime data) and a lower limit (for night-time data) were set for the 30-minute CO₂ flux measurements. After post-processing and filtering of spurious data, 57% of the CO₂ flux data were suitable for analysis. The unsuitable 43% was replaced by modeled (empirical regression) data.

Model description and parameterization

The model used in this study is PaSim 3.6 (v5) (Riedo et al., 1998; Riedo et al., 1999; Riedo et al., 2000; Riedo et al., 2001; Schmid et al., 2001; Riedo et al., 2002, Vuichard et al., in preparation). The first version was described by Riedo et al., 1998). The model has five submodels: soil physics; soil biology; plant; animal; and microclimate. This model is driven with hourly meteorological input data for: radiation; air temperature; vapor pressure; wind speed; precipitation and atmospheric concentration of CO₂ and ammonia (NH₃). PaSim

integrates the land management practices of grass cuttings, grazing and the application of fertilizer and slurry.

The soil biology submodel used in PaSim is derived from the CENTURY model (Parton et al., 1987). Organic carbon (C) and nitrogen (N) are divided into pools for plant residue and for organic matter. In order to run the model in a steady state, initial condition values for the concentrations of carbon and nitrogen in the different pools were those obtained at the end of a corresponding equilibrium run (Table 3). Equilibrium was reached when the change in C and N levels in the various pools was smaller than a prescribed threshold (here, the convergence criterion was reached when the change in the previous variables between two cycles was less than 2.5%).

All the meteorological input data were measured on site, except for the concentration of CO₂ and NH₃, which were taken as constants from the literature (IPCC, 2001; Seinfeld, 1986). In Figure 1, we show the monthly observations of air temperature and precipitation. There is a clear seasonality in the temperature with lows in the winter months (December and January) of ~ 5.5°C and highs in the summer months (July and August) of ~ 15°C. Precipitation occurs throughout the year with higher amounts in winter than in summer. There is no dry season and no frost season. Some soil parameters were determined from samples taken from the top 20 cm of soil and from 20 to 40 cm within the flux tower footprint. Other soil parameters were set according to the literature (Clapp and Hornberger, 1978) or determined by optimization of PaSim results and fall within the range of literature values (Table 2). The vertical soil profile was divided in three layers: layer 1 from 0 to 2 cm; layer 2 from 2 cm to 20 cm; layer 3 from 20 cm to 60 cm. The soil-rock interface was set at 2 m for modeling purposes. For modeling purposes, all fertilizer and slurry applications were temporally averaged in order to have 10 applications per year.

The current version of the model is known to produce too much biomass in winter, even though an additional stress parameter have been included to account for enhanced mortality in autumn and winter (Vuichard et al., (manuscript in preparation, 2005)). To

compensate for this we therefore include an extra cut at the end of each year to reset the biomass and leaf area index (LAI) to realistic values.

PaSim calculates the ecosystem GPP and the respiration of the soil, plants and the grazing animals. Here soil respiration is defined as microbial respiration only. We define the NEE as the difference between the modeled GPP and the sum of all the modeled respiration components (R_{tot}). In this study we use the standard biological convention in which fluxes from the biosphere to the atmosphere are negative.

3. Results

Figure 2 shows the cumulative NEE simulated by PaSim and observed by EC for the three years of study. As seen in this figure, the vegetation period (roughly April to October) can be divided in an active spring growing phase up to the first major grass cut (see arrow in Figure 2), and a less active phase thereafter.

The measured annual uptake is 1.9, 2.6 and 2.9 tC. ha⁻¹ for 2002, 2003, 2004, respectively, whereas the annual uptake computed with PaSim is 2.6, 2.7, 3.4 tC. ha⁻¹ (Table 4). For each year of the study, the modeled uptake is higher than the observed. Most of the carbon uptake occurs during the growing season in the months of April, May and June (Figure 2). The NEE simulated with PaSim captures the trends during the growing season very well. From June to September, the cumulative NEE shows neither net uptake nor loss, because of land management practices of silage cuttings and intensive grazing. The effects of the silage cuttings are visible as abrupt decreases in the cumulative modeled NEE (Figure 2). From the end of October to year's end, the cumulative NEE decreases as respiration exceeds photosynthesis.

To compare the evolution of NEE during the growing season of each year it is necessary to define the start and end dates of the season. The start date of the growing season varies within a fifteen day period from year to year. As there is no standard definition, we choose a growing season start date when the soil temperature at 7.5 cm depth is consistently above 6°C (see results in Table 4). However, the growth of the grass sometimes may begin

before this date (Keane and Collins, 2004). The end of the growing season is defined as the day of the first grass cut (Table 4). In the observations the growing season lasts between 89 and 106 days and in the model it is between 112 and 131 days. The gradient of the cumulative NEE curve represents the rate of change NEE. During the spring growing season, the gradient of uptake for the cumulative NEE observed is 2.8, 3.1, 2.7 gC. m⁻² day⁻¹ for the three consecutive years of the study. The gradient of uptake for the modeled NEE is similar to the observed (Table 4).

Figure 3 shows the model output of GPP and R_{tot}. The annual GPP increases from 19.9 tC. ha⁻¹ (2002) to 21.5 tC. ha⁻¹ for 2003 and 2004. The annual R_{tot} increases from 17.2 tC. ha⁻¹ (2002) to 18.9 tC. ha⁻¹ (2003) and then slightly decreases to 18.2 tC. ha⁻¹ (2004). The modeled interannual changes of GPP and R_{tot} are less than 9%. As NEE is the difference between GPP and R_{tot} (and is small relative to both), small interannual variation in NEE needs to be interpreted with caution. Figure 4 shows the modeled partitioning of R_{tot} as: R_{soil}, R_{plant} and R_{animal}. On average the soil respiration represents 55%, plants 40% and grazing animals 5%.

4. Discussion

Comparison of modeled and observed NEE

Figure 2 and Table 4 show that the modeled NEE broadly agree with the observations. However, the model overestimates the annual NEE by between 3% and 38%. Better agreement occurs during the growing season, with the rate of change being modeled accurately. PaSim has limitations in the last three months of each year (winter period) where it over predicts the uptake. It is currently acknowledged that PaSim produces too much biomass in winter, and this weakness in the model is currently being investigated (Vuichard et al., in preparation). The shape of the curve for the modeled NEE in the first months of 2002 is different from that in 2003 and 2004 (Figure 2). This is due to the over-sensitivity of PaSim to initial conditions, even when the ecosystem can be considered to be in equilibrium.

The result of our approximation of the spatially and temporally heterogeneous management activities with a single point simulation is that the model captures the cumulative NEE but does not account for the week-to-week variation in NEE. In the autumn and winter period the observations show a decreasing NEE (i.e., $R_{tot} > GPP$). The model does capture this trend better in 2003 and 2004 than in 2002.

For both model and observations, there is a year-to-year increase in NEE with the lowest NEE associated with the wettest year. The air temperature, incoming radiation and management practices over the three years were similar. The environmental variable that was most different between the three years was precipitation: 2002 was wetter than average (17% above the long-term annual average); 2003 was drier than average (19% below average); 2004 was 9% drier than average. The decrease in precipitation (from 2002 to 2003) results in an increase in NEE. Some of the observed interannual variation in NEE may be due to the uncertainty inherent in the EC method (Baldocchi, 2003). The fact that NEE was higher in the dry year by ($\sim 30\%$) than in the wet year, suggests that this ecosystem is robust enough to tolerate a wide annual precipitation range (1185 mm to 1835 mm).

Analysis of components of NEE

PaSim simulates GPP and R_{tot} . In Figure 3a, we show the cumulative GPP for each of the three years and in Figure 3b, the cumulative R_{tot} for the three years. We note in Figure 3a that the year with lowest GPP (19.9 tC. ha^{-1}) was the wettest year (1785 mm). We note from Figure 3b that the lowest R_{tot} (17.3 tC. ha^{-1}) was in the wettest year. In the wet year, GPP and R_{tot} are lower than in the drier years suggesting that productivity is dependent on a favorable soil moisture status.

GPP and R_{tot} are dependent on meteorological, hydrological, soil, vegetation and microbiological conditions. In Figures 5a and 5b, we examine the variation over the years of the soil moisture and soil temperature. Earlier we noted that both GPP and R_{tot} were lowest in the wet year. From the model study, the optimum NEE (largest difference between GPP and R_{tot}), corresponds to an annual precipitation close to the average annual precipitation ($\sim 1470 \text{ mm}$). Unlike the study of Xu and Baldocchi, (2004) of a grassland in California, the

variation in R_{tot} in our study can not be linked to daily precipitation events because the climate in Ireland is humid and temperate all the year round and consequently Irish soils are rarely subject to moisture deficit.

We used the model to examine the components of R_{tot} : R_{soil} ; R_{plant} and R_{animal} . The evolution of the cumulative respiration components is shown in Figure 4. There are few field scale studies partitioning respiration into its autotrophic (R_{plant}) and heterotrophic (R_{soil}) components for grassland ecosystems. In laboratory analysis, Tu, 2001) found that, for a grassland, the plant respiration accounted for $\sim 66\%$ of the ecosystem respiration. In forests, plant respiration is considered to account for $\sim 75\%$ of total respiration (Arneeth et al., 1998; Kinerson et al., 1977).

Conclusions

This study shows that the process oriented biogeochemical model (PaSim) for carbon cycling in this temperate humid grassland simulates well the eddy covariance measured NEE over the three-year study period. The model results and observed NEE are in especially good agreement during the spring growing season in each of the three years. However, departures from the observations were observed for the summer seasons. This may be due to the heterogeneous nature of land management in the summer period. The activities over the fifty small fields in the EC footprint is a mosaic of silage cutting fields and cattle grazing fields and we attempted to model these multiple activities with one grid cell.

The lowest NEE occurs in the wettest year, implying that the ecosystem is sensitive to precipitation at the upper end of the interannual range. However, the difference between the highest and lowest NEE is less than 35%. The model simulations of GPP and R_{tot} , also showed that GPP and R_{tot} were highest in the drier years and lowest in the wet year. From the observations and simulations it appears that for this ecosystem there may be an optimum precipitation (producing maximum NEE), which is approximately that of the current values of the long term average precipitation of ~ 1470 mm. Although we found that NEE is inversely proportional to precipitation amount, the fact that the interannual variation of NEE is within \sim

35% suggests that this grassland ecosystem which was established ~ 20 years ago is tolerant of a wide range of precipitation. Finally, this three-year study gives us confidence that this process-based model (PaSim) is reliable in modeling the carbon cycle of this grassland ecosystem. Now that the model has been validated with satisfactory results, we plan to simulate different management and climate change scenarios. Furthermore, PaSim shows promise as a tool for upscaling of ecosystem-scale CO₂ exchange measurements to the national level.

Acknowledgements

This work is part of the Environmental Research Technological Development and Innovation program, managed by the Irish EPA and financed by the Irish Government under the National Development Plan 2000-2006 (CELTICFLUX, 2001-CC-C2-M1). The first author is funded by the EU Erasmus program. The second author is funded by the European Union CARBOEUROPE-IP program. Adrian Birkby provided essential instrumentation and data collection support for this research. We very much appreciate the permission to use PaSim from Professor Jürg Fuhrer of the Swiss Federal Research Station for Agroecology and Agriculture.

References

- Arneeth, A., Kelliher, F.M., McSeveny, T.M. and Byers, J.N. (1998). Net ecosystem productivity, net primary productivity and ecosystem carbon sequestration in a *Pinus radiata* plantation subject to soil water deficit. *Tree Physiology*, 18, 785-793.
- Baldocchi, D.D. (2003). Assessing the eddy covariance technique for evaluating carbon dioxide exchange rates of ecosystems: past, present and future. *Glob. Change Biol.*, 9, 479-492.
- Baldocchi, D.D., Vogel, C.A. and Hall, B. (1997). Seasonal variation of carbon dioxide exchange rates above and below a boreal jack pine forest. *Agri. For. Meteorol.*, 83, 147-170.
- Barnard, R., Leadley, P.W. and Hungate, B.A. (2005). Global change, nitrification, and denitrification: A review. *Glob. Biogeochem. Cycles*, 19, doi:10.1029/2004GB002282.
- Bowling, D.R., Tans, P.P. and Monson, R.K. (2001). Partitioning net ecosystem carbon exchange with isotopic fluxes of CO₂. *Glob. Change Biol.*, 7, 127-145.
- Brown, J.F. (1998). *Mapping global grassland ecosystem: a comparison of four data sets*. Proceedings of the IEEE International Geoscience and Remote Sensing Symposium Proceedings, Seattle, Washington.
- Brutsaert, W. (1991). *Evaporation into the Atmosphere: Theory, History, and Applications*. Kluwer Academic Publishers, Boston.
- Campbell (1998). CSAT3 three dimensional sonic anemometer instruction manual. *Campbell Scientific, Inc.*, USA. <http://www.campbellsci.com/documents/manuals/csat3.pdf>.
- Campbell (2000). Tipping bucket rain gauges, ARG100. *Campbell Scientific, Inc.*, USA. <http://www.campbellsci.co.uk>.
- Campbell (2002). CS616 water content reflectometer. *Campbell Scientific, Inc.*, USA. www.campbellsci.co.uk/products/sensors/cs616.htm.
- Campbell (2003a). Model HMP45C temperature and relative humidity probe instruction manual. *Campbell Scientific, Inc.*, USA. <http://www.campbellsci.co.uk>.
- Campbell (2003b). Model 107 & 107B temperature probes instruction manual. *Campbell Scientific, Inc.*, USA. <http://www.campbellsci.co.uk>.
- Campbell (2005). TGA100A trace gas analyser overview. *Campbell Scientific, Inc.*, USA. http://www.campbellsci.com/documents/manuals/tga100a_ov.pdf.
- Campbell, S.G. and Norman, J.M. (1998). *An introduction to environmental Biophysics, second edition*. Springer-Verlag, New York.
- Cannell, M.G.R. and Thornley, J.M.H. (1998). N-poor ecosystem may respond more to elevated [CO₂] than N-rich ones in long term. A model analysis of grassland. *Glob. Change Biol.*, 4, 431-442.

- Cao, M. and Woodward, I. (1998). Net primary and ecosystem production and carbon stocks of terrestrial ecosystems and their response to climate change. *Glob. Change Biol.*, 4, 185-198.
- CarboEurope-GHG (2004). Greenhouse Gas Emissions from European Grasslands. <http://gaia.agraria.unitus.it/ceuroghg/ReportSS3.pdf>.
- Chen, D.-X., Hunt, H.W. and Morgan, J.A. (1996). Responses of a C3 and C4 perennial grass to CO₂ enrichment and climate change: Comparison between model predictions and experimental data. *Ecol. Model.*, 96, 11-27.
- Clapp, R.B. and Hornberger, G.M. (1978). Empirical equations for some hydraulic properties. *Water Resources Research*, 14, 601-604.
- Coughenour, M.B. and Chen, D.-X. (1997). Assessment of grassland and ecosystem responses to atmospheric change using linked plant-soil process models. *Ecol. Appl.*, 7, 802-827.
- Dabberdt, W.F., Lenschow, D.H., Horst, T.W., Zimmerman, P.R., Oncley, S.P. and Delany, A.C. (1993). Atmosphere-surface exchange measurements. *Science*, 260, 1472-1481.
- Daly, K. (1999). *An Environmental appraisal of the phosphorous of the Irish grassland soils*. PhD. Thesis, Trinity College, Dublin.
- DeRamus, H.A., Clement, T.C., Giampola, D.D. and Dickison, P.C. (2003). Methane emissions of beef cattle on forages. *Journal of Environmental Quality*, 32, 269-277.
- Dingman, S.L. (1994). *Physical Hydrology*. Macmillan Publishing Company, New York.
- Dobbie, K.E., McTaggart, I.P. and Smith, K.A. (1999). Nitrous oxide emissions from intensive agricultural systems: Variations between crops and seasons, key driving variables, and mean emission factors. *J. Geophys. Res.*, 104, 26,891-26,899.
- Dobbie, K.E. and Smith, K.A. (2003). Nitrous oxide emission factors for agricultural soils in Great Britain: the impact of soil water-filled pore space and other controlling variables. *Glob. Change Biol.*, 9, 204-218.
- Dorsey, J. (2002). UMIST, Atmospheric Physics Research Group, Introduction to the eddy covariance method. Manchester, UK. <http://cloudbase.phy.umist.ac.uk/people/dorsey/Edco.htm>.
- Edwards, G.C., Thurtell, G.C., Kidd, G.E., Dias, G.M. and Wagner-Riddle, C. (2003). A diode laser based gas monitor suitable for measurement of trace gas exchange using micrometeorological techniques. *Agri. For. Meteorol.*, 115, 71-89.
- EncyclopediaBritannica (2002).
- EnvironmentalMediaService (2003). Pentagon Report Describes Global Warming Dangers. http://www.ems.org/climate/pentagon_climate_change.html#report.
- EPA (2000). *Ireland's environment, chapter 4: Emissions to air, A Millennium Report*. Edited by Michael McGettigan

EPA (2003). *National Inventory Report 2003, Greenhouse gas emissions 1990-2001 reported to the United Nations framework convention on climate change*. Edited by Michael McGettigan and Paul Duffy

Falge, E., Baldocchi, D., Olson, R., Athoni, P., Aubinet, M., Bernhofer, C., Burba, G., Ceulemans, R., Clement, R., Dolman, H., Granier, A., Gross, P., Grünward, T., Hollinger, D., Jensen, N.-O., Katul, G., Keronen, P., Kowalski, A., Lai, C.T., Law, B.E., Meyers, T., Moncrieff, J., Moors, E., Munger, J.W., K., P., Rannik, Ü., Rebmann, C., Suyker, A., Tenhunen, J., Tu, K., Verma, S., Vesala, T., Wilson, K. and Wofsy, S. (2001). Gap filling strategies for defensible annual sums of net ecosystem exchange. *Agri. For. Meteorol.*, 107, 43-69.

Falge, E., Baldocchi, D., Tenhunen, J., Aubinet, M., Bakwin, P., Berbigier, P., Bernhofer, C., Burba, G., Clement, R. and Davis, K.J. (2002). Seasonality of ecosystem respiration and gross primary production as derived from FLUXNET measurements. *Agri. For. Meteorol.*, 113, 53-74.

FAO (1988). *Milk and dairy products: production and processing costs - FAO Animal production and health paper 62*. Food and Agriculture Organisation of the United Nations

FAO (1998). *Crop evapotranspiration - Guidelines for computing crop water requirements - FAO Irrigation and drainage paper 56*. Food and Agriculture Organisation of the United Nations, Rome.

Flanagan, L.B. and Johnson, B.G. (2005). Interacting effects of temperature, soil moisture and plant biomass production on ecosystem respiration in a northern temperate grassland. *Agri. For. Meteorol.*, 130, 237-253.

Flanagan, L.B., Wever, L.A. and Carlson, P.J. (2002). Seasonal and interannual variation in carbon dioxide exchange and carbon balance in a northern temperate grassland. *Glob. Change Biol.*, 8, 599-615.

Foken, T. and Wichura, B. (1996). Tools for quality assessment of surface-based flux measurements. *Agri. For. Meteorol.*, 78, 83-85.

Foy, J.K., Teague, W.R. and Hanson, J.D. (1999). Evaluation of the upgraded SPUR model (SPUR2.4). *Ecol. Model.*, 118, 149-165.

Frank, A.B. (2002). Carbon dioxide fluxes over a grazed prairie and seeded pasture in the Northern Great Plains. *Environmental Pollution*, 116, 397-403.

Frank, B.A. and Dugas, A.W. (2001). Carbon dioxide fluxes over a northern, semiarid, mixed-grass prairie. *Agri. For. Meteorol.*, 108, 317-326.

Franzluebbers, K., Franzluebbers, A.J. and Jawson, M.D. (2002). Environmental controls on soil and whole-ecosystem respiration from a tallgrass prairie. *Soil Sci. Soc. Am. J.*, 66, 254-262.

Franzluebbers, K., Franzluebbers, A.J. and Jawson, M.D. (2002). Environmental controls on soil and whole-ecosystem respiration from a tallgrass prairie. *Soil Sci Soc Am J*, 66, 254-262.

Garatt, J.R. (1992). *The Atmospheric Boundary Layer*. Cambridge University Press, Cambridge.

- Gardiner, M.J. and Radford, T. (1980). *Soil Associations of Ireland and Their Land Use Potential*. An Foras Talúntais, Dublin.
- Gordon, C., Cooper, C., Senior, C.A., Banks, H., Gregory, J.M., Johns, T.C., J.F.B., M. and Wood, R.A. (2000). The simulation of SST, sea ice extents and ocean heat transports in a version of the Hadley Centre coupled model without flux adjustments. *Climate Dynamics*, *16*, 147-168.
- Guenther, B.A. and Hills, A.J. (1998). Eddy covariance measurement of isoprene fluxes. *J. Geophys. Res.*, *103*, doi: 10.1029/97JD03283.
- Hamby, D.M. (1994). A review of techniques for parameter sensitivity analysis of environmental models. *Environ. Monit. Ass.*, *32*, 135-154.
- Hanninen, H. (1995). Assessing ecological implications of climatic change: can we rely on our simulation results? *Clim. Change*, *31*(1-4).
- Hanson, P.J., Edwards, N.T., Garten, C.T. and Andrews, J.A. (2000). Separating root and soil microbial contributions to soil respiration: A review of methods and observations. *Biogeochemistry*, *48*, 115-146.
- Hollinger, D.Y., Kelliher, F.M., Byers, J.N., Hunt, J.E., McSeveny, T.M. and Weir, P.L. (1994). Carbon dioxide exchange between an undisturbed old-growth temperate forest and the atmosphere. *Ecology*, *75*, 134-150.
- Hsieh, C.-I., Katul, G.G. and Chi, T.-W. (2000). An approximate analytical model for footprint estimation of scalar fluxes in thermally stratified atmospheric flows. *Advances in Water Resources*, *23*, 765-772.
- Hsieh, C.-I., Katul, G.G., Schieldge, J., Sigmon, J.T. and Knoerr, K.K. (1997). The Lagrangian stochastic model for fetch and latent heat flux estimation above uniform and non-uniform terrain. *Water Resources Res.*, *33*, 427-438.
- Hsieh, C.-I., Leahy, P., Kiely, G. and Li, C. (2005). The effect of future climate perturbations on N₂O emissions from a fertilised humid grassland. *Nutrient Cycling in Agroecosystems*, Submitted.
- Hunt, H.W., Trlica, M.J., Redente, E.F., Moore, J.C., Detling, J.K., Kittel, T.G.F., Walter, D.E., Fowler, M.C., Klein, D.A. and Elliott, E.T. (1991). Simulation model for the effects of climate change on temperate grassland ecosystems. *Ecol. Model.*, *53*, 205-246.
- IPCC (1996). *Climate Change 1995: The Science of Climate Change*. Contribution of Working Group 1 to the second assessment report of the Intergovernmental Panel on Climate Change; J. T. Houghton, Meira Filho, L.G., Callander, B.A., Harris, N., Kattenberg, A. and Maskell, K., eds.; Cambridge University Press, Cambridge, UK.
- IPCC (1996). Revised 1996 IPCC Guidelines for National Greenhouse Gas Inventories. <http://www.ipcc-nggip.iges.or.jp/public/gl/invs1.htm>.
- IPCC (1997). Revised 1996 IPCC Guidelines for National Greenhouse Gas Inventories. <http://www.ipcc-nggip.iges.or.jp/public/gl/invs1.htm>.
- IPCC (2000). *Special Report on Emissions Scenarios*. Nakicenovic, N., J. Alcamo, G. Davis, B. de Vries, J. Fenhann, S. Gaffin, K. Gregory, A. Grübler, T. Yong Jung, T. Kram, E.L. La Rovere, L. Michaelis, S. Mori, T. Morita, W. Pepper, H. Pitcher, L. Price, K. Riahi, A.

Roehrl, H.-H. Rogner, A. Sankovski, M. Schlesinger, P. Shukla, S. Smith, R. Swart, S. van Rooijen, N. Victor and Z. Dadi (eds.). A Special Report of Working Group III of the intergovernmental Panel on Climate Change, Cambridge University Press, Cambridge, UK.

IPCC (2001). *Climate Change 2001: The Scientific Basis*. Intergovernmental Panel on Climate Change; D. J.T. Houghton, Y. , Griggs, D.J., Noguer, M., van der Linden, P.J., Dai, X., Johnson, C.A., Maskell, K., eds.; Cambridge University Press, Cambridge, U.K.

Jain, A.K., Khesghi, H.S. and Wuebbles, D.J. (1994). Integrated Science Model for Assessment of Climate Change. *Lawrence Livermore National Laboratory*, UCRL-JC-116526.

Jaksic, V. (2004). *Observations and modelling of carbon dioxide and energy fluxes from an Irish grassland for a two year campaign*. M.Eng.Sc. Thesis, University College, Cork, Ireland.

Johnson, K.A. and Johnson, D.E. (1995). Methane Emissions from Cattle. *J. Anim. Sci.*, 73, 2483-2492.

Joos, F., Bruno, M., Fink, R., Siegenthaler, U. and Stocker, T.F. (1996). An efficient and accurate representation of complex oceanic and biospheric models of anthropogenic carbon uptake. *Tellus*, 48B, 397-417.

Jordan, C. (1997). *Mapping of rainfall chemistry in Ireland 1972-94*. Biology and Environment: Proceedings of the Royal Irish Academy.

Keane, T. and Collins, J.F. (2004). *Climate, Weather and Irish Agriculture*. AGMET, Dublin.

Kiely, G. (1997). Global climate change-greenhouse gases. In *Environmental Engineering*. McGraw-Hill Publishing Company, UK, pp. 358-362.

Kinerson, R.S., Ralston, C.W. and Wells, C.G. (1977). Carbon cycling in a loblolly pine plantation. *Oecologia*, 29, 1-10.

Kipp and Zonen (2000). CNR1 Net-Radiometer instruction manual. *Kipp & Zonen*, Delft, Netherlands. http://www.campbellsci.ca/CampbellScientific/Catalogue/CNR1_Br.pdf.

Kipp and Zonen (2001). PAR LITE Sensor for photosynthetic photon flux. *Kipp & Zonen*, Delft, Netherlands. http://www.campbellsci.ca/CampbellScientific/Catalogue/PAR_Lite_Br.pdf.

KyotoProtocol (1997). The text of the Kyoto Protocol is available at: www.unfccc.de.

Laville, P., Jambert, C., Cellier, P. and Delmas, R. (1999). Nitrous oxide fluxes from a fertilised maize crop using micrometeorological and chamber methods. *Agri. For. Meteorol.*, 96, 19-38.

Lawton, D., Leahy, P., Kiely, G., Byrne, K. and Calanca, P. (2005). Observations and process-based modeling of the net ecosystem exchange and its components for a humid grassland ecosystem. *Glob. Change Biol.*, submitted.

Le Bris, C. (2002). *Observations and modelling of carbon dioxide flux from an Irish Grassland for a one year campaign*. M.Eng.Sc. Thesis, University College, Cork, Ireland.

- Leahy, P., Kiely, G. and Scanlon, T.M. (2004). Managed grasslands: A greenhouse gas sink or source? *Geophysical Research Letters*, 31, doi:10.1029/2004GL021161.
- Leggett, J., Pepper, W.J., Swart, R.J., Edmonds, J., Meira Filho, L.G., Mintzer, I., Wang, M.X. and Watson, J. (1992). Emissions Scenarios for the IPCC: an Update. In *Climate Change 1992: The Supplementary Report to The IPCC Scientific Assessment*. Cambridge University Press, UK, pp. 68-95.
- Leiros, M.C., Trasar-Cepeda, C., Seoane, S. and Gil-Sotres, F. (1999). Dependence of mineralization of soil organic matter on temperature and moisture. *Soil Biol. Biochem.*, 31, 327-335.
- Lewis, C. (2003). *Phosphorus, nitrogen and suspended sediment loss from soil to water from agricultural grassland*. M.Eng.Sc. Thesis, University College, Cork, Ireland.
- Li, C., Frolking, S. and Harriss, R. (1994). Modeling carbon biogeochemistry in agricultural soils. *Global Biogeochem. Cycles*, 8, 237-254.
- Liang, X., Xie, Z. and Huang, M. (2003). A new parameterization for surface and groundwater interactions and its impact on water budgets with the variable infiltration capacity (VIC) land surface model. *Journal of Geophysical Research*, 108, doi:10.1029/2002JD003090.
- LI-COR (2001). LI-7500 Product Information. *LI-COR, Inc*, USA. <http://www.licor.com>.
- Mengelkamp, H.T., Warrach, K. and Raschke, E. (1999). SEWAB – a parameterization of the Surface Energy and Water Balance for atmospheric and hydrologic models. *Advances in Water Resources*, 23, 165-175.
- Mosier, A.R., Duxbury, J.M., Freney, J.R., Heinemeyer, O. and Minami, K. (1996). Nitrous oxide emissions from agricultural fields: Assessment, measurement and mitigation. *Plant and Soil*, 181, 95-108.
- Novick, K.A., Stoy, P.C., Katul, G.G., Ellsworth, D.S., Siquiera, M.B.S., Juang, J. and Oren, R. (2004). Carbon dioxide and water vapour exchange in a warm temperate grassland. *Oecologia*, 138, 259-274.
- Ojima, D.S., Dirks, B.O.M., Glen, E., Owensby, V.C. and Scurlock, J.M.O. (1993). Assessment of C budget for grasslands and drylands of the world. *Water, Air and, Soil Pollution*, 70, 95-109.
- Parton, W.J., Schimel, D.S., Cole, C.V. and Ojima, D.S. (1987). Analysis of factors controlling soil organic matter levels in Great Plains grasslands. *Soil Sci. Soc. Am. J.*, 51, 1173-1179.
- Parton, W.J., Scurlock, J.M.O., Ojima, D.S., Schimel, D.S. and Hall, D.O., Scopegram Group Members (1995). Impact of climate change on grassland production and soil carbon worldwide. *Glob. Change Biol.*, 1, 13-22.
- Pattey, E., Strachan, I.B., Desjardins, R.L. and Massheder, J. (2002). Measuring nighttime CO₂ flux over terrestrial ecosystems using eddy covariance and nocturnal boundary layer methods. *Agri. For. Meteorol.*, 113, 145-158.

- Picon-Cochard, C., Teyssonneyre, F., Besle, J.M. and Soussana, J.-F. (2004). Effects of elevated CO₂ and cutting frequency on the productivity and herbage quality of a semi-natural grassland. *Europ. J. Agronomy*, 20, 363-377.
- Pope, V.D., Gallani, M.L., R., R.P. and Stratton, R.A. (2000). The impact of new physical parametrizations in the Hadley Centre climate model -- HadAM3. *Climate Dynamics*, 16, 123-146.
- Rastetter, E.B., Agren, G.I. and Shaver, G.R. (1997). Responses of N-limited ecosystems to increased CO₂: a balanced-nutrition, coupled element-cycles model. *Ecol. Appl.*, 7, 444-460.
- Rastetter, E.B. and Shaver, G.R. (1992). A model of multiple-element limitation for acclimating vegetation. *Ecology*, 73, 1154-1174.
- REPS (2002). *Agri-Environmental Specifications For REPS 2000*. Departement of Agriculture, Food and Rural Development.
- Riedo, M., Grub, A., Rosset, M. and Fuhrer, J. (1998). A pasture simulation model for dry matter production, and fluxes of carbon, nitrogen, water and energy. *Ecol. Model.*, 105, 141-183.
- Riedo, M., Gyalistras, D., Fischlin, A. and Fuhrer, J. (1999). Using an ecosystem model linked to GCM-derived local weather scenarios to analyse effects of climate change and elevated CO₂ on dry matter production and partitioning, and water use in temperate managed grasslands. *Glob. Change Biol.*, 5, 213-223.
- Riedo, M., Gyalistras, D. and Fuhrer, J. (2001). Pasture responses to elevated temperature and doubled CO₂ concentration: assessing the spatial pattern across an alpine landscape. *Clim. Res.*, 17, 19-31.
- Riedo, M., Gyalistras, D. and Furher, J. (2000). Net primary production and carbon stocks in differently managed grasslands: simulation of a site-specific sensitivity to an increase in atmospheric CO₂ and to climate change. *Ecol. Model.*, 134, 207-227.
- Riedo, M., Milfort, C., Schmid, M. and Sutton, M.A. (2002). Coupling soil-plant-atmosphere exchange of ammonia with ecosystem functioning in grasslands. *Ecol. Model.*, 158, 83-110.
- Ryden, J.C. (1981). N₂O exchange between a grassland soil and the atmosphere. *Nature*, 292, 235-236.
- Saigusa, N., Oikawa, T. and Liu, S. (1998). Seasonal variations of the exchange of CO₂ and H₂O between a grassland and the atmosphere: An experimental study. *Agri. For. Meteorol.*, 89, 131-139.
- Salètes, S., Fiorelli, J.L., Vuichard, N., Cmabou, J., Olesen, J.E., Hacala, S., Sutton, M.A., Fuhrer, J. and Soussana, J.F. (2004). *Proceedings of the International Conference "Greenhouse gas emissions from agriculture - Mitigations options and strategies"*, Leipzig, 10-12th February 2004.
- Sarmiento, J.L. and Gruber, N. (2002). Sinks for anthropogenic carbon. *Physics Today*, 55, 30-36.
- Scanlon, T.M., Kiely, G. and Xie, Q. (2004). A nested catchment approach for defining the hydrological controls on non-point phosphorus transport. *Journal of Hydrology*, 291, 218-231.

- Schmid, M., Neftel, A., Riedo, M. and Fuhrer, J. (2001). Process-based modelling of nitrous oxide emissions from different nitrogen sources in mown grassland. *Nutrient Cycling in Agroecosystems*, 60, 177-187.
- Schmid, P.H. (2002). Footprint modelling for vegetation atmosphere exchange studies: a review and perspective. *Agri. For. Meteorol.*, 113, 159-183.
- Seinfeld, J. (1986). *Atmospheric Chemistry and Physics of Air Pollution*. John Wiley, New-York.
- Sims, P.L. and Bradford, J.A. (2001). Carbon dioxide fluxes in a southern plains prairie. *Agri. For. Meteorol.*, 109, 117-134.
- Soussana, J.-F., Loiseau, P., Vuichard, N., Ceschia, E., Balesdent, J., Chevallier, T. and Arrouays, D. (2004). Carbon cycling and sequestration opportunities in temperate grasslands. *Soil Use and Management*, 20, Special Issue 1, 219-230.
- Thornley, J.M.H. (1998). *Grassland Dynamics. An Ecosystem Simulation Model*. CAB International, Oxon.
- Thornley, J.M.H. and Cannell, M.G.R. (1997). Temperate grassland responses to climate change: an analysis using the Hurley Pasture Model. *Annals of Botany*, 80, 205-221.
- Trogler, W.C. (1999). Physical properties and mechanisms of formation of nitrous oxide. *Coord. Chem. Rev.*, 187, 303-327.
- Tu, K.P. (2001). *Partitioning ecosystem respiration using stable carbon isotopes in a mixed C3 annual grassland*. American Geophysical Union, Fall Meeting 2001, San Francisco, Ca.
- UNFCCC (1992). United Nations Framework Convention on Climate Change. <http://unfccc.int/resource/docs/convkp/conveng.pdf>.
- Volpe Horii, C., Zahniser, M.S., Nelson, D.D.J., McManus, J.B. and Wofsy, S.C. (1999). Nitric acid and nitrogen dioxide flux measurements: a new application of tunable diode laser absorption spectroscopy. *SPIE*, 3758, 152-161.
- Vuichard, N., Ciais, P., Viovy, N., Ammann, C., Calanca, P., Clifton-Brown, J., Fuhrer, J., Jones, M., Martin, C. and Soussana, J.-F. (2005). Estimating the greenhouse gas fluxes of European grasslands with a process driven model: Part 1. Model evaluation from in-situ measurements. *in preparation*.
- Webb, E.K., Pearman, G.I. and Leuning, R. (1980). Correction of flux measurements for density effects due to heat and water vapor transfer. *Q.J.R. Met. Soc.*, 106, 85-100.
- Williams, D.L., Ineson, P. and Coward, P.A. (1999). Temporal variations in nitrous oxide fluxes from urine-affected grassland. *Soil Biol. Biochem.*, 31, 779-788.
- Xu, L. and Baldocchi, D.D. (2004). Seasonal variation in carbon dioxide exchange over a Mediterranean annual grassland in California. *Agri. For. Meteorol.*, 123, 79-96.
- Young (2001). Model 81000 Ultrasonic anemometer, manual PN 81000-90. *RM Young Company*, Michigan, USA. <http://www.youngusa.com/81000.pdf>.

Figure 1: (a) Monthly average air temperature, (b) monthly totals of precipitation, for 2002, 2003 and 2004.

Figure 2: Modeled (___) and measured (_ _ _) cumulative net ecosystem exchange for 2002, 2003 and 2004 (tC. ha^{-1}). The arrows indicate the timing of the first cut and so the end of the first active “spring” growing season.

Figure 3: (a) Cumulative gross primary production (GPP) in tC. ha^{-1} , (b) Cumulative total respiration of the ecosystem (R_{tot}) in tC. ha^{-1} . GPP is positive in accordance with the biological sign convention.

Figure 4: The three components of total respiration: (a) soil, (b) plant, (c) grazing animal, in tC. ha^{-1} .

Figure 5: (a) Modeled time integrated soil moisture of the 2nd layer, (b) Modeled time integrated soil temperature for the 2nd layer, for the three year of the study.

Table 1. Physical and climatic characteristics of the site

Location	52.14° N		
	8.66° W		
Altitude above sea level (m)	200		
Soil type	loam		
	2002	2003	2004
Average daily radiation ($W m^{-2}$)	46.75	48.03	52.47
No. of days $T_{air} > 5^{\circ}C$	331	317	320
Average daily mean temperature ($^{\circ}C$)	9.6	9.6	9.5
Total precipitation ($mm yr^{-1}$)	1785	1178	1340

Table 2. Soil parameters

^a Soil pH	5.6
^a Main rooting depth (m)	0.25
^a Sand:Silt:Clay (%)	42:41:17
^a Depth of the 3 layers (m)	0.02 ; 0.20 ; 0.60
^a Bulk density (g/cm ³)	1.0 ; 1.0 ; 1.7
^b Saturated soil water content (m ³ /m ³)	0.60 ; 0.43 ; 0.40
^c Air entry potential (mm)	-50.0 ; -100.0 ; -100.0
^c Saturated hydraulic conductivity (mm day ⁻¹)	188.0 ; 18.0 ; 18.0
^d Parameter b	5.4

^a Soil samples.

^b Literature.

^c Model optimization.

^d Clapp and Hornberger, (1978).

Table 3. Initial conditions for carbon and nitrogen in the various pools

	Carbon [kgC. m ⁻²]	Nitrogen [kgN. m ⁻²]
Wstruct ^a	1.693	-
Wmetab ^b	0.109	0.010
Wactive ^c	0.305	0.043
Wslow ^d	5.701	0.378
Wpassive ^e	5.054	0.455

^a Structural dead plant material, ^b Metabolic dead plant material, ^c Active soil organic matter,

^d Slow soil organic matter, ^e Passive soil organic matter

Table 4. Comparison of the observed and modeled NEE

Annual sum of NEE			
	2002	2003	2004
Observed (tC. ha ⁻¹ yr ⁻¹)	1.91	2.59	2.95
Modeled (tC. ha ⁻¹ yr ⁻¹)	2.64	2.66	3.36

Growing season for observed NEE

	2002	2003	2004
Starting date (julian day)	79	78	98
Finishing date (julian day)	184	167	204
Length (days)	105	89	106
Gradient (gC. m ⁻² day ⁻¹)	2.8	3.1	2.7

Growing season for modeled NEE

	2002	2003	2004
Starting date (julian day)	79	68	73
Finishing date (julian day)	195	180	204
Length (days)	116	112	131
Gradient (gC. m ⁻² day ⁻¹)	2.3	2.5	2.8

Figure 1

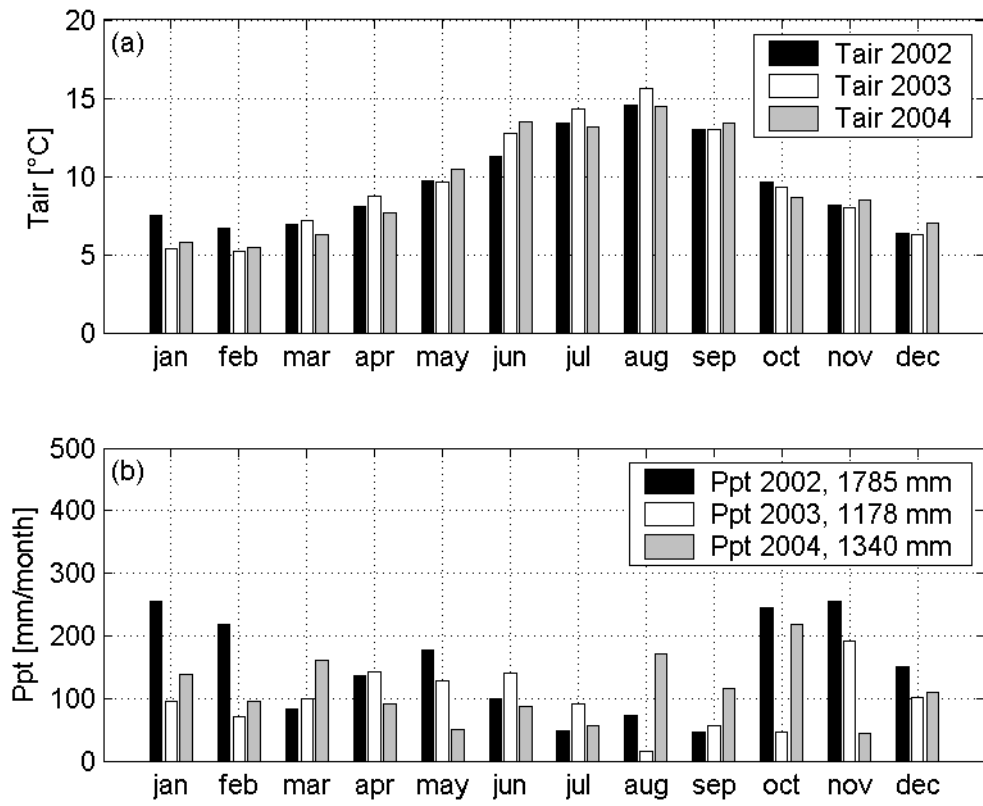


Figure 2

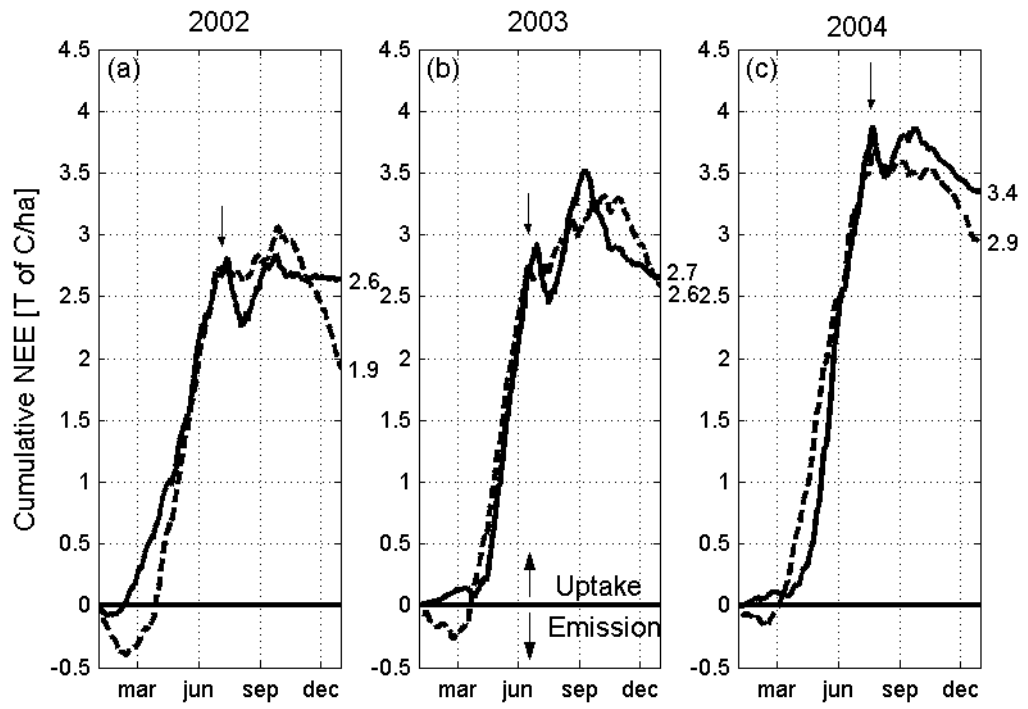


Figure 3

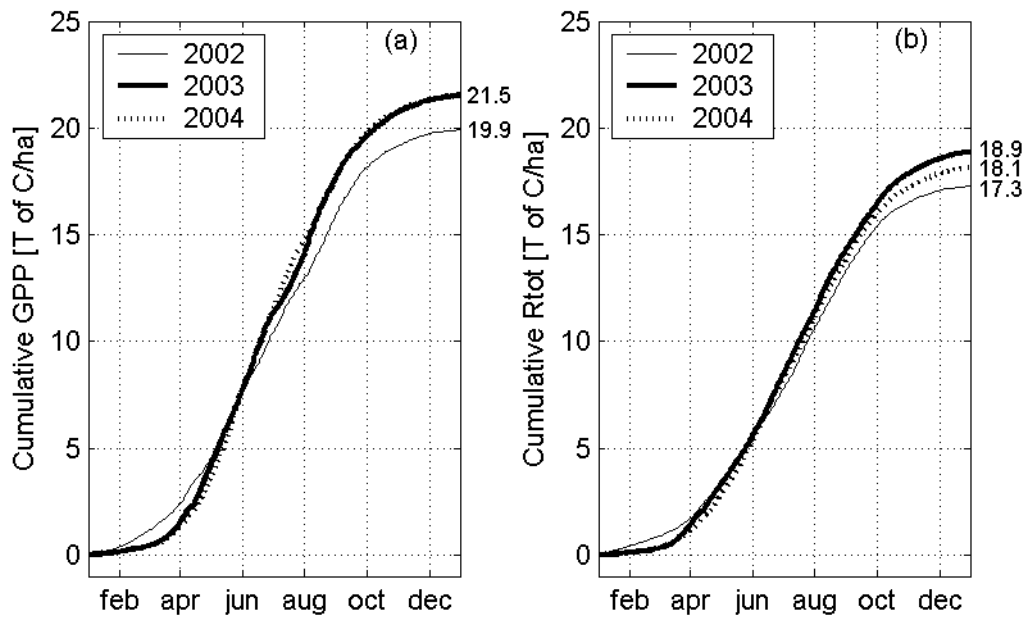


Figure 4

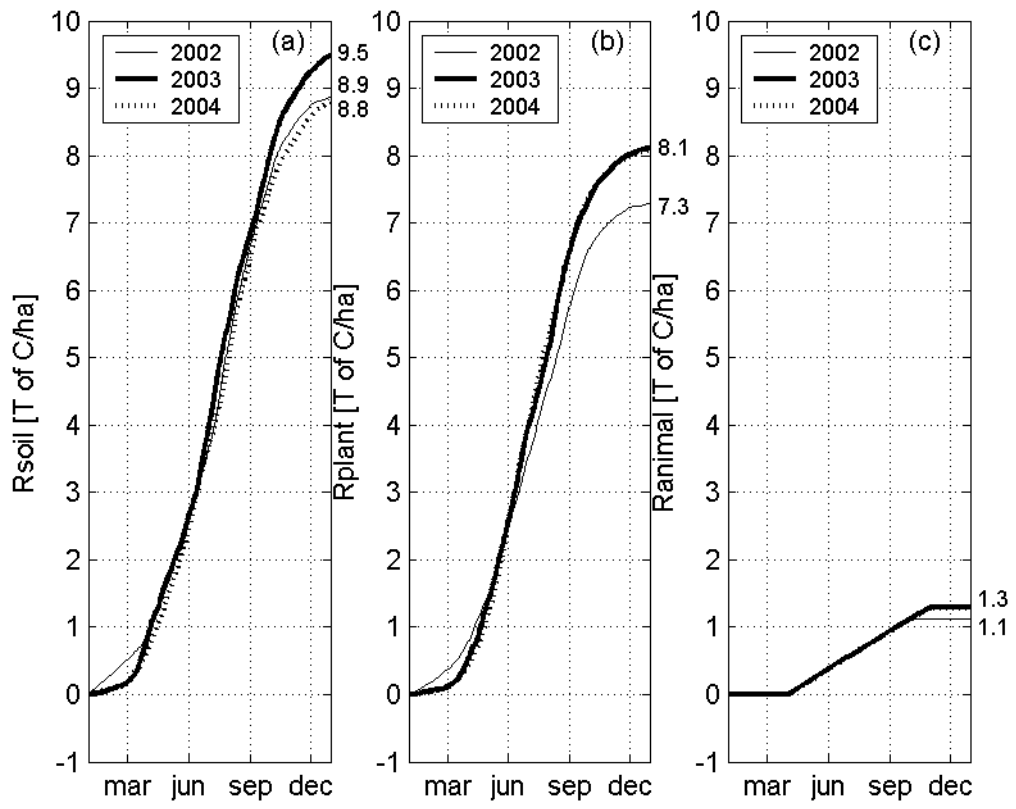


Figure 5

